UCRL-17696

cy. 2

University of California

Ernest O. Lawrence Radiation Laboratory

QUANTUM NUMBERS OF BOSON RESONANCES

Gerson Goldhaber

July 1967

DISCLAIMER

Lecture Series Presented at the "1967 CERN School of Physics"
Rättvik, Sweden – May 21 to June 3, 1967

UCRL-17696

UNIVERSITY OF CALIFORNIA
Lawrence Radiation Laboratory
Berkeley, California

AEC Contract No. W-7405-eng-48

QUANTUM NUMBERS OF BOSON RESONANCES

Gerson Goldhaber

July 1967

Recently discovered Ancient Proverb
(author unknown):

"One Valley Is Worth Two Peaks"

Contents

QUANTUM NUMBERS OF BOSON RESONANCES

Gerson Goldhaber

Lawrence Radiation Laboratory and Department of Physics
University of California, Berkeley, California

Lecture I: THE ESTABLISHED BOSON NONETS

During the past six years, three boson nonets have been clearly established. These are the pseudoscalar octet and singlet, or nonet ($J^P = 0^-$), the vector nonet ($J^P = 1^-$), and $J^P = 2^+$ nonet. The general features of these have been reviewed at the Berkeley Conference.[1] Therefore I will be very brief here.*)

1. THE PSEUDOSCALAR OCTET AND SINGLET

The first eight pseudoscalar mesons $\pi[I = 1, (2I + 1 = 3)]$, $\eta[I = 0, (2I + 1 = 1)]$, K and $\bar{K}$, $[I = 1/2, 2(2I + 1) = 4]$ fit the Gell-Mann–Okubo (mass-squared) formula for an octet, $\hat{M}_K = (3\hat{M}_\eta + \hat{M}_\pi)/4$, fairly well. Here $\hat{M}_i = (M_i)^2$. If we use $\hat{M}_K$ and $\hat{M}_\pi$ as input we find $(\hat{M}_\eta)_{\text{predicted}} = 0.318\ (\text{GeV})^2$, compared with $(\hat{M}_\eta)_{\text{exptl}} = 0.301\ (\text{GeV})^2$ -- only a 5.7% discrepancy (see Fig. I-1). There are at present two candidates for the $J^P = 0^-$ unitary singlet: the $X^0(960)$ (or η') and more recently the $E(1410) \to K\bar{K}\pi$ meson. The latter appears to be strongly preferred as a 0^- rather than a 1^+ particle. This "embarras de richesse" of unitary singlets can be understood. On the quark model, for example, we would have to assume that one of these two is the η' with very little mixing between the η and η'. The other one can be the singlet corresponding to the next radial excitation state, with principal quantum number n = 2. We still have to learn, of course, how reliable the spin determination for the E meson is!

---

*) In these lectures I concentrate on new data obtained since the 1966 Berkeley Conference. However, the selection is entirely on the basis of data available to me, and no attempt at completeness has been made. Much of the new data was presented at the April 1967 Washington Meeting of the American Physical Society.

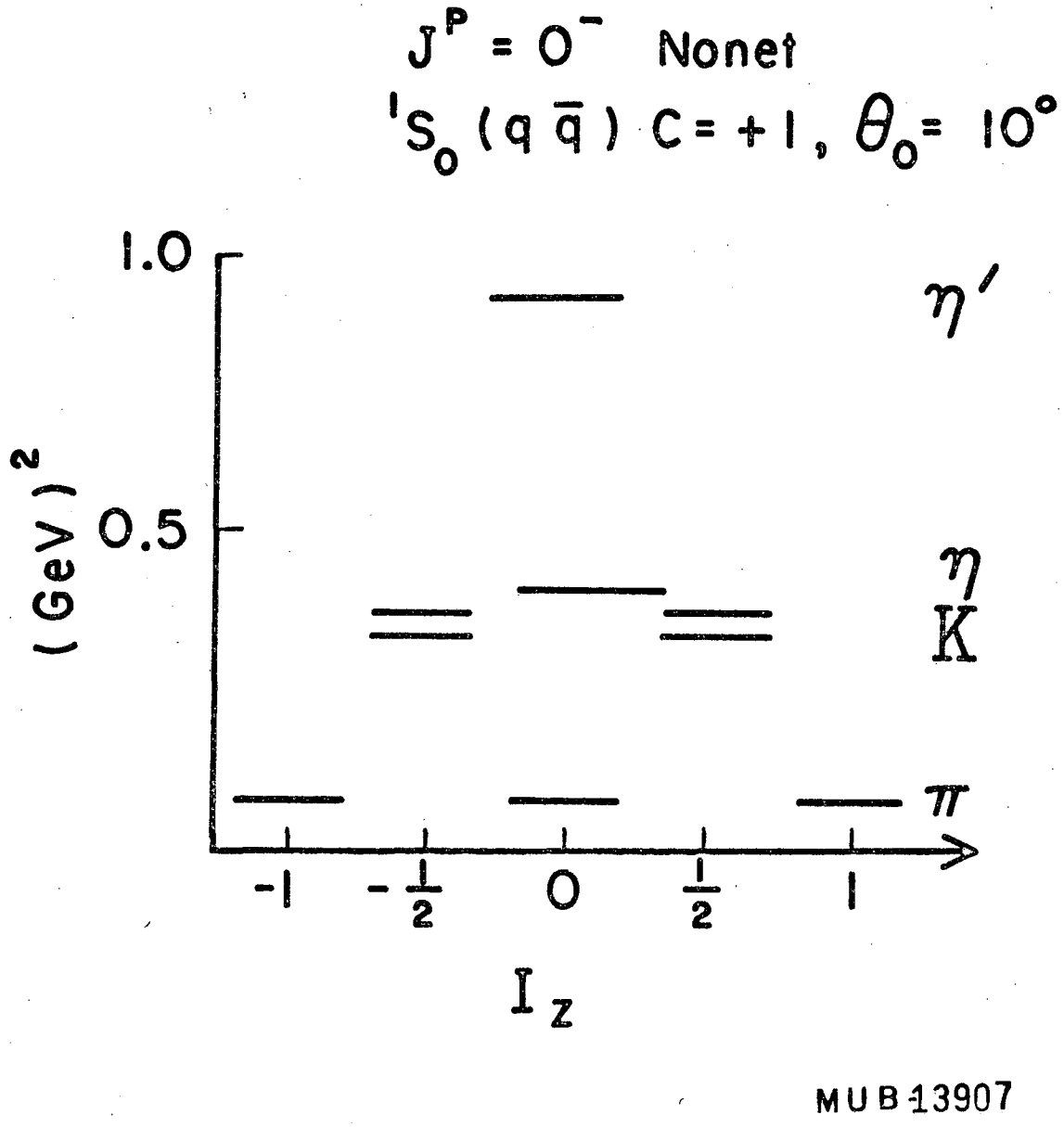

Fig. I-1. The energy-level diagram for the pseudoscalar nonet.

Again on the quark model, the unitary singlet is the completely symmetric state:

$$\eta_1 = \frac{1}{\sqrt{3}}\, a^k a_k = \frac{1}{\sqrt{3}}\,(\bar{p}p + \bar{n}n + \bar{\lambda}\lambda).$$

On removing this state we can express the ideal octet as the traceless tensor,

$$P^i_j = a^i a_j - \frac{1}{3}\,\delta^i_j\, a^k a_k = \begin{pmatrix} \frac{\eta_8}{\sqrt{6}} + \frac{\pi^0}{\sqrt{2}} & \pi^+ & K^+ \\ \pi^- & \frac{\eta_8}{\sqrt{6}} - \frac{\pi^0}{\sqrt{2}} & K^0 \\ K^- & \bar{K}^0 & -\sqrt{\frac{2}{3}}\,\eta_8 \end{pmatrix},$$

where $\eta_8 = (1/\sqrt{6})\,(\bar{p}p + \bar{n}n - 2\bar{\lambda}\lambda)$ and $\pi^0 = (1/\sqrt{2})\,(\bar{p}p - \bar{n}n)$. The physical η is very close to η_8, but contains a small admixture of η_1.

The mixing angle θ_0 is about 10°. If it should turn out that the E is the η' then the mixing angle is even smaller.

I find it a remarkable coincidence that the $\delta(964)$ and $X^0(960)$ should both have very small decay widths and near mass degeneracy! Perhaps there is some correlation between them, a point of view discussed by Tuan and Wu, for example.[2] If this were the case it would of course eliminate the $X^0(960)$ as a member of the 0^- nonet. Here we ought to remember, however, that our acceptance of the δ as a particle relies heavily on the mass coincidence between two distinct experiments (see Figs. I-2 and I-3). No direct indication of the δ has been observed in any other experiment. More work on this particle certainly appears very worthwhile.

2. THE VECTOR NONET

Here the situation is quite different from the pseudoscalar mesons. The eight vector mesons ρ, ϕ, and K^* or ρ, ω, and K^* are nowhere near to the octet mass relation (see Fig. I-4). Thus there is very strong $\phi\,\omega$ mixing, with mixing angle θ_1 given by

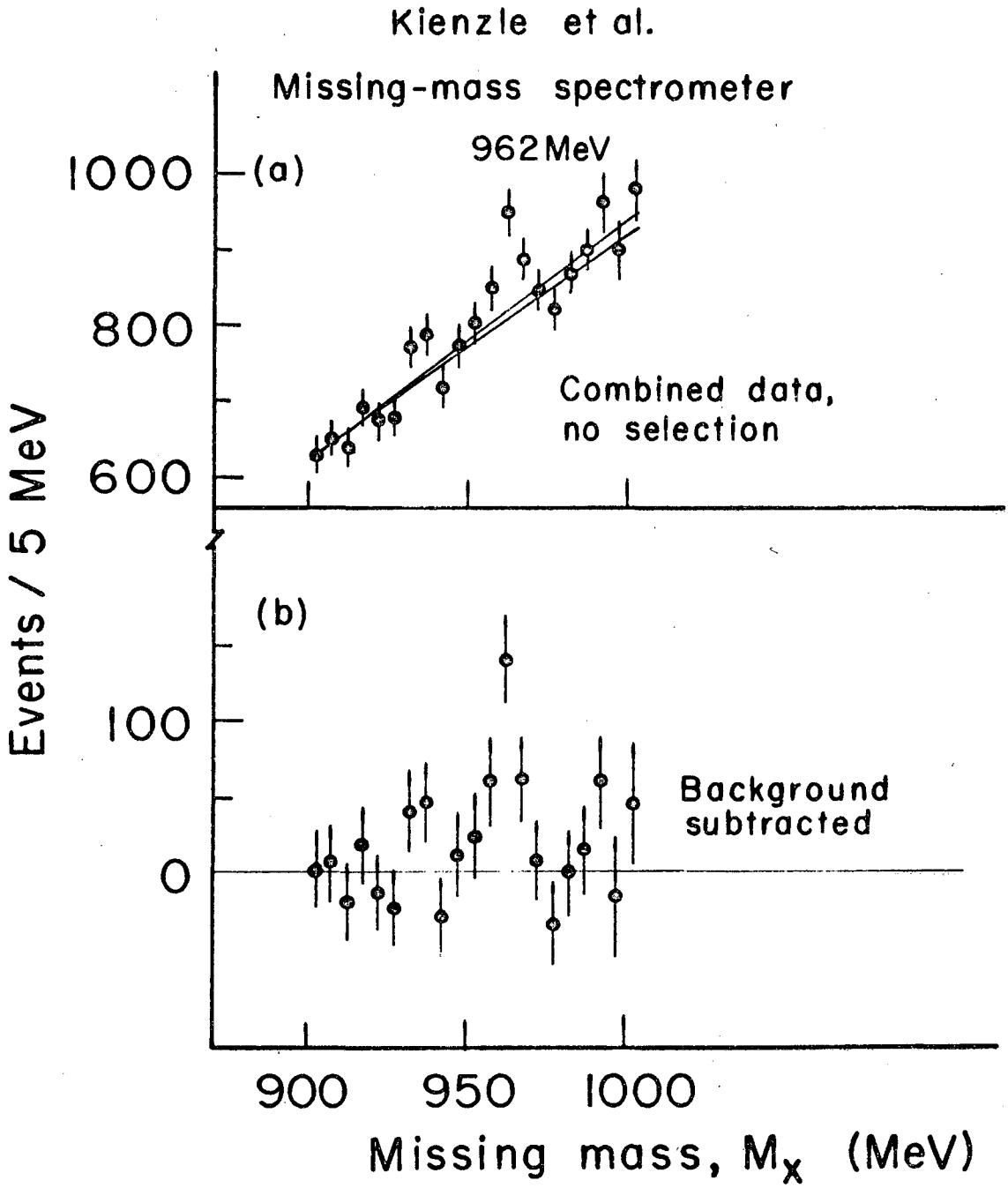

Fig. I-2. The first evidence for the δ^- particle, from CERN.

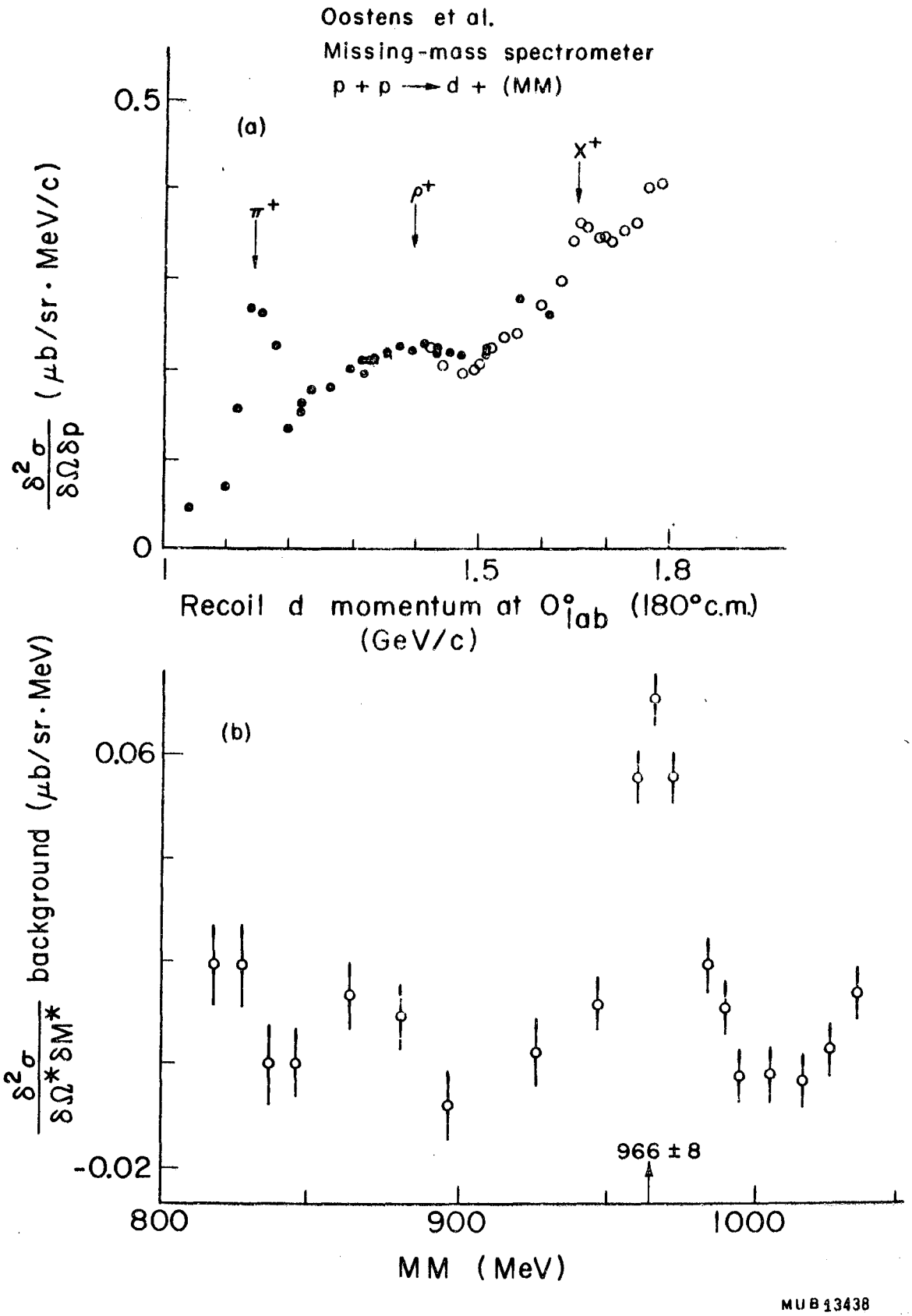

Fig. I-3. The corroborative evidence for the δ particle, from Saclay.

3. THE $J^P = 2^+$ NONET

Here again the nonet form appears more appropirate (see Fig. I-5). If we insert the experimental mass values in the Schwinger equation we find $J \approx 1$ within 15% in this case also.

For this nonet all particles are reasonably well established, although a few questions remain:

i) the spin of the A_2 is still under discussion. The latest suggestion by Morrison is that a second particle with $J^P = 2^-$ or 1^+ is formed at higher bombarding momenta (p = 8 GeV/c).[3]

ii) The remarkable splitting of the A_2 observed in the CERN missing-mass spectrometer experiment appears reconfirmed in more recent work.

iii) The lesser decay modes for all these resonances, such as $A_2 \rightarrow \eta\pi$, are not yet well determined.

Thus while the broad outlines appear established for this nonet, many of the detailed questions are yet unanswered.

4. GLASHOW'S UNIVERSAL MASS PLOT

Glashow has noted an amusing empirical relation which is illustrated in Fig. I-6. He found that the masses of both the bosons and baryons fell on a (nearly) straight line if one plotted $J + (1/2)\,N + M + F$ versus $(\text{mass})^2$.

Here J is the spin, N the number of nonstrange quarks in the particle, M the number of strange quarks, and F the orbital angular momentum or the number of extra $q\bar{q}$ pairs needed to make up the particle. As yet he has no explanation for this empirical relation.

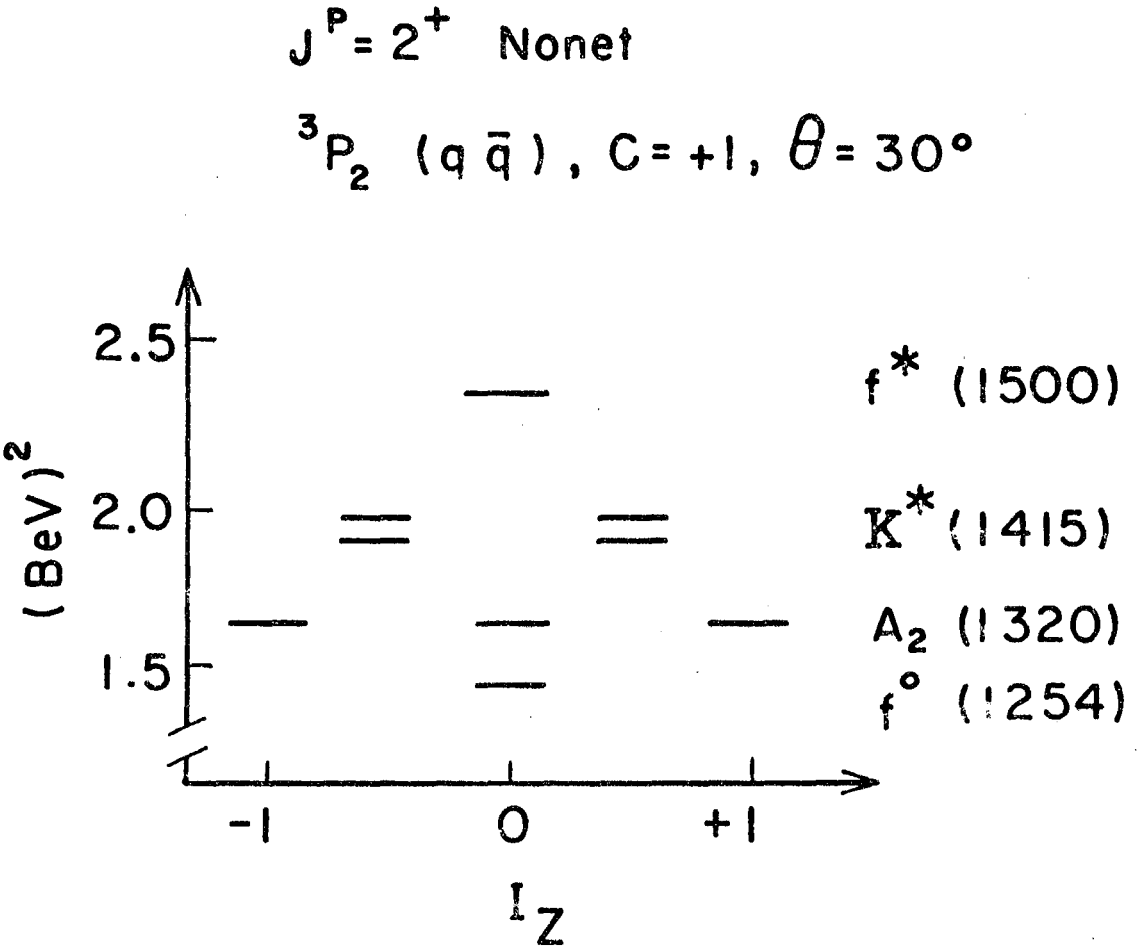

Fig. I-5. The energy-level diagram for the 2^+ nonet.

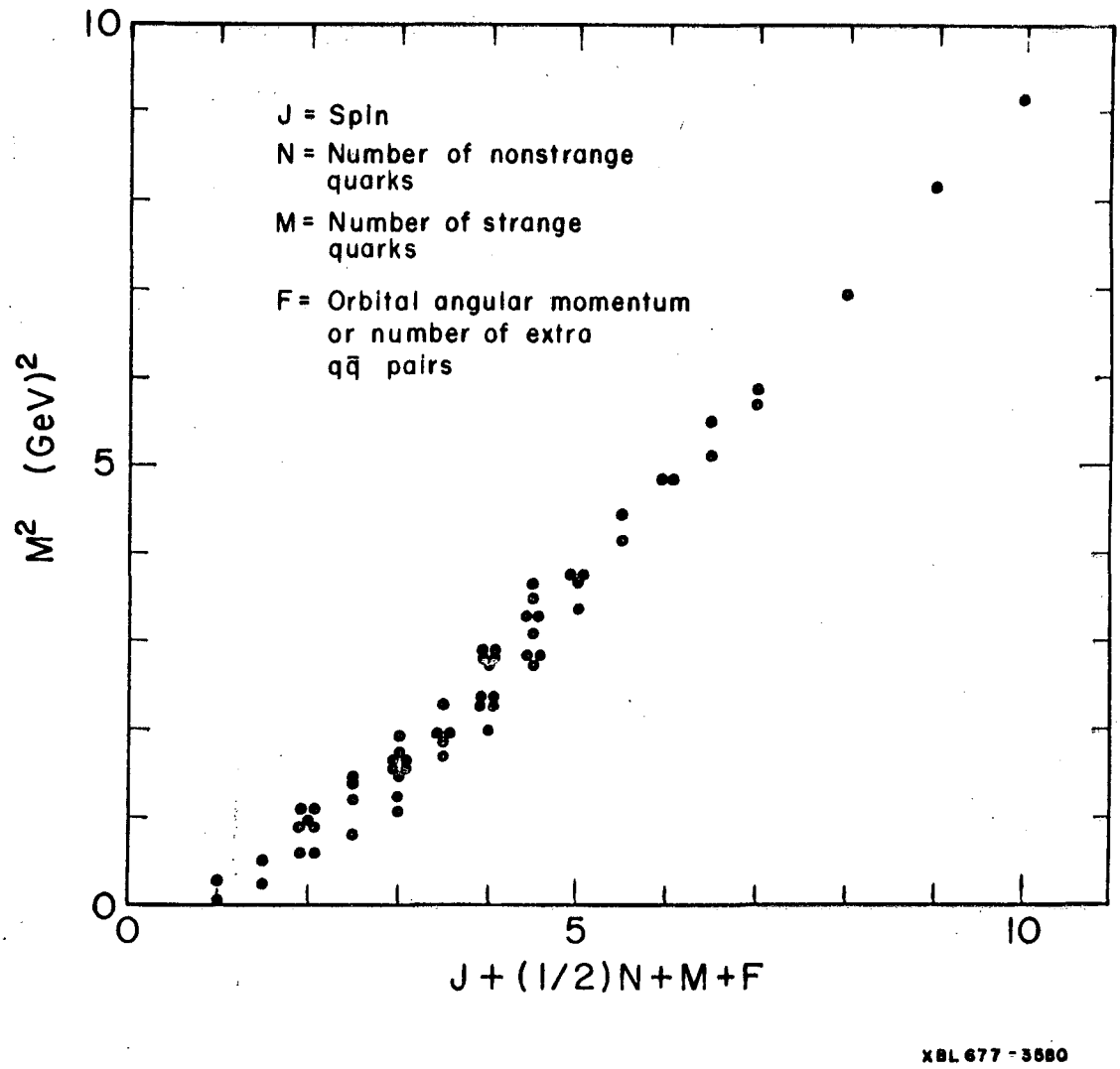

Fig. I-6. Glashow's universal mass plot (all baryons and bosons).

ACKNOWLEDGMENTS

I wish to thank Dr. A. Firestone, Mr. C. M. Fu, Mrs. B. L. Mossman, Dr. B. C. Shen, and Dr. C. Wohl for help on various aspects of these lectures.

REFERENCES, SECTION I

1) Gerson Goldhaver, Rapporteur Talk, "Boson Resonances," in Proceedings of the XIIIth International Conference on High Energy Physics, Berkeley, September 1966 (University of California Press, Berkeley and Los Angeles, 1967) page 103. This article contains references to the original papers. No attempt has been made to duplicate these here.

2) S. F. Tuan and T. T. Wu, Phys. Rev. Letters 18, 349 (1967).

3) D. R. O. Morrison, The Possible Existence of a ($\pi\rho$) Resonance Near 1300 MeV with Spin-Parity Assignment of 2^- or 1^+ (CERN preprint D. Ph. II/PHYSICS 67-15), submitted to Phys. Letters.

Lecture II. HINTS OF OTHER BOSON NONETS

1. TWO 1^+ NONETS, C = +1 AND C = -1

If we interpret the 2^+ nonet on the quark model we can assume that it corresponds to the $^3P_2$ state of the $q\bar{q}$ system. We can then expect that the $^3P_0$, $^3P_1$, and $^1P_1$ states should also exist. This is discussed in greater detail in Lecture III.

We have candidates for the I = 1 members of the two axial vector nonets: the $A_1(1080)$, which decays into $\pi + \rho$ and thus has G = -1 and which from the relation $G = C(-1)^I$ must have C = +1; the B(1220), which decays into $\pi+\omega$ and thus has G = +1 and C = -1. We also have one candidate each for each nonet of the I = 0 states: the $D(1286) \rightarrow K\bar{K}\pi$, which is probably a C = +1 state; and the $H(970) \rightarrow \pi\rho$, which has C = -1.

A new and particularly interesting situation develops for the two K^*'s. The Y = 1 states are not eigenstates of C. The charge conjugation C = ±1 indicates the quark structure of the two K^*'s as $^3P_1$ or $^1P_1$.* Unless for some reason the total quark spin is a conserved quantum number, the two 1^+ K^*'s may undergo mixing. Thus not only can there be mixing between the two sets of two singlets, but further mixing can occur between the two K^*'s, the I = 1/2 states. Furthermore, we might also expect peculiar interference effects in the mass distributions for two adjacent states with the same quantum numbers.

2. IS THERE EVIDENCE FOR TWO 1^+ K^*'s?

If we look at the recent available data on the $K\pi\pi$ system in the 1.1- to 1.5 GeV region we notice a rather peculiar behavior, which at first glance gives the impression that the different experiments are not in agreement with each other.

---

*) A wider generalization of C, designated as unitary-parity, has been introduced by Dothan, and is referred to as $\mathcal{C}$ in the literature. The precise definition and references are given by B. W. Lee in High Energy Physics and Elementary Particles, 1965 Trieste Seminars (International Atomic Energy Agency, Vienna, 1965). See also G. L. Kane, Some Consequences of SU(3) and Charge Conjugation Invariance for K-Meson Resonances, University of Michigan preprint (unpublished).

2.1 THE C MESON OBSERVED IN $\bar{p}p$ ANNIHILATIONS AT REST

It has been a mystery of long standing why the C meson, $M_C \approx 1220$ MeV, occurs only in the neutral form.[1,2] This situation was not helped by the fact that a less pronounced enhancement occurred at $\approx$ 1320 MeV in the charged mode (see Figs. II-1 and II-2). More recent results indicate that the C mass is probably higher, namely 1240 to 1250 MeV.

2.2 THE K^+p AND K^-p REACTIONS AT VARIOUS MOMENTA

We can next consider the behavior of the large $K\pi\pi$ enhancement observed in various experiments as a function of incident momentum.

i) The work on $K^-p \to \bar{K}^0 \pi^0 \pi^- p$ at 2.6 and 2.7 GeV/c at Lawrence Radiation Laboratory[3] shows a clear separation between the 1400-MeV peak and a lower-mass peak. The lower peak appears centered at 1280 MeV. No evidence for a 1320-MeV peak is observed (see Fig. II-3).

ii) Our data[4] for 4.6-GeV/c K^+p show a clear separation between the 1430-MeV peak and a narrow lower peak--which, however, occurs at 1320 MeV, $\Gamma \approx$ 80 MeV. The peaks are superimposed on a considerable background about equal in height to that of the peaks (see Fig. II-4).

iii) The recent Bruxelles–CERN data[5] for 5-GeV/c K^+p represent a very considerable increase in statistics. Here they now obtain a clear separation between the 1420-MeV peak and the lower peak, just as in our data at 4.6 GeV/c. The lower-mass peak is, however, much broader now (see Fig. II-5).

iv) As we continue to higher-momenta K^-p at 4.6 and 5 GeV/c[6] (Figs. II-6 and II-7) and at 5.5 GeV/c[7] (Fig. II-8), and K^+p at 5.5[8] (Fig. II-9) and 7.3 GeV/c[9] (Fig. II-10), we note the same general features--the broad $K\pi\pi$ peak either is not resolved or shows slight indications of structure.

v) In our new data[10] for 9-GeV/c K^+p we note that the 1420 peak is no longer clearly resolved. On the other hand, there appears evidence for a resolved 1250-MeV peak as well as an enhancement in the 1340-MeV region (see Figs. II-11 and II-12).

vi) The work of the ABCLV collaboration, 10-GeV/c K^-p, indicates a large peak centered at 1320 MeV which is, however, not

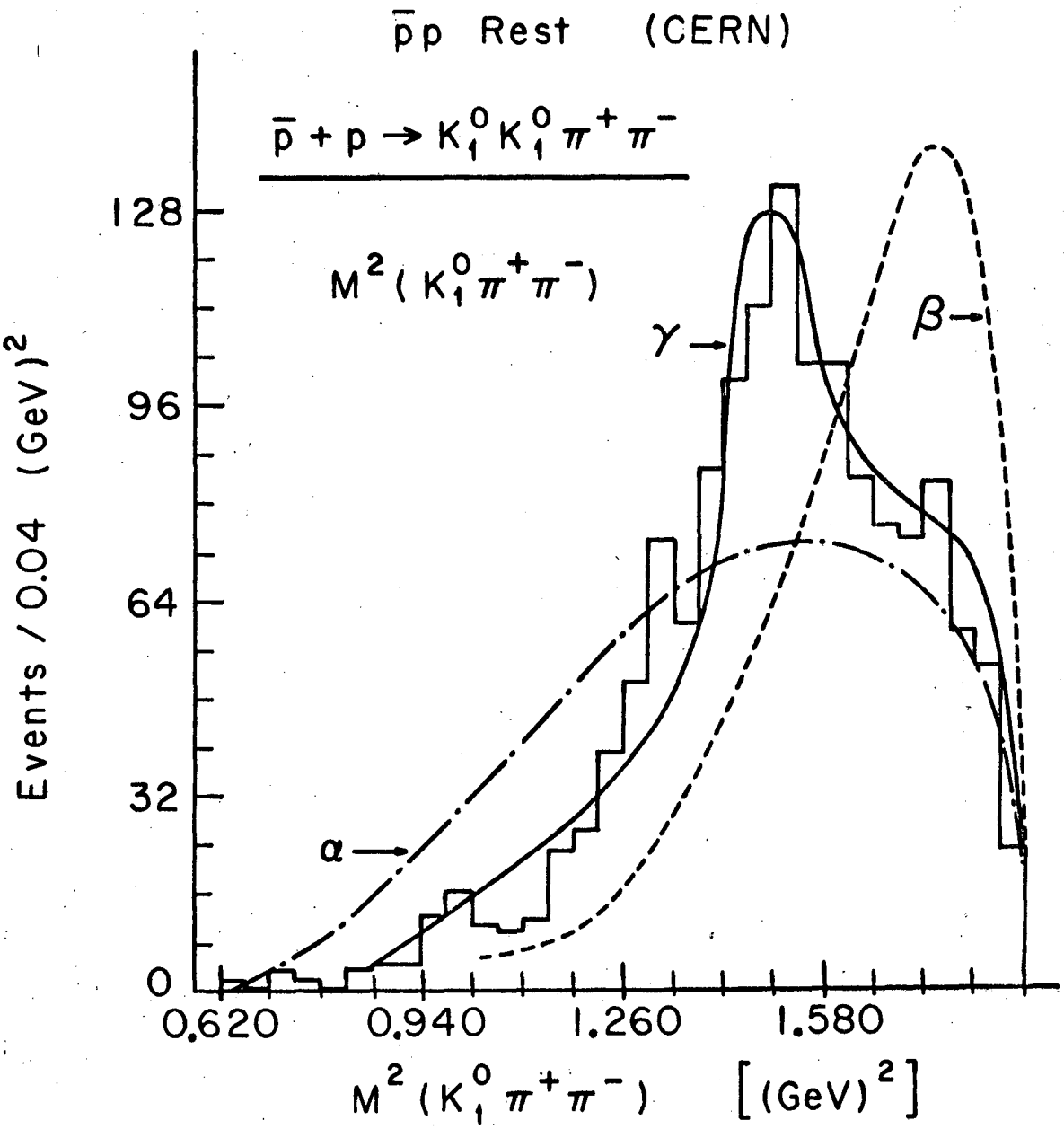

Fig. II-1 XBL677-3569

$\bar{p}p$ Annihilations at rest - CERN.
Curve α: phase space
Curve β: (Kp) phase space in $\bar{p}p \rightarrow K_1^0 K_1^0 p$
Curve γ: 40% phase space,
+ 60% $\bar{p}p \rightarrow K^0 C^0$ with $C^0 \rightarrow K^0 p^-$
M(c) = 1215 MeV; Γ (c) = 60 MeV

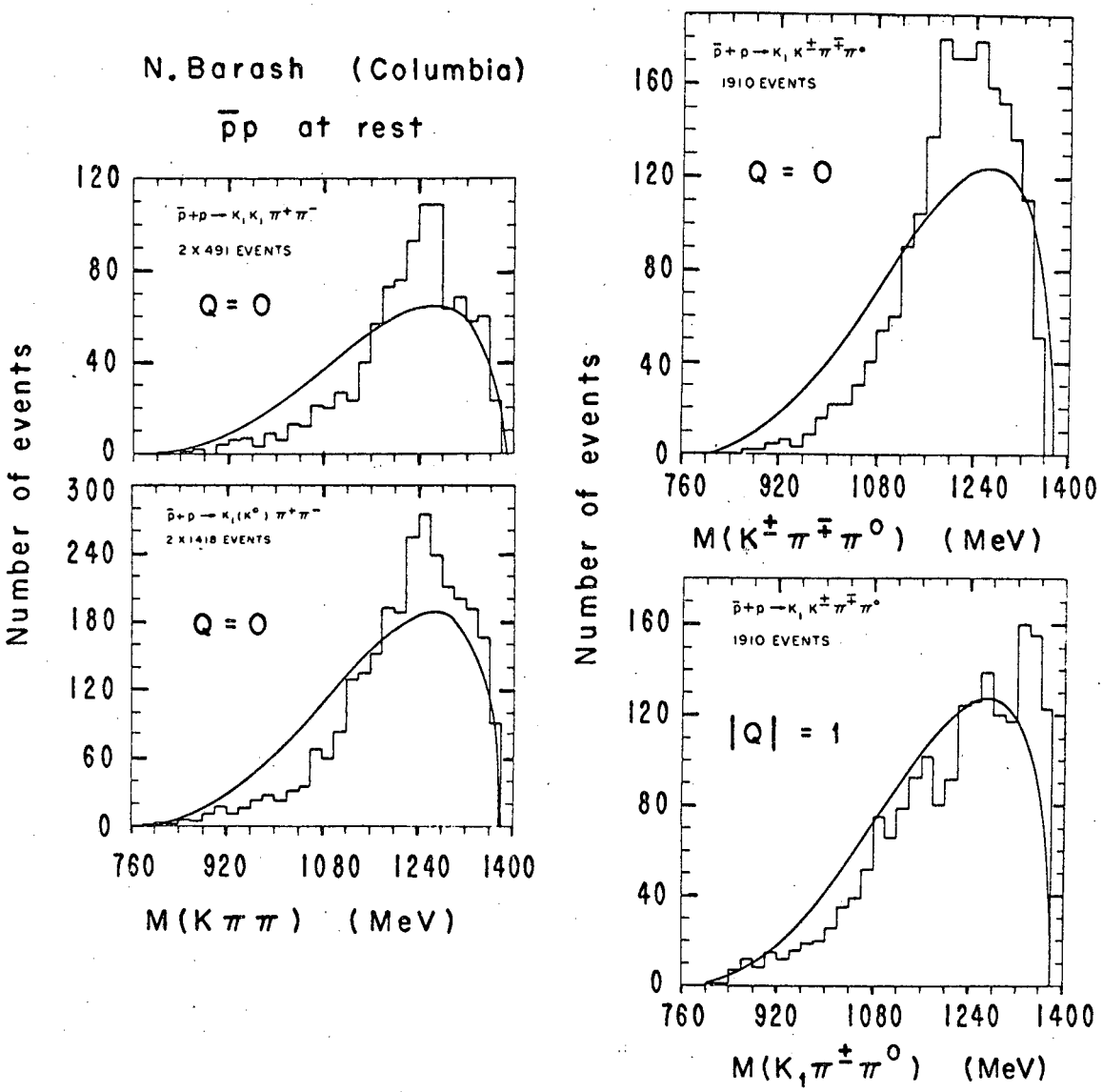

Fig. II-2 XBL677-3570

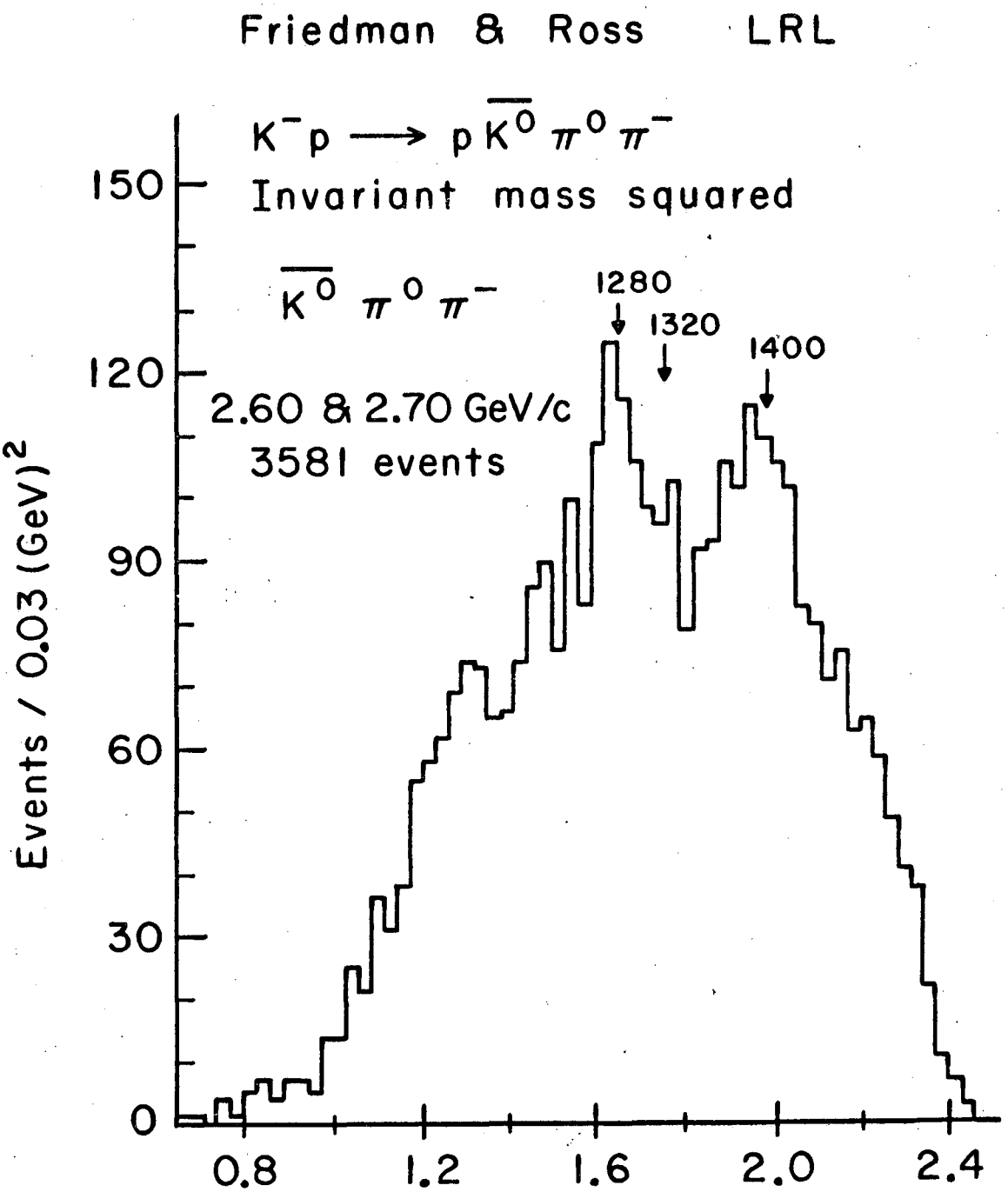
Friedman & Ross LRL
$K^- p \longrightarrow p \overline{K^0} \pi^0 \pi^-$
Invariant mass squared
$\overline{K^0} \pi^0 \pi^-$
2.60 & 2.70 GeV/c
3581 events
1280
1320
1400
Events / 0.03 (GeV)^2
150
120
90
60
30
0
0.8
1.2
1.6
2.0
2.4
XBL677-3571

Fig. II-3

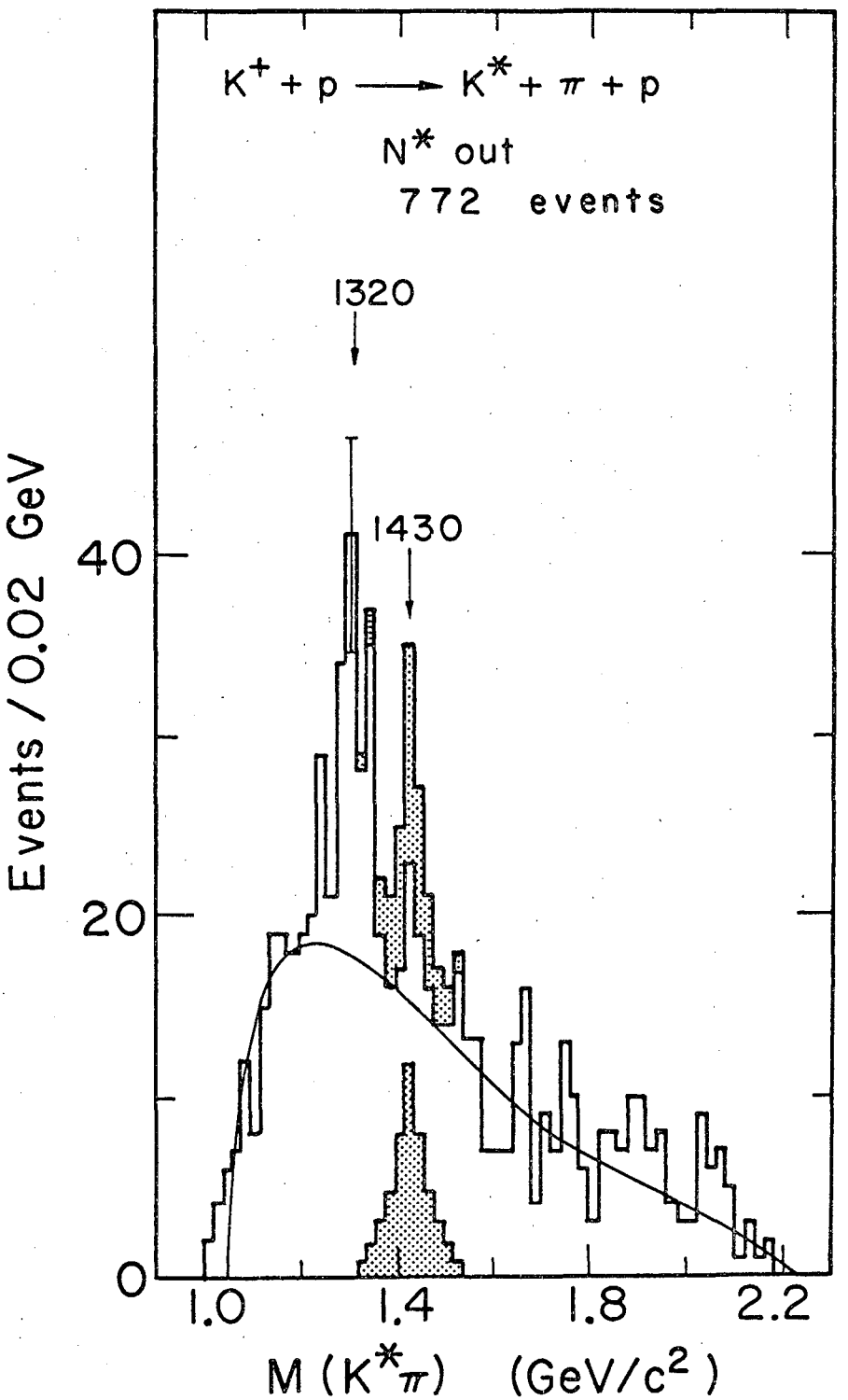

Fig. II-4 MUB-13440

Data of Shen et al. K^+p at 4.6 GeV/c, evidence for $K^*(1320)$ formation. The curve corresponds to the computed contribution from the Deck mechanism normalized to the experimental height at 1.2 GeV. The shaded portion corresponds to the contribution from $K^*(1430)$ decay as estimated from the three-particle in the final-state reactions.

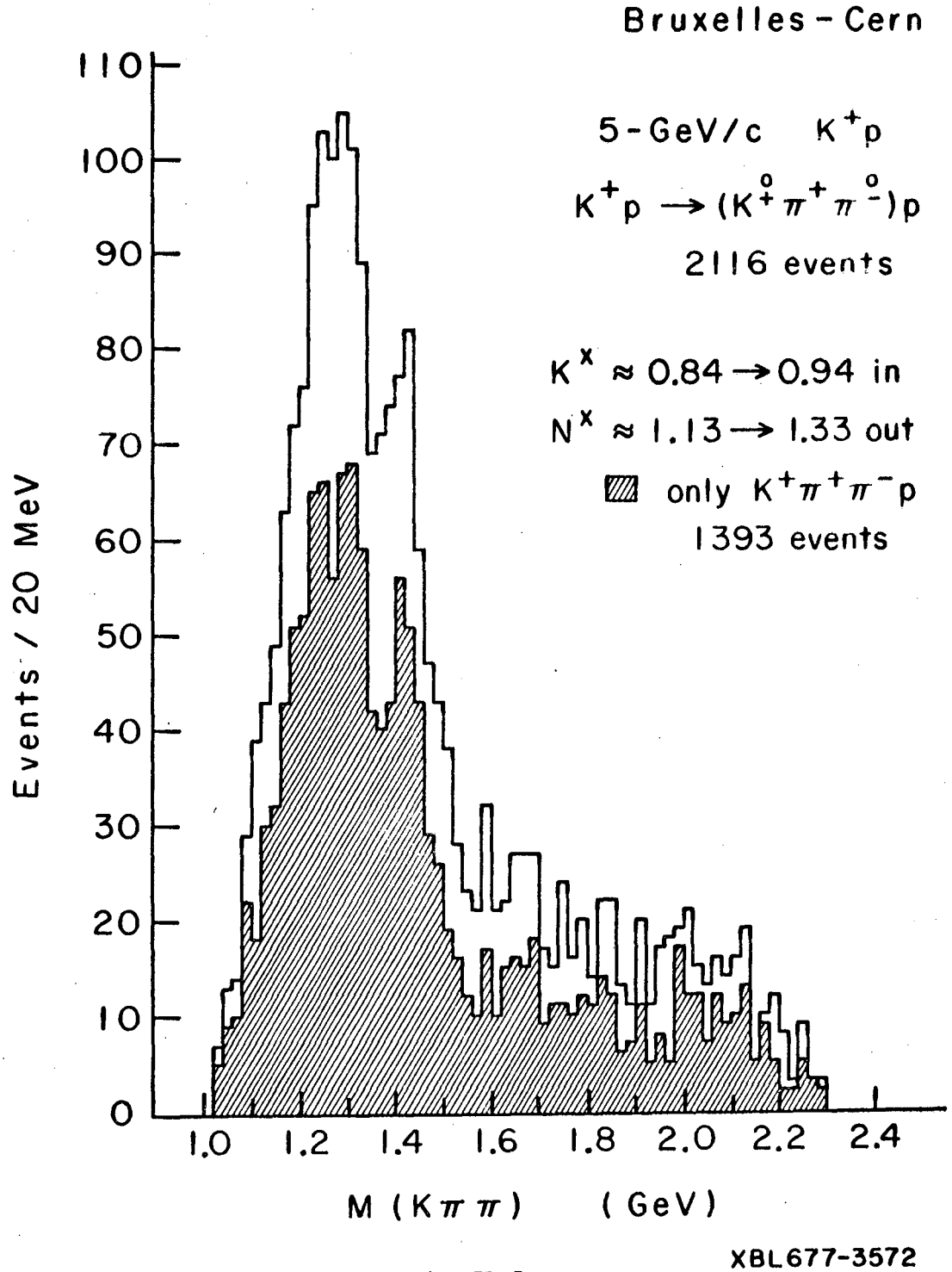
Bruxelles - Cern
5 - GeV/c K+p
K+p → (K+0 π+ π-0) p
2116 events
K^x ≈ 0.84 → 0.94 in
N^x ≈ 1.13 → 1.33 out
only K+π+π-p
1393 events
Events / 20 MeV
0
10
20
30
40
50
60
70
80
90
100
110
1.0
1.2
1.4
1.6
1.8
2.0
2.2
2.4
M (Kππ) (GeV)
XBL677-3572

Fig. II-5

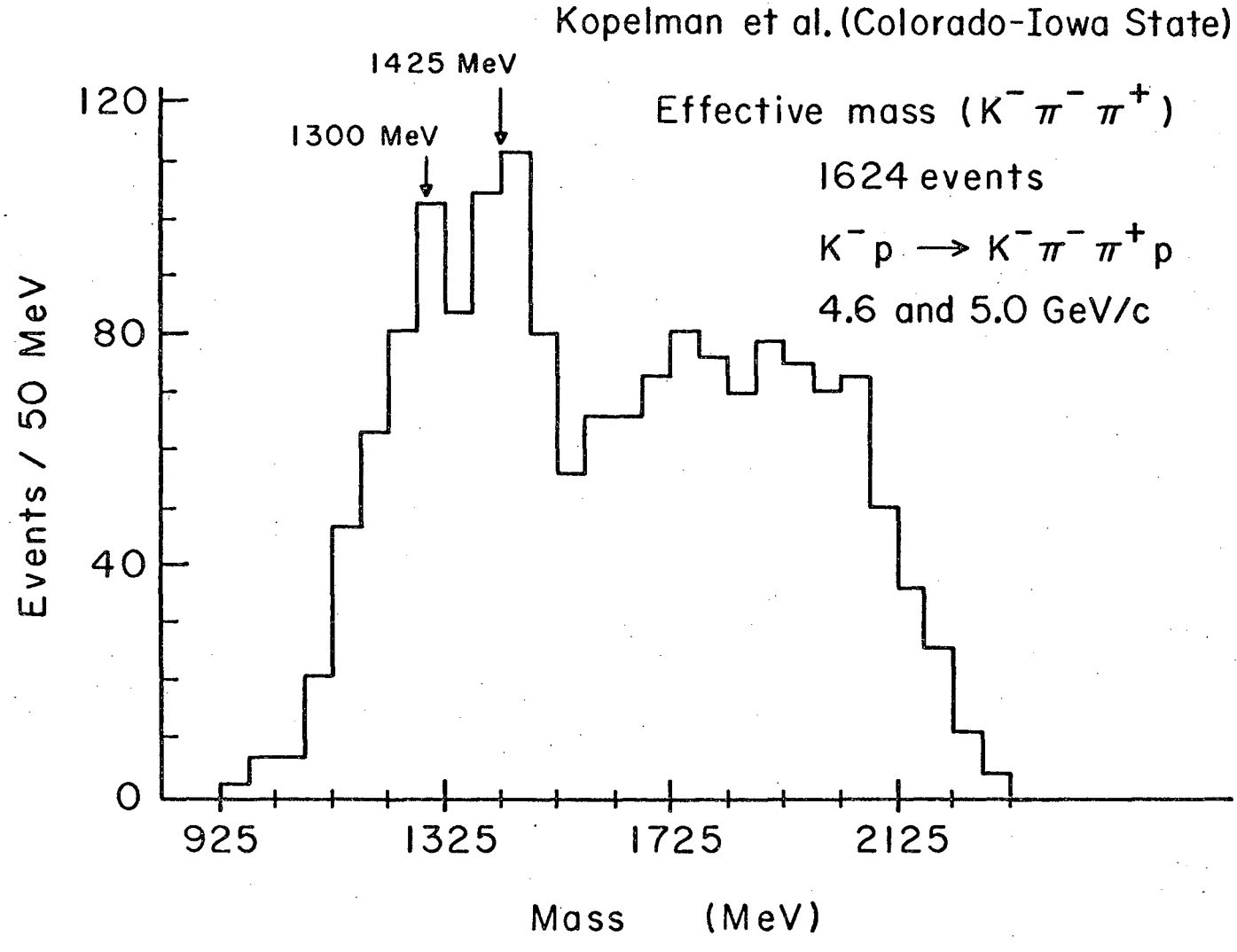

Fig. II-6 XBL677-3573

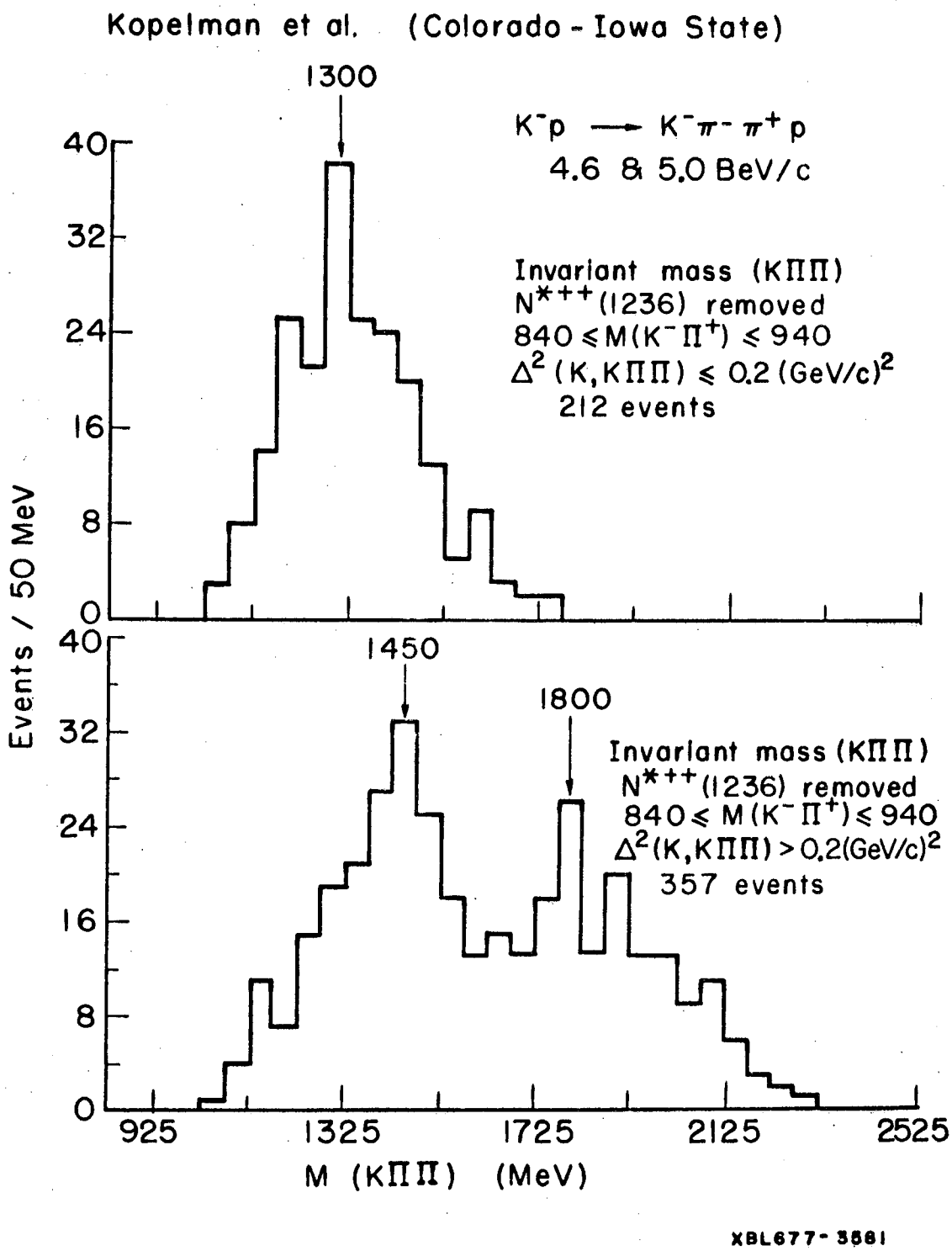
Kopelman et al. (Colorado - Iowa State)
1300
$K^-p \longrightarrow K^-\pi^-\pi^+p$
4.6 & 5.0 BeV/c
Invariant mass (KΠΠ)
$N^{*++}(1236)$ removed
$840 \leq M(K^-\Pi^+) \leq 940$
$\Delta^2(K, K\Pi\Pi) \leq 0.2\ (GeV/c)^2$
212 events
1450
1800
Invariant mass (KΠΠ)
$N^{*++}(1236)$ removed
$840 \leq M(K^-\Pi^+) \leq 940$
$\Delta^2(K, K\Pi\Pi) > 0.2(GeV/c)^2$
357 events
Events / 50 MeV
0
8
16
24
32
40
925
1325
1725
2125
2525
M (KΠΠ) (MeV)
XBL677-3581

Fig. II-7

Wangler et al. (Argonne-Northwestern-Illinois)

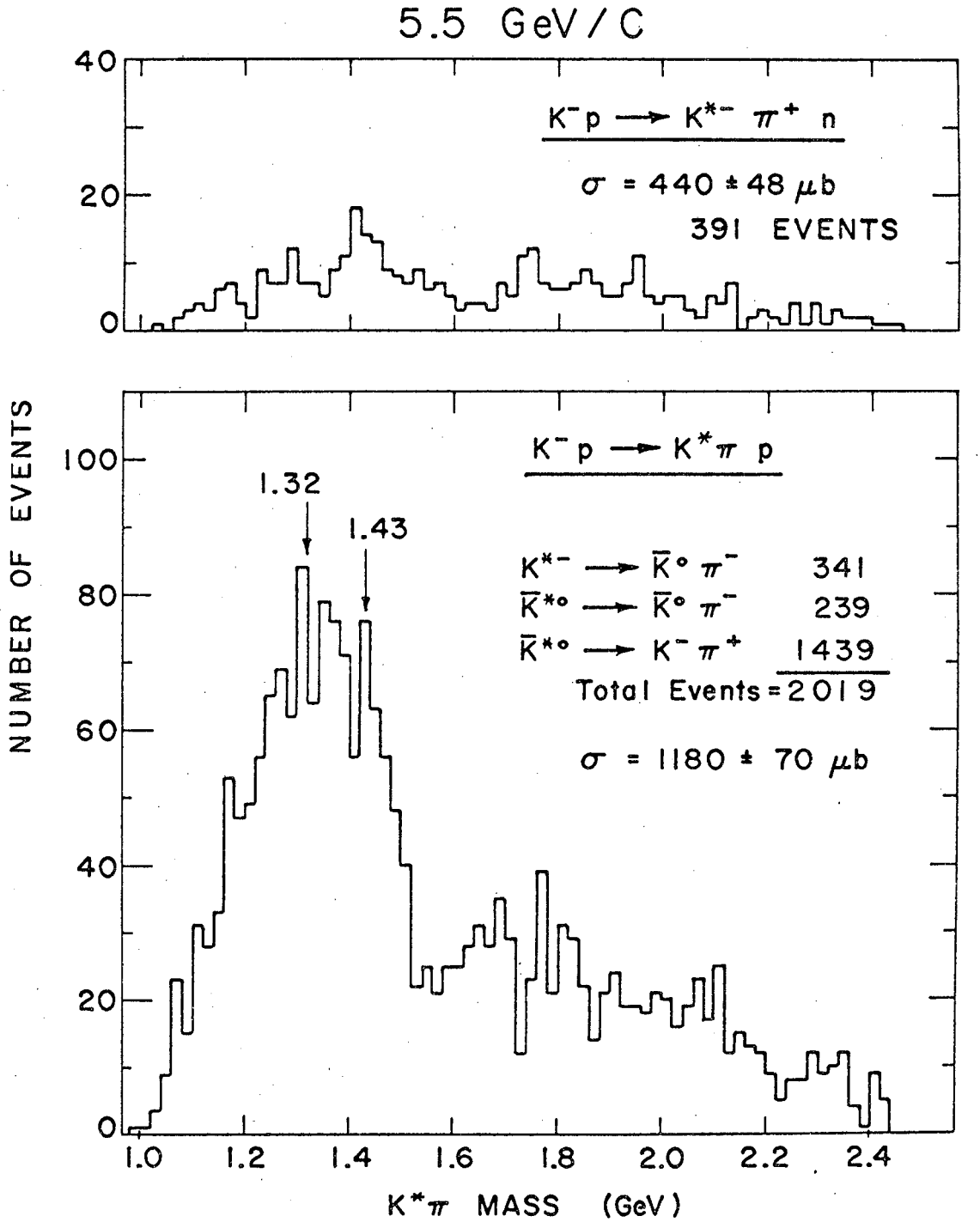

XBL678-3615

Fig. II-8

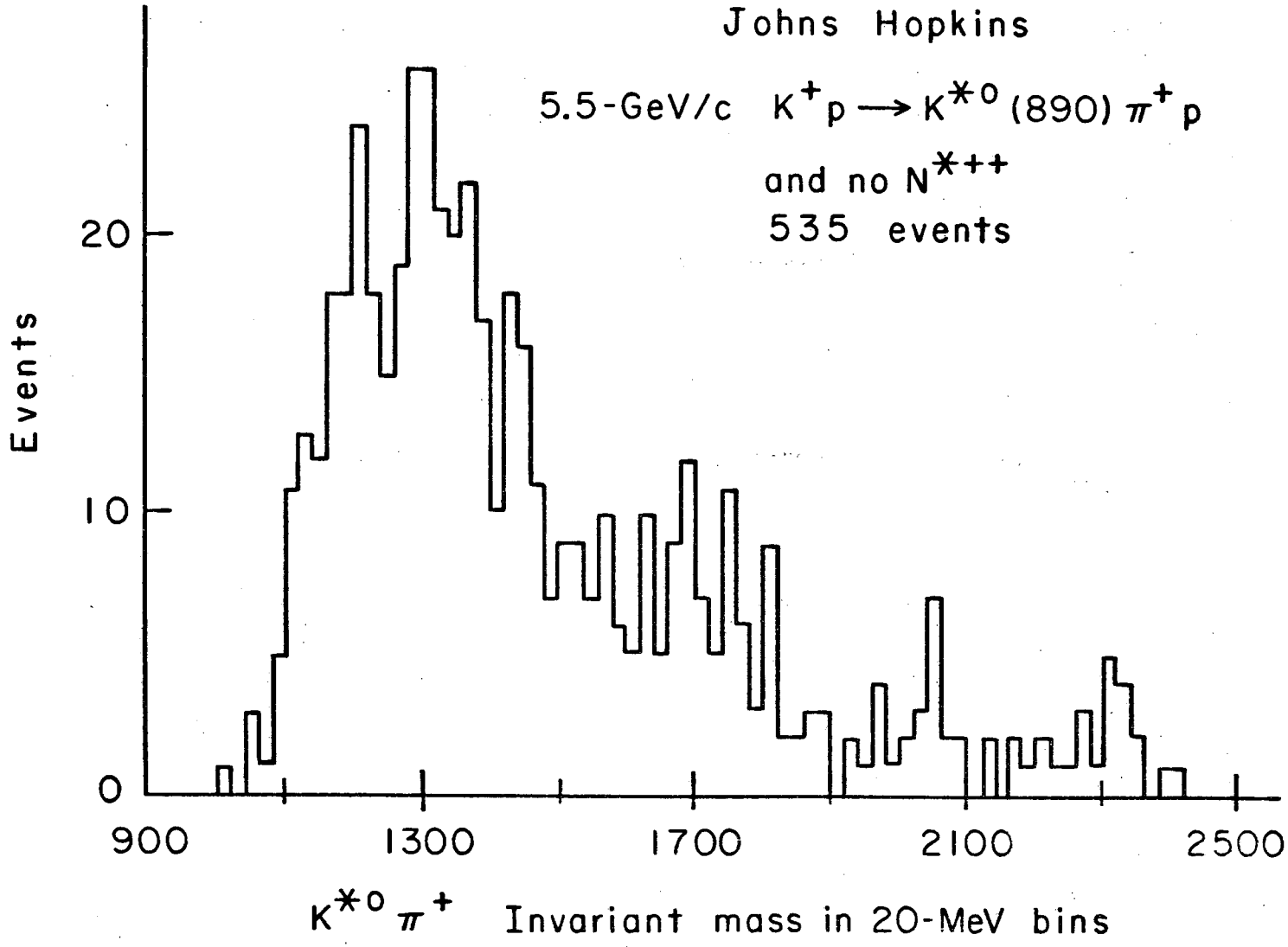

XBL677-3574

Fig. II-9

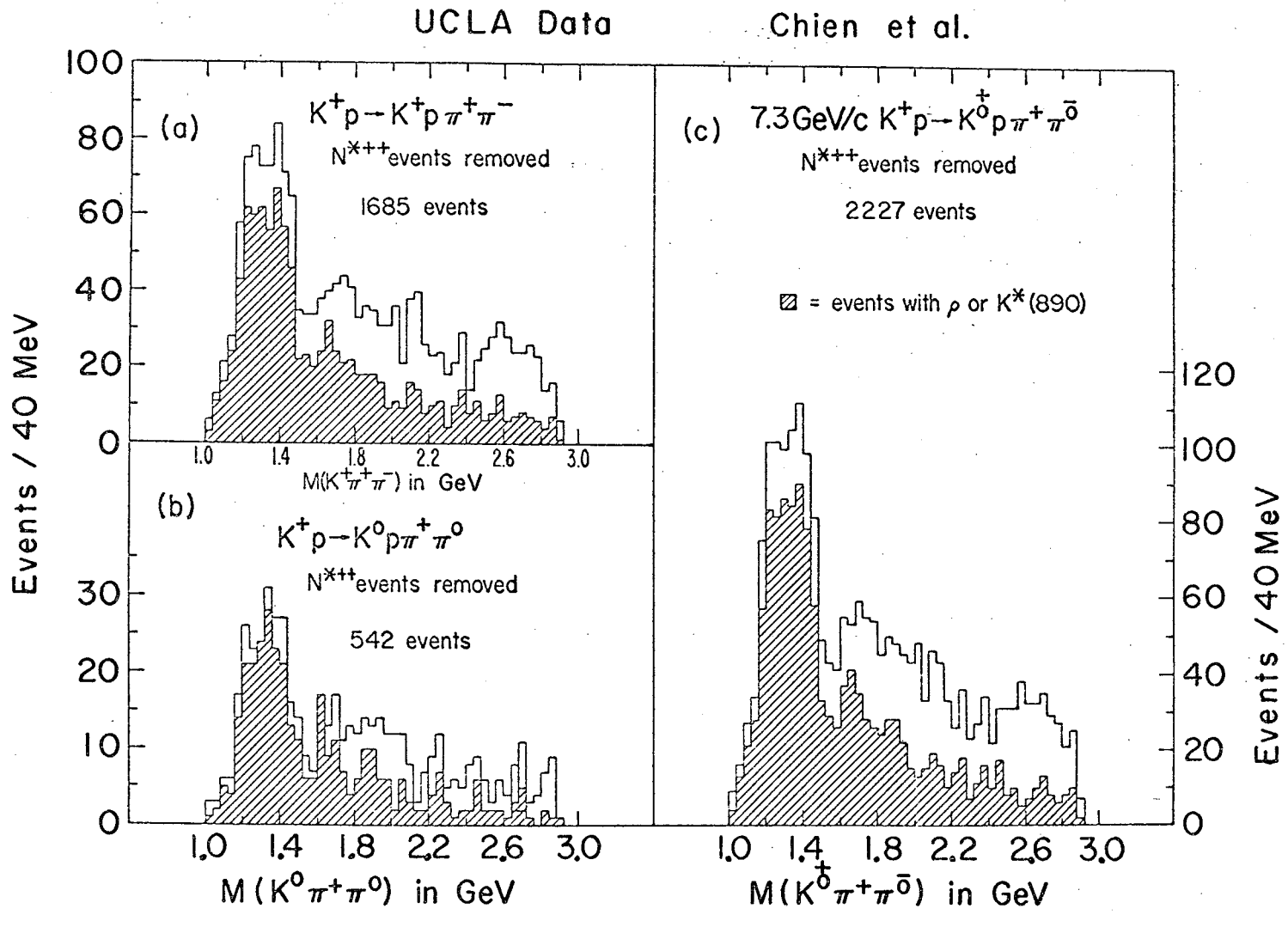
UCLA Data
Chien et al.
(a)
$K^+p \to K^+p\pi^+\pi^-$
N^{*++}events removed
1685 events
$M(K^+\pi^+\pi^-)$ in GeV
(b)
$K^+p \to K^0p\pi^+\pi^0$
N^{*++}events removed
542 events
$M(K^0\pi^+\pi^0)$ in GeV
(c)
7.3GeV/c $K^+p \to K^{\overline{0}}p\pi^+\pi^{\overline{0}}$
N^{*++}events removed
2227 events
▨ = events with ρ or $K^*(890)$
$M(K^{\overline{0}}\pi^+\pi^{\overline{0}})$ in GeV
Events / 40 MeV
Events / 40 MeV
XBL677-3582

Fig. II-10

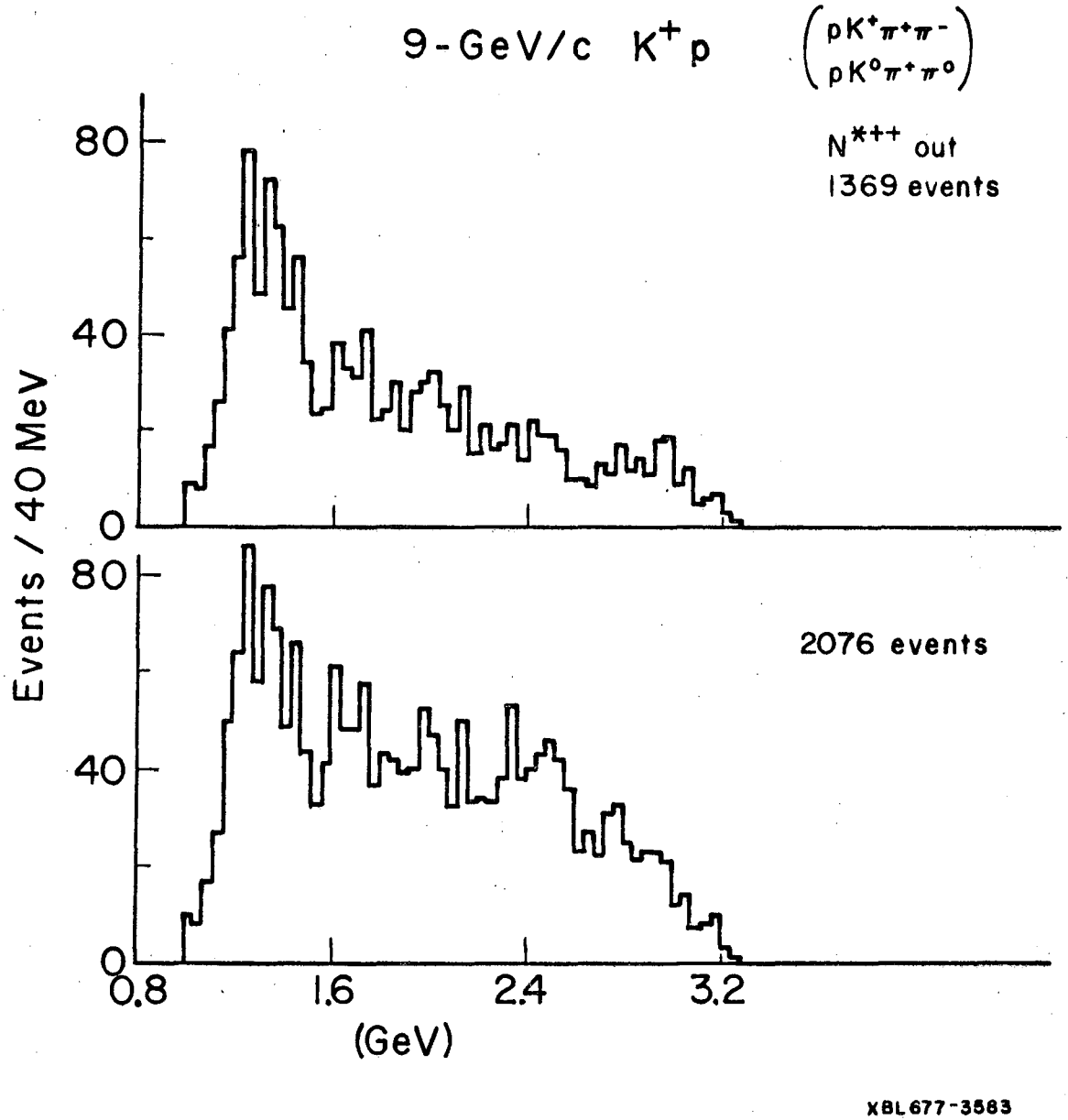
9-GeV/c K+p
(pK+π+π-
pK°π+π°)
N*++ out
1369 events
2076 events
Events / 40 MeV
80
40
0
0.8
1.6
2.4
3.2
(GeV)
XBL677-3583

Fig. II-11

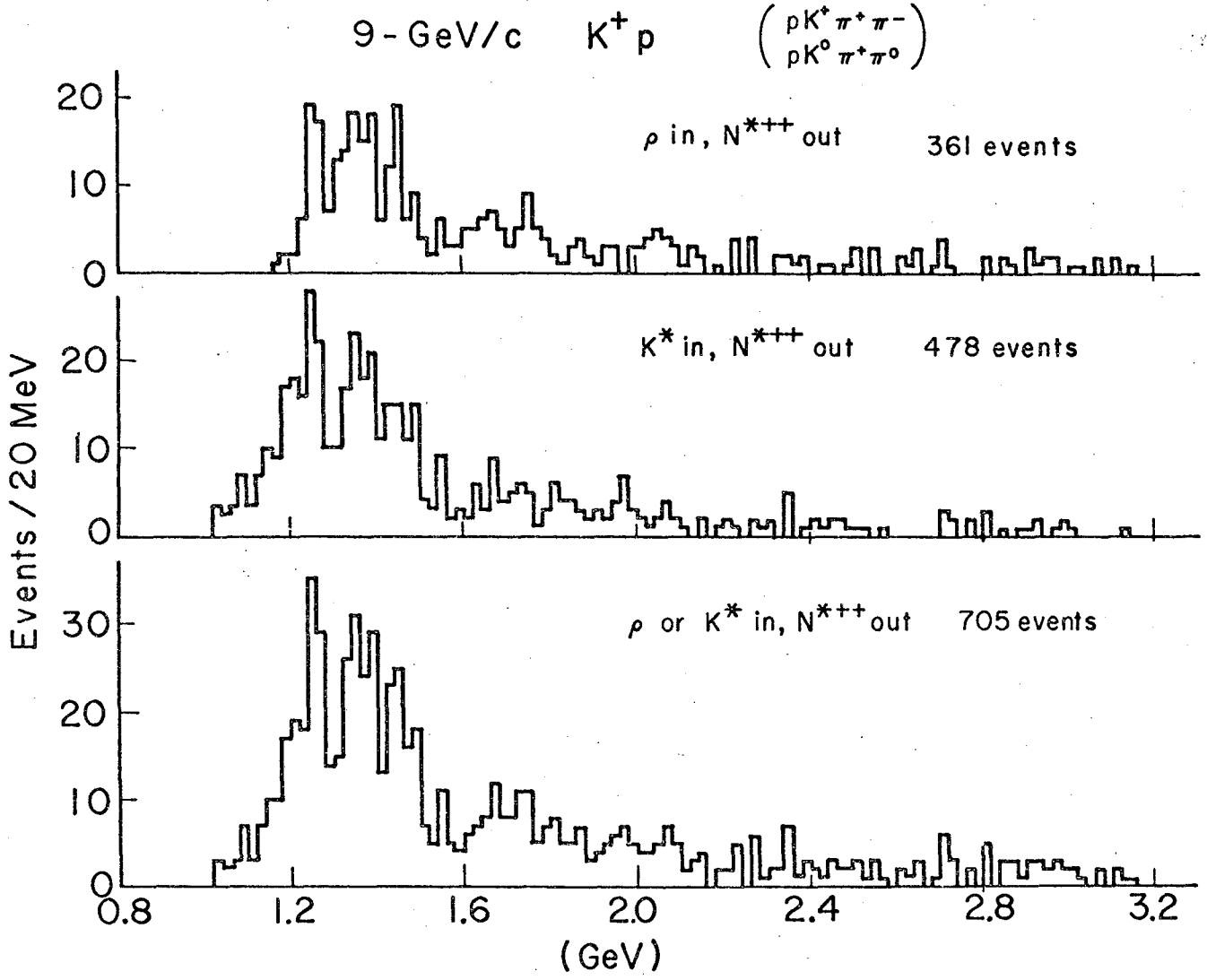

Fig. II-12

XBL677-3584

resolved.[11] (see Fig. II-13). These data also showed the first bubble chamber evidence for the L meson at 1790 MeV. This I will discuss later. The data also indicate clearly that only the 1420-MeV peak remains when p to n charge exchange occurs at the nucleon vertex. This same feature is stressed in the Argonne-Northwestern-Illinois data (see Fig. II-8), also by Dornan et al.[12]

vii) The highest momentum studied to date is represented by the K^-p data from Yale[13] and the K^+p data from Rochester,[14] both at 12.6 GeV/c. Here the K^-p data show a peak at 1250 MeV--possibly resolved from some effect at 1420 MeV--while the K^+p data show an unresolved peak at 1320 MeV (see Figs. II-14 and II-15).

2.3 THE REACTION $\pi^-p \to \Lambda (K\pi\pi)^0$

Very recently the group at Brookhaven[15] has observed a $K\pi\pi$ enhancement in a 6-GeV/c π^-p experiment. In this reaction one does not expect complications due to the Deck effect, as the baryon vertex involves a strangeness change. They observe two distinct peaks in the $K\pi\pi$ mass distribution at 1300 and 1440 MeV (see Fig. II-16).

3. VARIATIONS OF THE CROSS SECTION WITH MOMENTUM

The 1420-MeV peak is of course well known and has the feature that its cross section decreases with increasing momentum, as can be ascertained most readily from the $K\pi$ decay modes. In Fig. II-17 I give a compilation by Morrison[16] of this cross section, which indicates that $\sigma \doteq \text{const} \times (p_{in})^{-n}$ holds with $n = 2.2 \pm 0.2$. According to Morrison, the above relation, with various values for n, holds for all two-body or quasi-two-body process for incident laboratory-system momenta p_{in} sufficiently high above threshold. In particular for reactions corresponding to pomeron exchange, or what has alternatively been described as "diffraction dissociation," the cross sections remain essentially constant with p_{in}, i.e., $n \approx 0$. For Pomeron exchange to occur the incident particle and outgoing resonance must be "similar" in the sense that $\Delta Q = 0$, $\Delta I = 0$, $\Delta S = 0$, $\Delta G = 0$, and thus presumably $\Delta C = 0$ also. On the other hand, angular momentum ℓ together with the corresponding parity $P = (-1)^\ell$ can be transferred to the resonance.

Thus for 0^- incident particles (π or K) we get $J = \ell$ and $P = -(-1)^\ell$ as the allowed states. In other words the series of resonances $J^{PC} = 0^{-+}$,

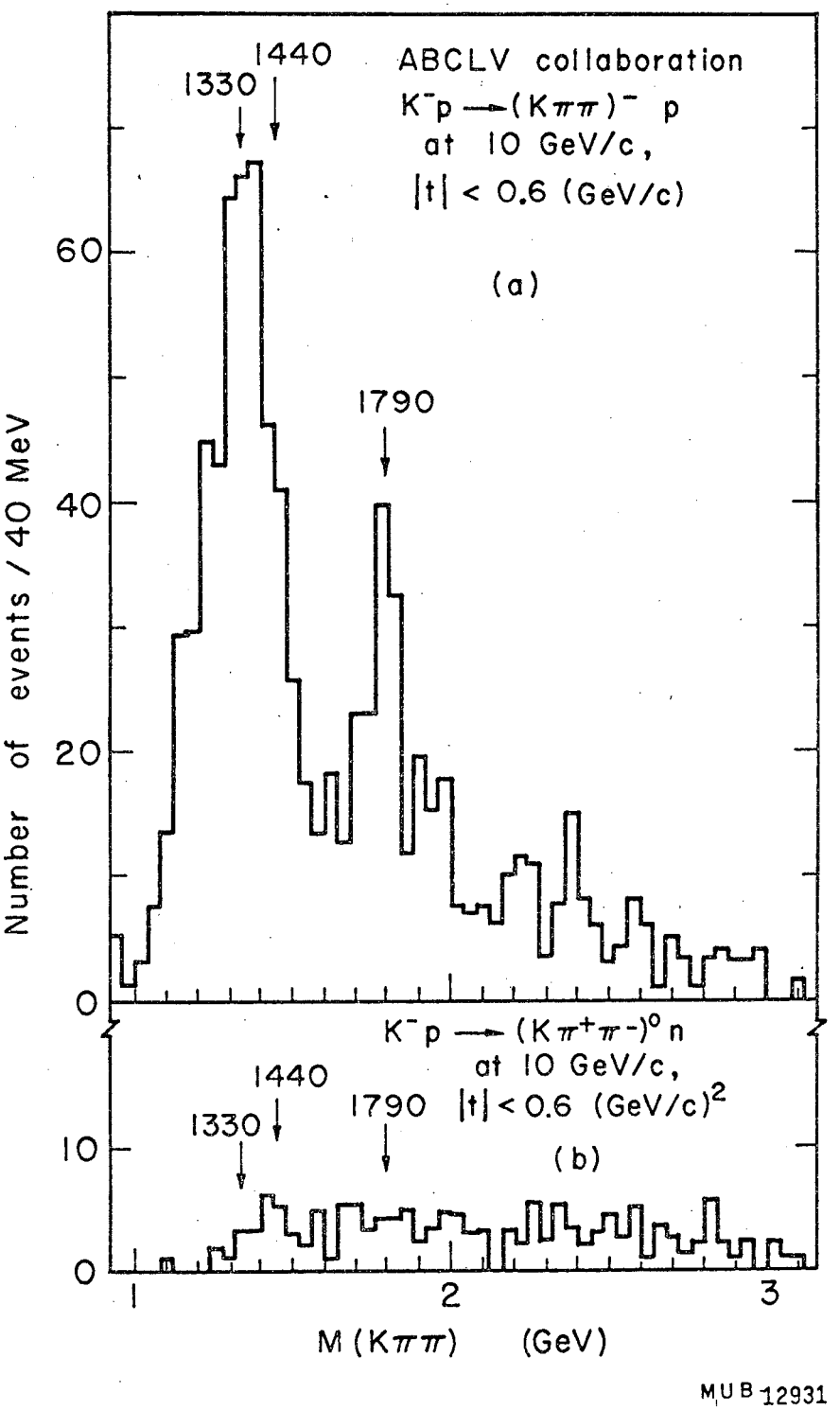
1330
1440
1790
ABCLV collaboration
K⁻p → (Kππ)⁻ p
at 10 GeV/c,
|t| < 0.6 (GeV/c)
(a)
Number of events / 40 MeV
60
40
20
0
K⁻p → (Kπ⁺π⁻)⁰ n
at 10 GeV/c,
|t| < 0.6 (GeV/c)²
(b)
10
0
1
2
3
M (Kππ) (GeV)
MUB 12931

Fig. II-13

LUDLAM ET AL. (YALE)

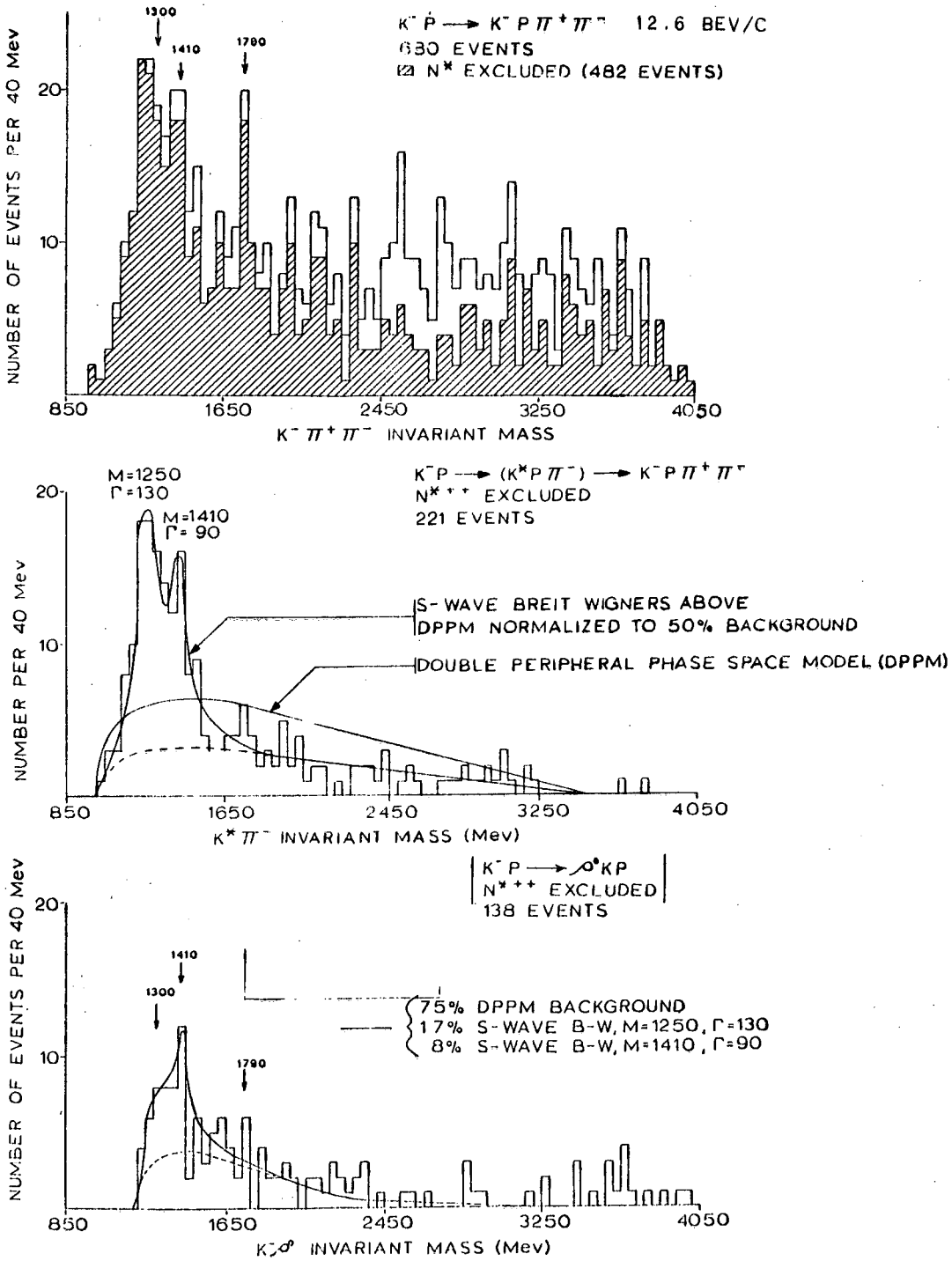

Fig. II-14

XBL678-3618

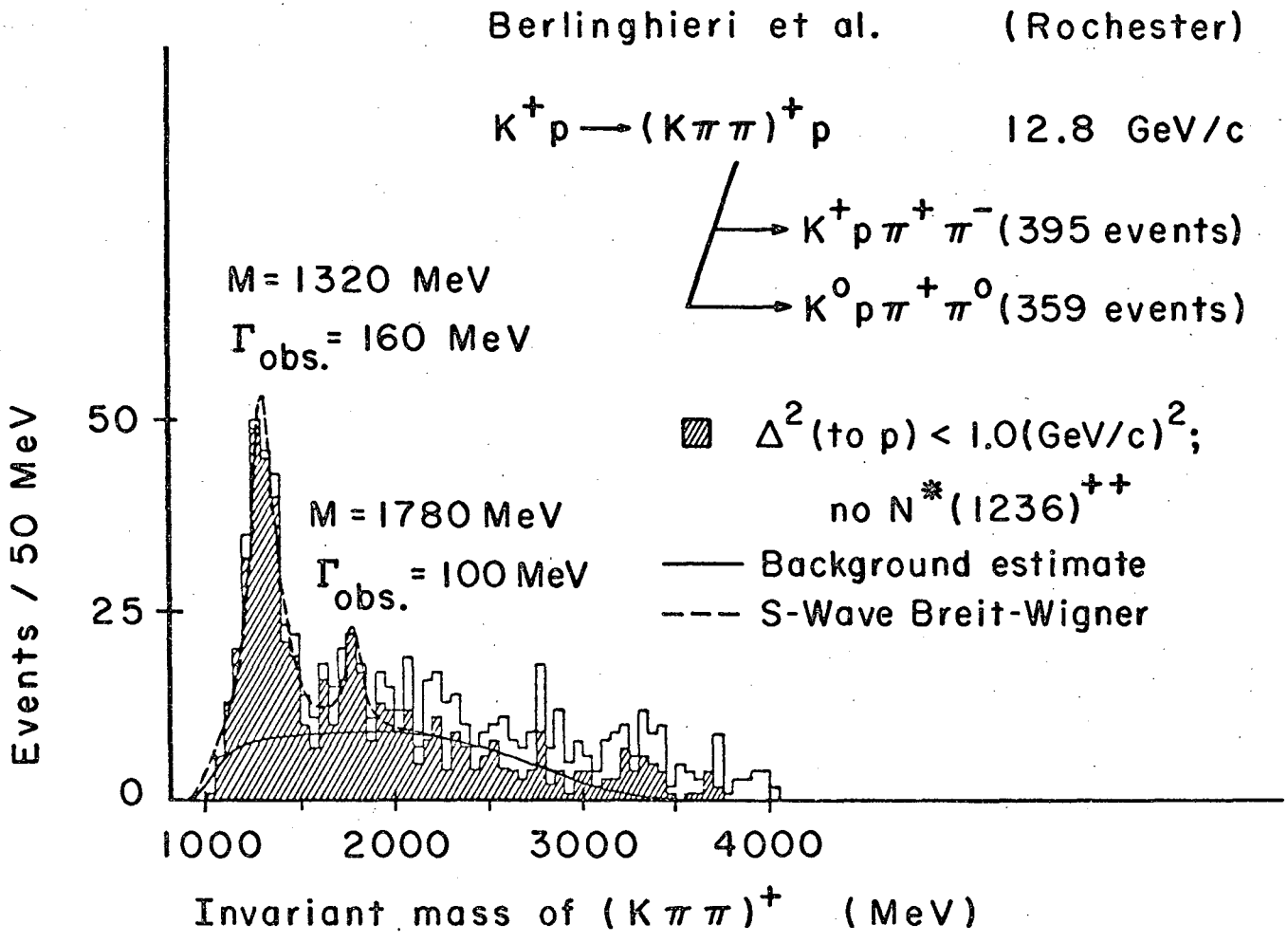

Fig. II-15

XBL677-3575

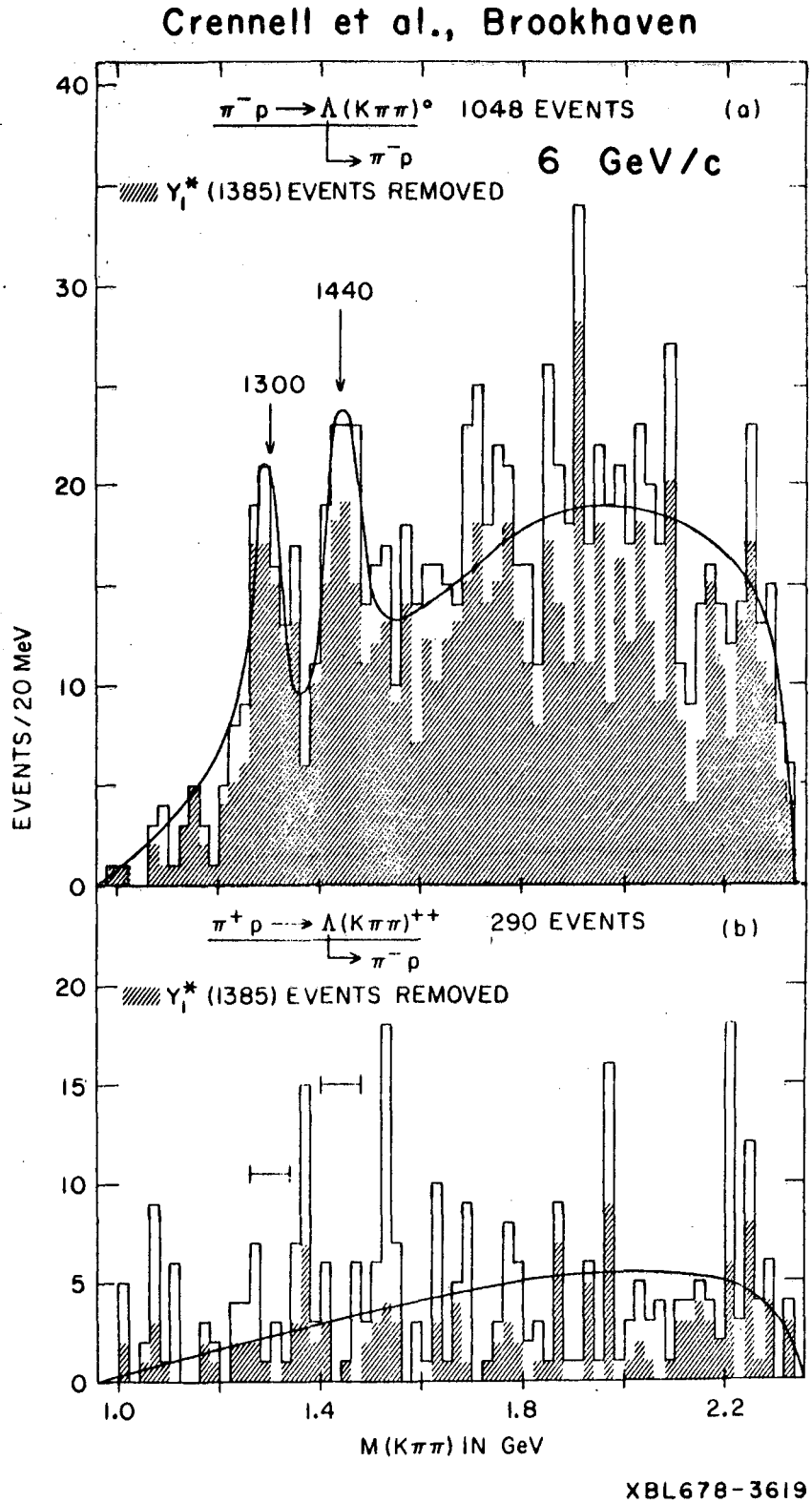
Crennell et al., Brookhaven
$\pi^- p \rightarrow \Lambda(K\pi\pi)^0$ 1048 EVENTS (a)
$\rightarrow \pi^- p$
6 GeV/c
Y_1^* (1385) EVENTS REMOVED
1440
1300
$\pi^+ p \rightarrow \Lambda(K\pi\pi)^{++}$ 290 EVENTS (b)
$\rightarrow \pi^- p$
Y_1^* (1385) EVENTS REMOVED
EVENTS / 20 MeV
M(Kππ) IN GeV
XBL678-3619

Fig. II-16

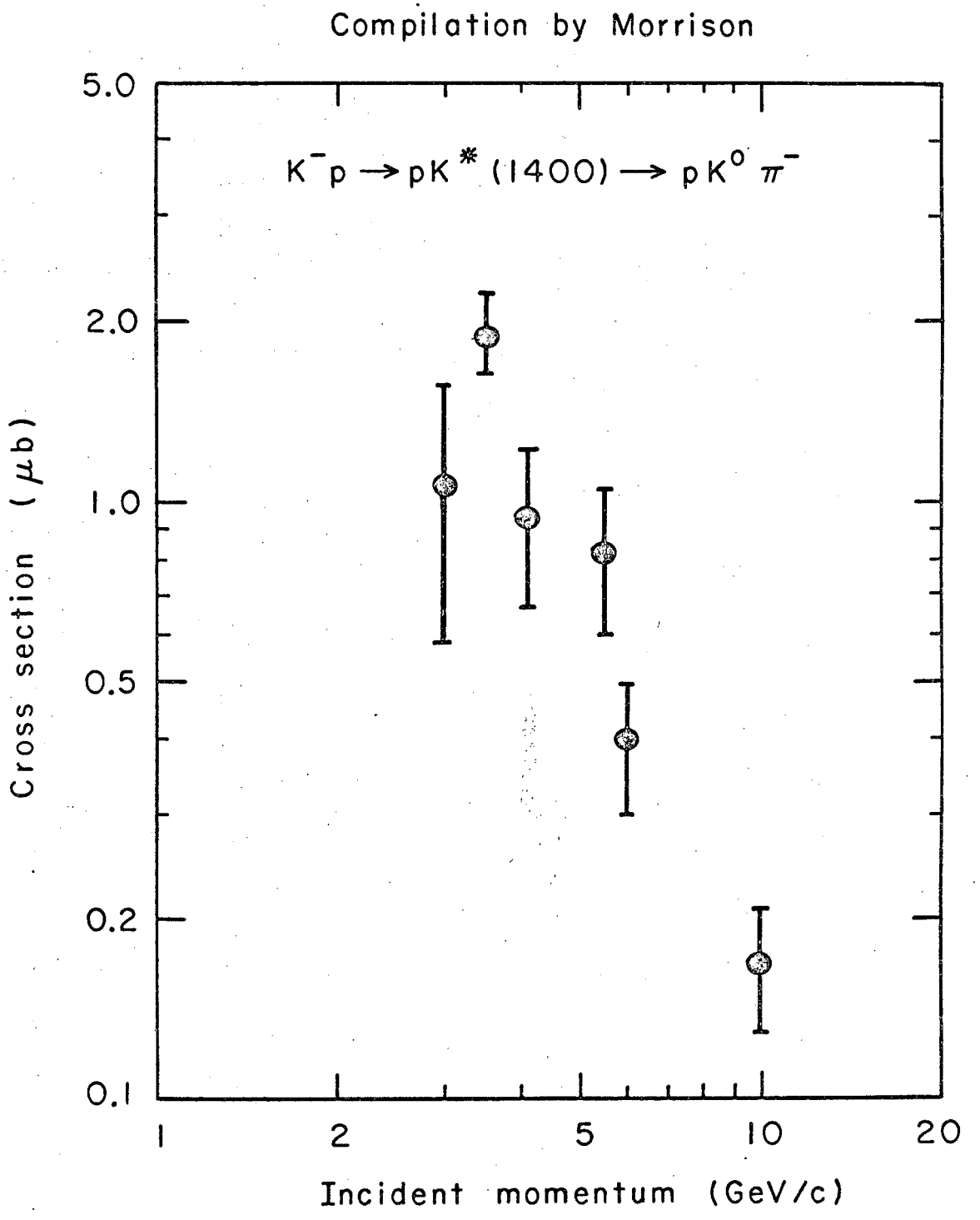
Compilation by Morrison
$K^- p \rightarrow p K^*(1400) \rightarrow p K^0 \pi^-$
Cross section (μb)
5.0
2.0
1.0
0.5
0.2
0.1
1
2
5
10
20
Incident momentum (GeV/c)
XBL677-3576

Fig. II-17

1^{++}, 2^{-+}, 3^{++}, etc. can be produced by pomeron exchange.

Here again as the meaning of C and G are well defined for the I=0 I = 1 resonances, we expect, for example, A_1 production ($J^{PC} = 1^{++}$) to occur with nearly constant cross section for reactions such as $\pi^{\pm} p \rightarrow A_1^{\pm} p$, while the cross sections for B production ($J^{PC} = 1^{+-}$) in a similar reaction should decrease with increasing momentum. There remains the interesting question: How will the two 1^+ K^*'s behave? We might expect that the cross section of the $J^{PC} = 1^{++}$--i.e., $^3P_1$ resonance-- will stay constant, while the $J^{PC} = 1^{+-}$-- i.e., $^1P_1$ resonance-- will decrease in cross section with incident momentum. In principle this gives us a means of distinguishing between them. However, all indications are that the cross section of the entire 1250- and 1320-MeV composite peaks (if this is the correct interpretation of the peak) changes very little with incident momentum. This may mean either that the two physical particles are mixtures of the two states or that the $\Delta C = 0$ selection rule is not applicable to K^* resonances. The question, therefore, is now: Can all these different experimental results be reconciled?

It appears to me that if we are indeed dealing with two 1^+ K^*'s the apparent discrepancy between various sets of data can be understood. Namely two 1^+ K^*, both of which are decaying into the $K\pi\pi$ decay mode, will give rise to interference effects in the mass distribution. Here we must remember that, in general, if we consider a mass distribution it corresponds to averaging over all angular distributions. Thus two adjacent resonances with different J^P values will just add incoherently. This is not the case for two resonances with the <u>same</u> J^P values, however. For these the amplitudes add coeherently. If one assumes an arbitrary phase angle ϕ between the two amplitudes, which can, for instance, be a function of the incident momentum, then we can get momentum-dependent interference effects. Such effects could perhaps account for the differences between the various experimental data. Thus it is tempting to ascribe all the data discussed primarily to three resonances--namely, two 1^+ resonances at nominal mass values of 1250 and 1320 MeV, which interfere with each other and possibly also with a general "diffraction dissociation" type of background, and a 2^+ resonance, the $K^*(1420)$. Here the "1250 MeV" peak is probably the same effect as the C_0 meson.

I should emphasize here that the suggested interpretation given to the experimental data does not necessarily reflect the opinion of the various authors whose data are quoted. In fact a number of authors are attempting to identify the general $K\pi\pi$ enhancement purely with kinematic effects of one sort or another. In particular, in recent work, the Brookhaven-Syracuse Group[17] is emphasizing this point of view. A detailed discussion of the arguments for and against the kinematic enhancement effect has been given by the author and Sulamith Goldhaber.[18]

REFERENCES, SECTION II

1) R. Armenteros, D. N. Edwards, T. Jacobsen, L. Montanet, J. Vandermeulen, C. d'Andlau, A. Astier, P. Baillon, J. Cohen-Ganouna, C. Defoix, J. Siaud, and P. Rivet, 1964 International Conference on High Energy Physics, Dubna (1964).

2) N. Barash, The Annihilation of Stopping Antiproton into K Mesons (thesis), Columbia University Report CU-1932-261 Nevis 157, 1967.

3) Jerome H. Friedman and Ronald R. Ross, Bull. Amer. Phys. Soc. II 12, 539 (1967).

4) B. Shen, I. Butterworth, C. Fu, G. Goldhaber, S. Goldhaber, and G. Trilling, Phys. Rev. Letters 17, 726 (1966).

5) Y. Goldschmidt-Clermont, R. Jongejans, and V. Henri (CERN), private communication.

6) E. M. Urvater, J. B. Kopelman, L. Marshall-Libby, R. E. Juhalla, and J. I. Rhode, Bull. Amer. Phys. Soc. II 12, 540 (1967).

7) T. P. Wangler, M. Derrick, L. G. Hyman, J. G. Loken, F. Schweingruber, R. G. Ammar, R. E. P. Davis, W. Kropac, J. Mott, and J. Park, Bull. Amer. Phys. Soc. 12, 540 (1967).

8) Richard Zdanis, Bull. Amer. Phys. Soc. II 12, 567 (1967), and A. Pevsner (Johns Hopkins University), private communication.

9) T. G. Trippe, C. Y. Chien, E. I. Malamud, P. E. Schlein, W. E. Slater, D. H. Stork, and H. K. Ticho, Bull. Amer. Phys. Soc. II 12, 506 (1967).

10) A. Firestone, R. W. Bland, G. Goldhaber, J. A. Kadyk, B. C. Shen, and G. H. Trilling, Bull. Amer. Phys. Soc. II 12, 539 (1967).

11) J. Bartsch et al., Phys. Letters 22, 357)1966).

12) P. J. Dornan et al. (Brookhaven-Syracuse), Bull. Amer. Phys. Soc. 11, 342 (1966).

13) T. Ludlam, J. Kim, J. Lach, J. Sandweiss, and H. Taft, Bull. Amer. Phys. Soc. II 12, 540 (1967).

14) M. S. Farber, J. Berlinghieri, T. Ferbel, B. Forman, A. C. Melissinos, T. Yamanouchi, and H. Yuta, Bull. Amer. Phys. Soc. II 12, 540 (1967).

15) David J. Crennell, George R. Kalbfleisch, Kwan Wu Lai, J. Michael Scarr, and Thomas G. Schumann, Phys. Rev. Letters 19, 44 (1967).

16) D. R. O. Morrison, The Possible Existence of a $(\pi\rho)$ Resonance Near 1300 MeV with Spin-Parity Assignment of 2^- or 1^+ (CERN preprint D. Ph. II/PHYSICS 67-15), submitted to Phys. Letters.

17) P. J. Dornan, V. E. Barnes, G. R. Kalbfleisch, I. O. Skillicorn, M. Goldberg, B. Goz, R. Wolf and J. Leitner, Phys. Rev. Letters 19, 271 (1967).

18) G. Goldhaber and S. Goldhaber, "The A_1 and $K^{**}(1320)$ Phenomena, Kinematic Enhancement or Mesons?" in Proceedings of the 4th Anniversary Symposium at the Institute of Mathematical Sciences, Madras, India, on January 3-11, 1966 (UCRL-16744, March 1966), to be published.

Lecture III. BOSON L CLUSTERS

The evidence that baryons lie on Regge trajectories is very good at present. That the same is true for bosons is still not yet fully established. However, the data from the missing-mass-spectrometer work at CERN,[1] as well as from other experiments,[2] suggests that bosons may also lie on Regge trajectories.

It is particularly attractive to consider this phenomenon by looking at the bosons as $q\bar{q}$ structures. To reproduce the Regge behavior we introduce orbital angular momentum L in the $q\bar{q}$ system. This combines with the total quark spin S to give the total angular momentum J for the state. We need not take the quarks literally--as real particles; rather we can for the moment consider them as the basis for the simplest model that gives results in agreement with the experimental data.

I intend in this lecture to explore the experimental consequences of this model in some detail. This will give us a basis to decide to what extent the experimental facts are in agreement (or disagreement) with the model.*

1. SOME OF THE EXPERIMENTAL EVIDENCE

1.1 The CERN missing-mass-spectrometer experiment

A critical discussion of this experiment has been presented recently[3] and therefore I will be very brief. What is relevant here is that the experiment gives evidence for a series of "Major" peaks, ρ, A_2, $R(R_1 R_2 R_3)$, S, T, and U, which lie on a straight line when the order number is plotted against M^2 (see Figs. III-1 and III-2 and Table III-1. If the order number is interpreted as J, the spin of the boson, the line coincides in slope and intercept with the ρ trajectory of Regge theory. It is this feature, together with the known spin of the ρ ($J^P = 1^-$) and

---

*) Various ideas on the classification of higher boson resonances have been recently discussed by Sutherland and also by Cline, reporting on work by Barger. These differ from my discussion here mainly in that attempts have been made to predict definite mass values of the bosons in the various L clusters. My point of view has been that we will be lucky to identify the clusters first-the fine structure will come later. See D. G. Sutherland, Some Remarks on Higher Mesons, CERN TH-768 (unpublished); D. Cline, Classification of Baryons and Mesons on Regge Trajectories, appearing in Argonne Symposium on Regge Poles, 1966 (unpublished).

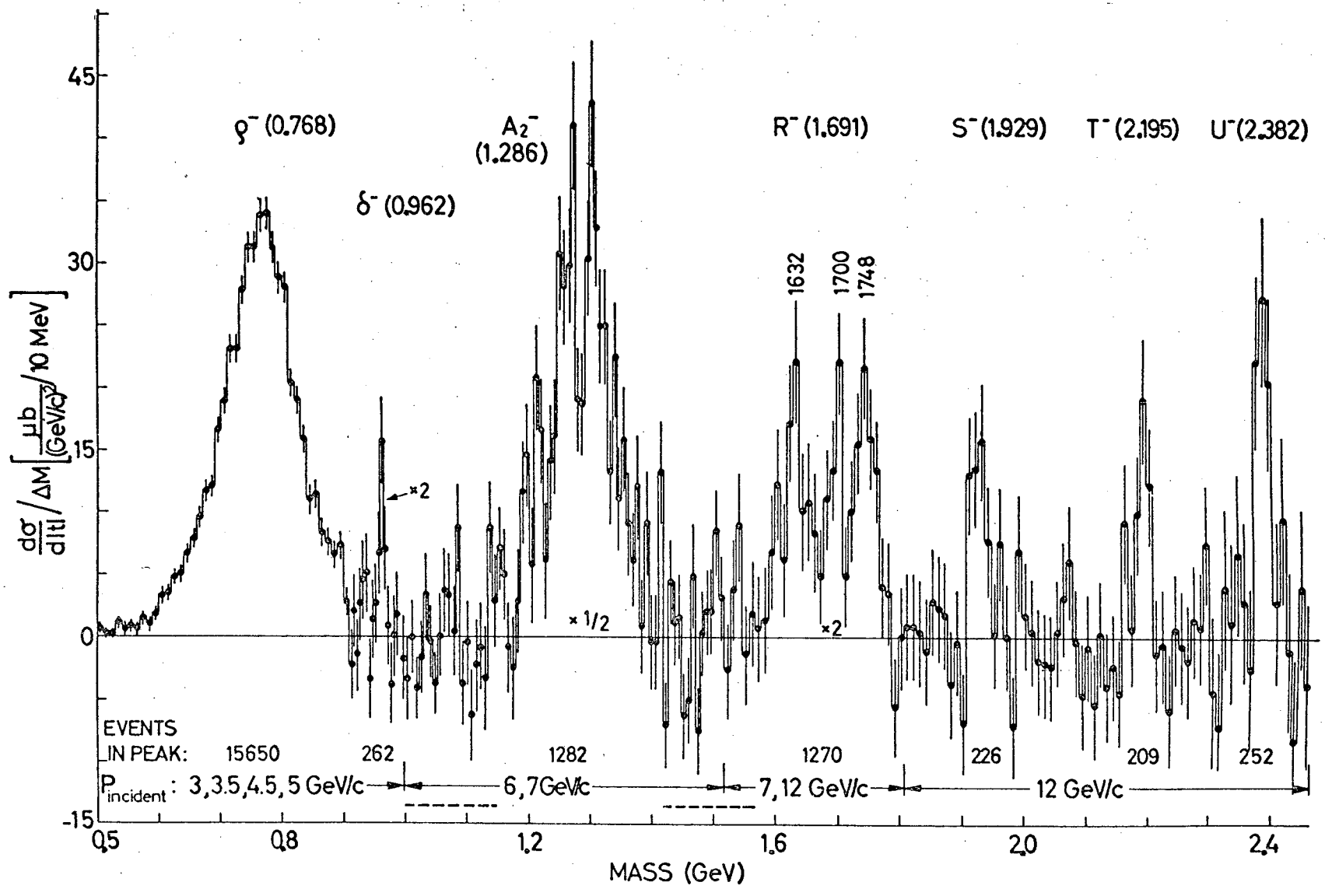

Fig. III-1

MUB-13748

Boson mass spectrum from the missing-mass spectrometer at CERN.

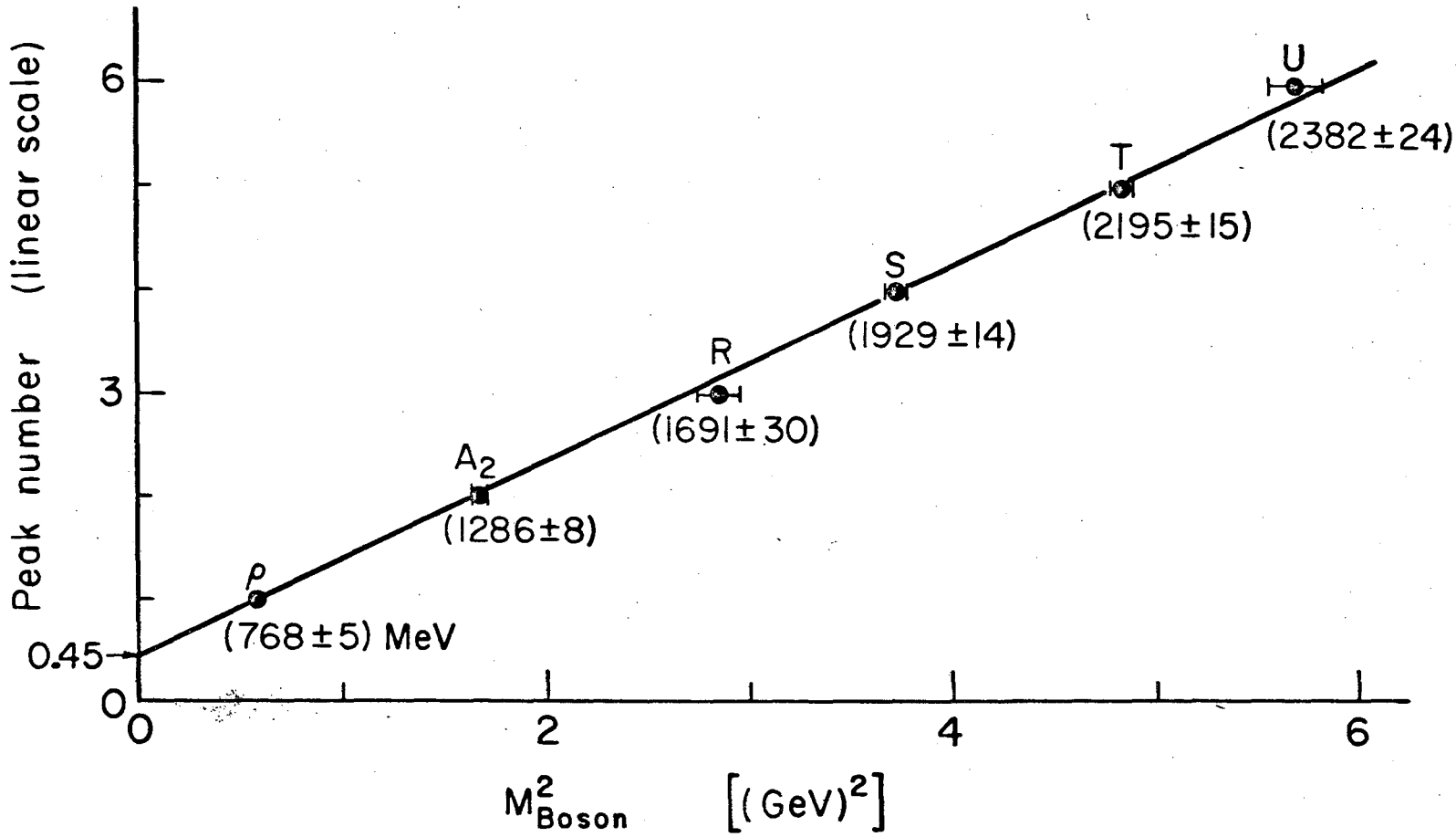

Fig. III-2 MUB-13206

The data of Focacci et al. in a plot of the major peak number versus the mass squared.

Table III-1

Measurements on bosons with the CERN missing mass spectrometer.

Column headings:

a. particle name,

b. central mass value, in MeV,

c. experimental resolution (which changes with mass region studied),

d. physical width of resonance deduced from the observations,

e. incident π^- momentum, p_1,

f. statistical significance, stated either as number of standard deviations or probability for the particular interpretation (such as the splitting or not splitting of the A_2 which is listed as equally probable),

g. number of events in peak above background and the statistical error on this number,

h. the signal-to-background ratio,

i. the intervals in momentum transfer squared, t, over which the phenomenon was studied,

j. $\frac{d\sigma}{dt}$,

k. the decay mode, expressed as the ratio between the different numbers of charged particles observed, namely 1C (single charged particle), 3C (three charged particles), and >3C (more than three charged particles).

Table III-1

Measurements on bosons with the CERN missing mass spectrometer

a	b	c	d	e	f	g	h	i	j	k
particle name	central mass value (in MeV)	expt. resolution	physical width Γ (deduced)	incident π⁻ momentum, P_1	statistical significance (st. dev.)	events in peak above background and statistical error	signal-to-background ratio	t limits	dσ/dt	decay mode
ρ^-	768 ± 5	28 ± 5	127 ± 5	3.0 3.5 4.5 5.0		15600 ± 170	1.6:1	0.10 - 0.14 0.14 - 0.17 0.17 - 0.22 0.22 - 0.26	770 ± 150[x] 770 ± 170 580 ± 100 370 ± 110	1c > 97.4%
δ^-	962.5 ± 5	24 ± 4	≤5	3.0 3.5 4.5 5.0	5.0	262 ± 52	1:5	0.11 < t < 0.21	8.9 ± 3[y]	$\frac{1c}{\geq 3c} = 1.3^{+0.9}_{-0.7}$
A_2	1286 ± 8	36 ± 4	98 ± 5	6.0 7.0	17	1282 ± 63	1:1.5	0.31 < t < 0.39	400 ± 120	$\frac{1c}{3c} = 1.05 \pm 0.1$
A_2' A_2''	1260 ± 10 1312 ± 10			6.0 7.0	1 peak and 2 peaks equally probable: P = 5% to 10%	$\frac{A_2'}{A_2''} \approx 1:1$	1:6			$\frac{1c}{3c} \approx 1$
R	1691 ± 15	31 ± 3	116 ± 3	7.0 12.0	11.6 1 peak: P = 1% 2 peak: P = 1% 3 peak: P = 20 to 60% ($R_{1,2,3}$)	973 ± 84	1:6	0.23 < t < 0.28	125 ± 30	1c = 0.30 ± 0.06[z] 3c = 0.67 ± 0.10 >3c = 0.03 ± 0.03
R_1	1632 ± 15	34 ± 3	<21		6.7	360 ± 70	1:4.7		35 ± 10	1c = 0.37 ± 0.13 3c = 0.59 ± 0.21 >3c = 0.04 ± 0.04
R_2	1700 ± 15	30 ± 3	<30	7.0 12.0	6.1	485 ± 73	1:3.3		43	1c = 0.42 ± 0.11 3c = 0.56 ± 0.14 >3c = 0.01 ± 0.01
R_3	1748 ± 15	28 ± 3	<38		7.3	425 ± 74	1:3.5		47	1c = 0.14 ± 0.08 3c = 0.80 ± 0.18 >3c = 0.05 ± 0.05
S	1929 ± 14	22 ± 2	≤35	12.0	5.5	226 ± 41	1:7	0.22 < t < 0.36	35 ± 12	$1c = 0.06^{+0.15}_{-0.06}$ $3c = 0.92^{+0.08}_{-0.20}$ $>3c = 0.02^{+0.13}_{-0.02}$
T	2195 ± 15	39 ± 4	≤13	12.0	5.1	209 ± 41	1:7	0.22 < t < 0.36	29 ± 10	$1c = 0.04^{+0.11}_{-0.04}$ $3c = 0.94^{+0.06}_{-0.19}$ $>3c = 0.02^{+0.13}_{-0.02}$
U	2382 ± 24	62 ± 6	≤30	12.0	5.9	252 ± 43	1:6	0.28 < t < 0.36	42 ± 14	1c = 0.30 ± 0.10 3c = 0.45 ± 0.15 >3c = 0.25 ± 0.10

x. dσ/dt normalized to 4 GeV/c (average momentum).
y. dσ/dt weighted between p_1 = 3, 3.5, and 4.5 GeV/c.
z. errors are one standard deviation.

$A_2(J^P = 2^+)$ and a probable assignment[4] of J = 3 for the charged g meson (presumably the same as one of the R mesons) which at the moment is the basis for the conjecture on J. Thus, strictly from an experimental point of view, the evidence for the Regge interpretation is still very flimsy indeed. On the other hand, the idea implied by such a model is very appealing.

1.2 The Brookhaven precision total $\bar{p}p$ and $\bar{p}d$ cross section measurements

The $\bar{p}p$ and $\bar{p}n$ systems have baryon number zero and hence can have all the quantum numbers of the nonstrange boson states of mass >2Mp. As part of a series of precision total cross section measurements, Abrams, Cool, Giacomelli, Kycia, Leontić, Li, and Michael[2] have measured the $\bar{p}p$ and $\bar{p}d$ cross sections for momenta from 1.0 to 3.4 GeV/c. The remarkable feature of these measurements is that despite the very large cross sections (75 to 120 mb for $\bar{p}p$ and 130 to 210 mb for $\bar{p}d$), they note distinct peaks of the order of a few mb. See Figs. III-3 to III-6. One straightforward interpretation of the data is that the peaks represent higher bosons. In particular it is noteworthy that the peaks are consistent in mass--but not width-with the T and U mesons of Foccaci, Kienzle, Maglić, et al.[1] One difficulty which is not yet resolved is that the lower peak also corresponds in mass to the threshold of the reaction,

$$\bar{p}p \rightarrow \bar{N}^* N \text{ or } N^* \bar{N}, \qquad M = 2180 \text{ MeV}.$$

Because of the large cross section for N^* production this reaction could in principle give rise to a peak in the total cross section which does not necessarily correspond to a boson resonance, i.e., a t-channel rather than an s-channel effect. If this is so the situation is analogous to the peak of Cool et al.[5] in the K^+p system at 1910 MeV, which has been interpreted on the basis of nonresonant KN^* production.[6] We can compare these data with precision total cross section measurement on the pp system by Bugg et al.[7]. In that experiment prominent structures generally ascribed to the production of various N^*'s in the t channel have been observed. However, the structures occur at somewhat different masses than in the $\bar{p}p$ system (see Fig. III-7). Interpretation of the peaks in the $\bar{p}p$ system is thus not possible without more detailed studies of the reaction products.

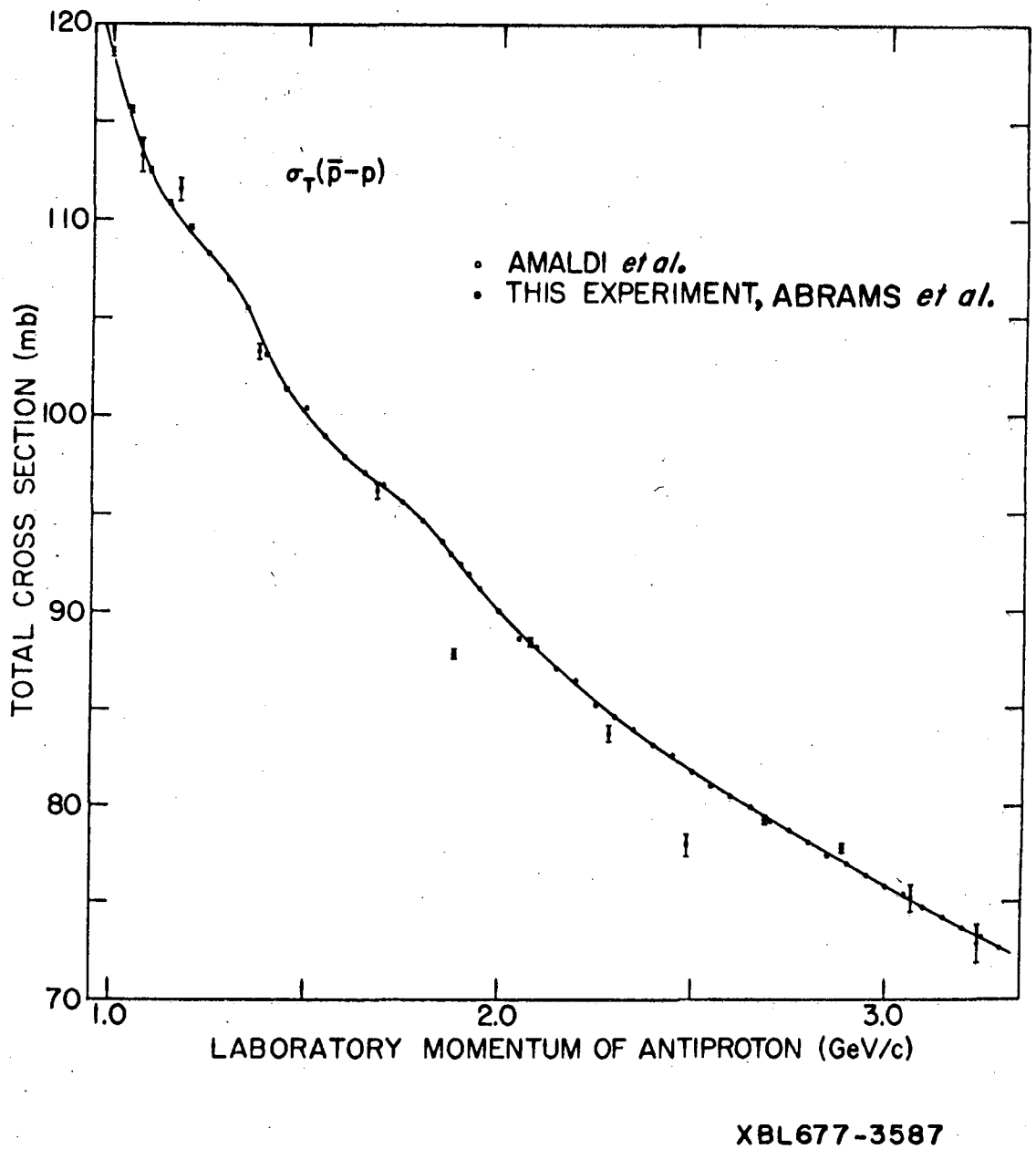
120
110
100
90
80
70
$\sigma_T(\bar{p}-p)$
AMALDI *et al.*
THIS EXPERIMENT, ABRAMS *et al.*
TOTAL CROSS SECTION (mb)
1.0
2.0
3.0
LABORATORY MOMENTUM OF ANTIPROTON (GeV/c)
XBL677-3587

Fig. III-3

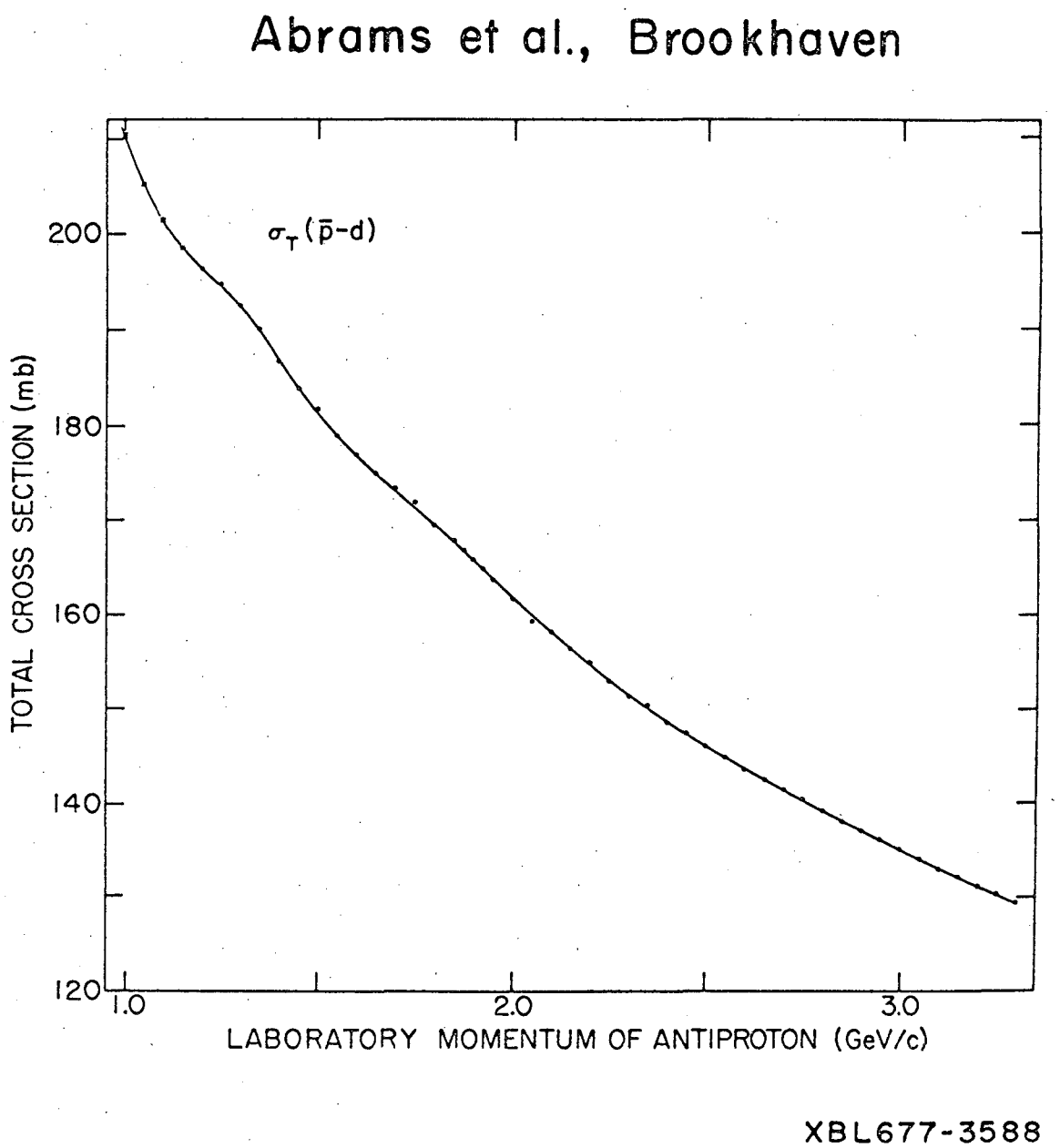
Abrams et al., Brookhaven
$\sigma_T(\bar{p}\text{-}d)$
TOTAL CROSS SECTION (mb)
200
180
160
140
120
1.0
2.0
3.0
LABORATORY MOMENTUM OF ANTIPROTON (GeV/c)
XBL677-3588

Fig. III-4

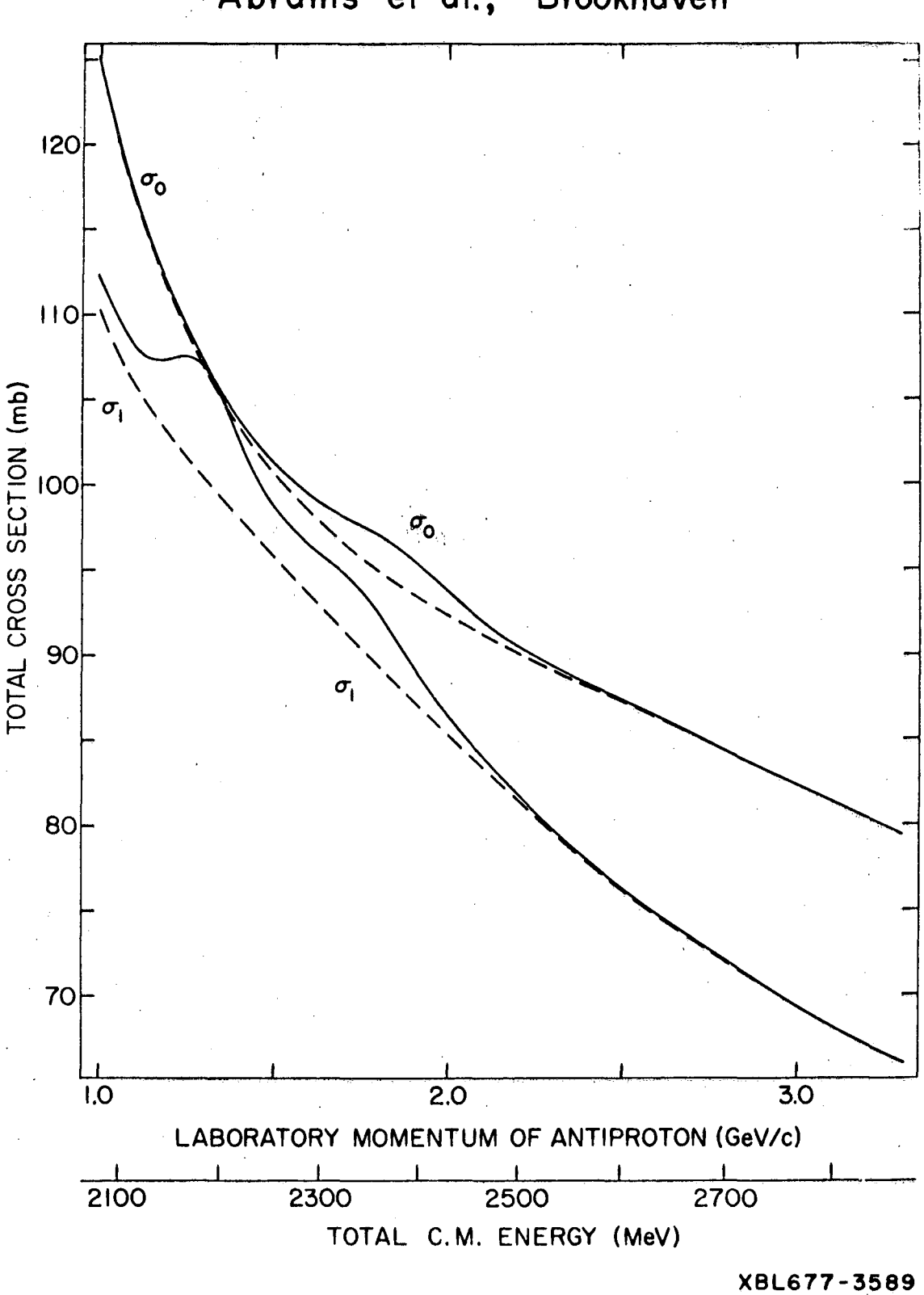
Abrams et al., Brookhaven
120
110
100
90
80
70
TOTAL CROSS SECTION (mb)
σ_0
σ_1
σ_0
σ_1
1.0
2.0
3.0
LABORATORY MOMENTUM OF ANTIPROTON (GeV/c)
2100
2300
2500
2700
TOTAL C.M. ENERGY (MeV)
XBL677-3589

Fig. III-5

Kycia (Brookhaven)

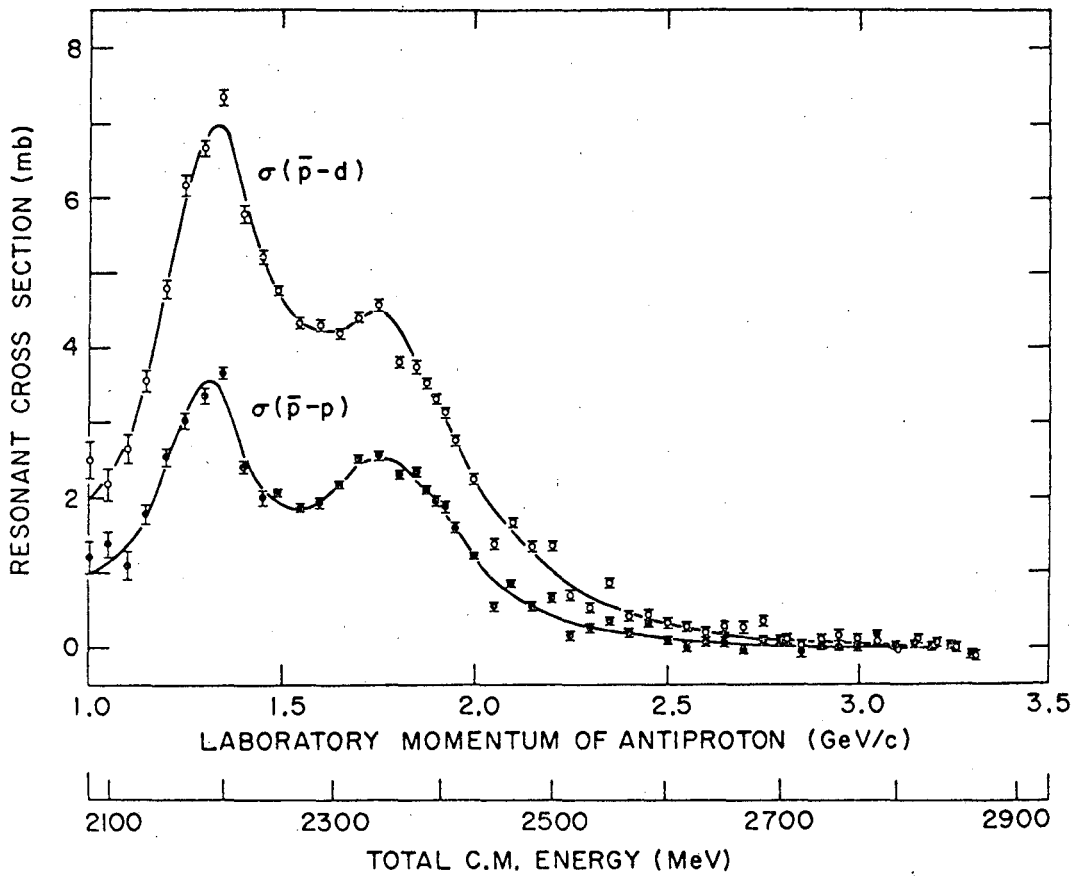

Some Parameters of the Antinucleon-Nucleon Structures[a]

Isotopic Spin	Laboratory Momentum (GeV/c)	Total Energy, c.m. (MeV)	Full Width, c.m. (MeV)	Height (mb)	$4\pi\lambda^2$ (mb)	$\frac{1}{2}(J+\frac{1}{2})\kappa$
1	1.32	2190 ± 5	85	6	15.4	0.4
1	1.76	2345 ± 10	140	3	9.9	0.3
0	1.86	2380 ± 10	140	2	9.1	0.2

a) These values are preliminary.

XBL678-3620

Fig. III-6

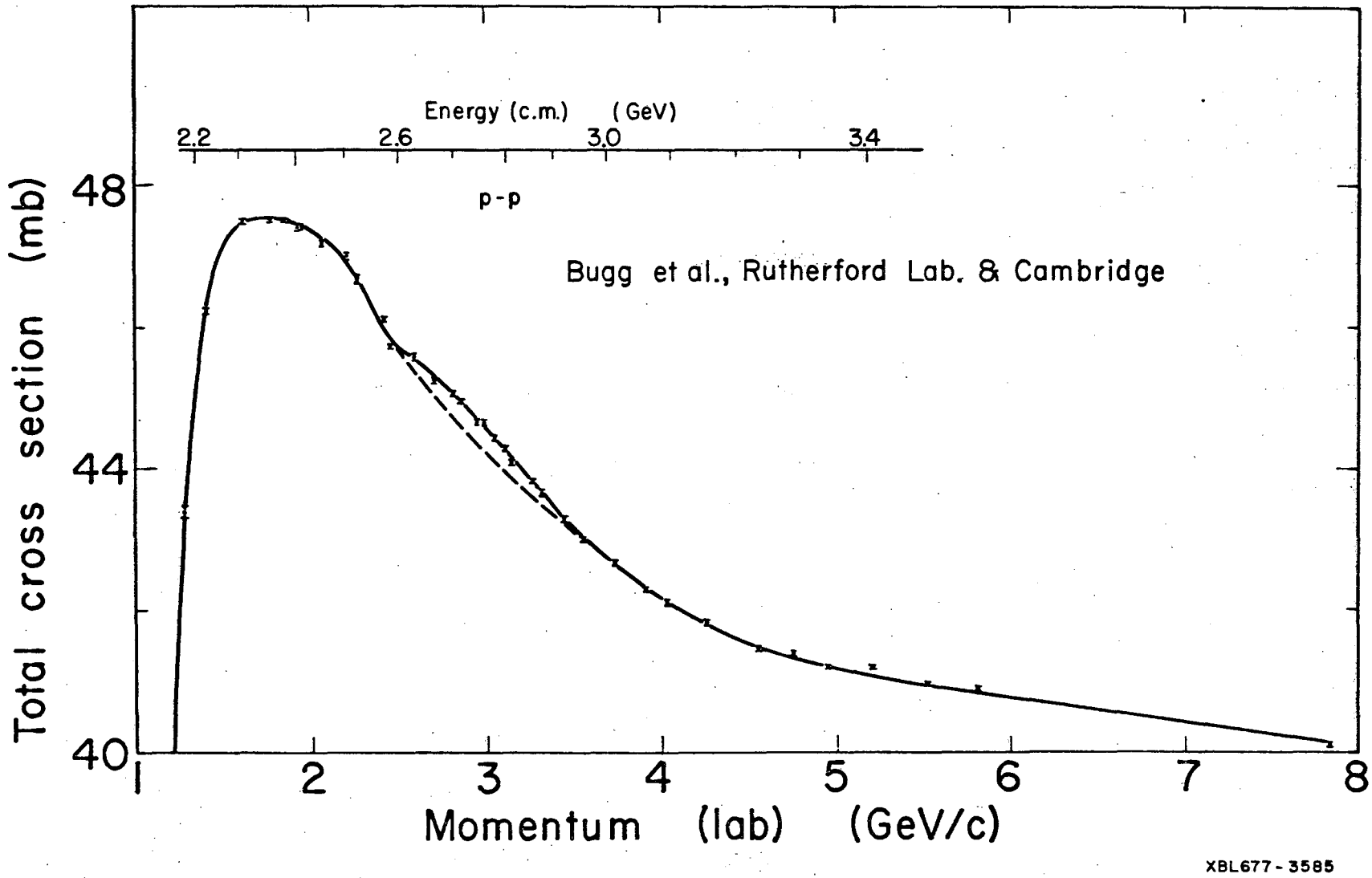

Fig. III-7a

p-p Total cross section, Bugg et al.

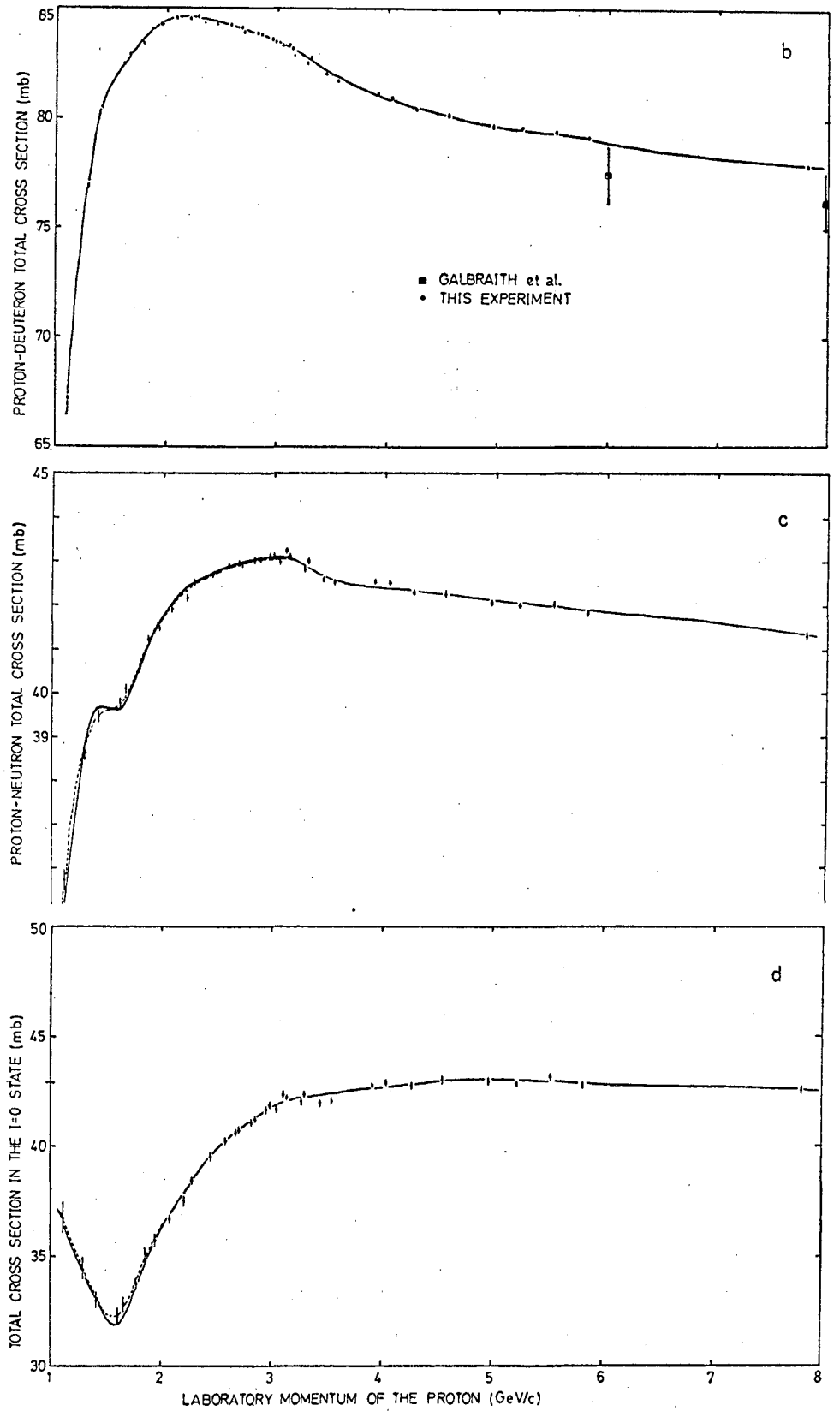

Fig. III-7b, c, d XBL677-3610

Total cross sections for (b) p-d scattering, (c) p-n scattering, (c) scattering in I = 0 state. Data of Bugg et al.

2. THE $q\bar{q}$ MODEL OF THE BOSONS

Here we consider the $q\bar{q}$ system as a tightly bound system in a very deep potential well. Many of these considerations were given by Dalitz in his Rapporteur talk at the 1966 Berkeley Conference.[8)]

i) The effect of angular momentum L

If we treat the $q\bar{q}$ system similarly to a diatomic molecule, the energy splitting due to different angular momentum states is given by a centrifugal term of the form

$$\delta (E^2) = L(L+1) \left\langle \frac{1}{r^2} \right\rangle_L .$$

To account for the observed Regge behavior, namely a linear dependence of L with mass squared, we have to assume that the $\left\langle \frac{1}{r^2} \right\rangle_L$ term does not remain roughly constant as is the case for molecules, but rather that it falls off like $1/(2L+1)$ as L increases. As Dalitz points out, this can be achieved with a harmonic oscillator potential of the form

$$V(r) = V_0 + \lambda r^2 .$$

If this were the only mass-splitting effect, we would obtain clusters of four boson nonets for each L value, namely the four states which can be formed by combining L with the total quark spin S for $S = 1$ or $S = 0$. These are the nonets ${}^3L_{L-1}$, ${}^3L_L$, ${}^1L_L$, ${}^3L_{L+1}$, where the symbol stands for ${}^{2S+1}L_J$ in the usual spectroscopic notation. An exception to this is the case for $L=0$ where we only have two such states, the ${}^1S_0$ and ${}^3S_1$ nonets. Indications from experiment suggest that the mass splittings for different L values are greater than those between the four nonets corresponding to a given L values. Thus we might expect to observe clusters of boson resonances which are clearly separated from each other but in which the four nonets may not always be clearly resolved. I will call these "boson L clusters."

The first such boson cluster observed was the A meson, which was later resolved into the A_1 and A_2 mesons. These are believed to correspond to the P-wave $q\bar{q}$ system. The $I = 1/2$ $K\pi\pi$ boson cluster centered at 1320 MeV was the next such example. Here again at least two objects, $K^*(1320)$ and $K^*(1400)$, have been resolved. There is the possibility of a third object, presumably the C meson also, as was discussed in Lecture II.

ii) Spin-orbit splitting

If we look at the above-mentioned $\pi\pi\pi$ and $K\pi\pi$ boson clusters, we can note the effect of spin-orbit splitting. In particular let us consider the I = 1 members of the four nonets $^3P_0$, $^3P_1$, $^1P_1$, and $^3P_2$. The currently popular (though yet tentative) assignment for the last three is $A_1(1080)$, $B(1220)$, and $A_2(1310)$. We note that these represent (roughly) equal $(\text{mass})^2$ splitting. If we ascribe the observed splitting to a spin-orbit potential

$$\overline{V}_{so} = (\underline{\sigma} + \overline{\underline{\sigma}}) \cdot \underline{L}\, V_{so}(r) = \underline{S} \cdot \underline{L}\, V_{so}(r),$$

with the mass-splitting coefficient

$$\underline{S} \cdot \underline{L} = \frac{1}{2}[J(J+1) - L(L+1) - S(S+1)],$$

then for the four nonets this takes on the values given below:

	$^3L_{L-1}$	^3L_L	^1L_L	$^3L_{L+1}$
S	1	1	0	1
L	L	L	L	L
J	L-1	L	L	L+1
$\underline{S} \cdot \underline{L}$	-(L+1)	-1	0	+L

Hence on the basis of the experimental mass sequence of the A_1, B, and A_2, Dalitz suggests that we are dealing with a repulsive spin-orbit potential, that is, $V_{so}(r) > 0$. For L = 1 this gives equal $(\text{mass})^2$ splitting in accordance with experiment. For L = 2 this $(\text{mass})^2$ splitting is 2:1:2 (see Fig. III-8). Dalitz also points out that a tensor force, which in principle could also split a given L cluster, is probably small, as it would give rise to unequal splitting for the L = 1 case.

iii) Spin-spin splitting

The L = 0 nonets are an anomaly in that we have only spin-spin forces available for splitting the $^1S_0$ and $^3S_1$ states. These are very considerable, however, in view of the large $\pi\rho$ mass difference. The surprising feature is that this force appears to have died out for L = 1. This behavior can be explained[8] by making the spin-spin force of sufficiently short range.

$q\bar{q}$ model

Distributions of nonets

(Not to scale)

SU_3 splitting not shown.

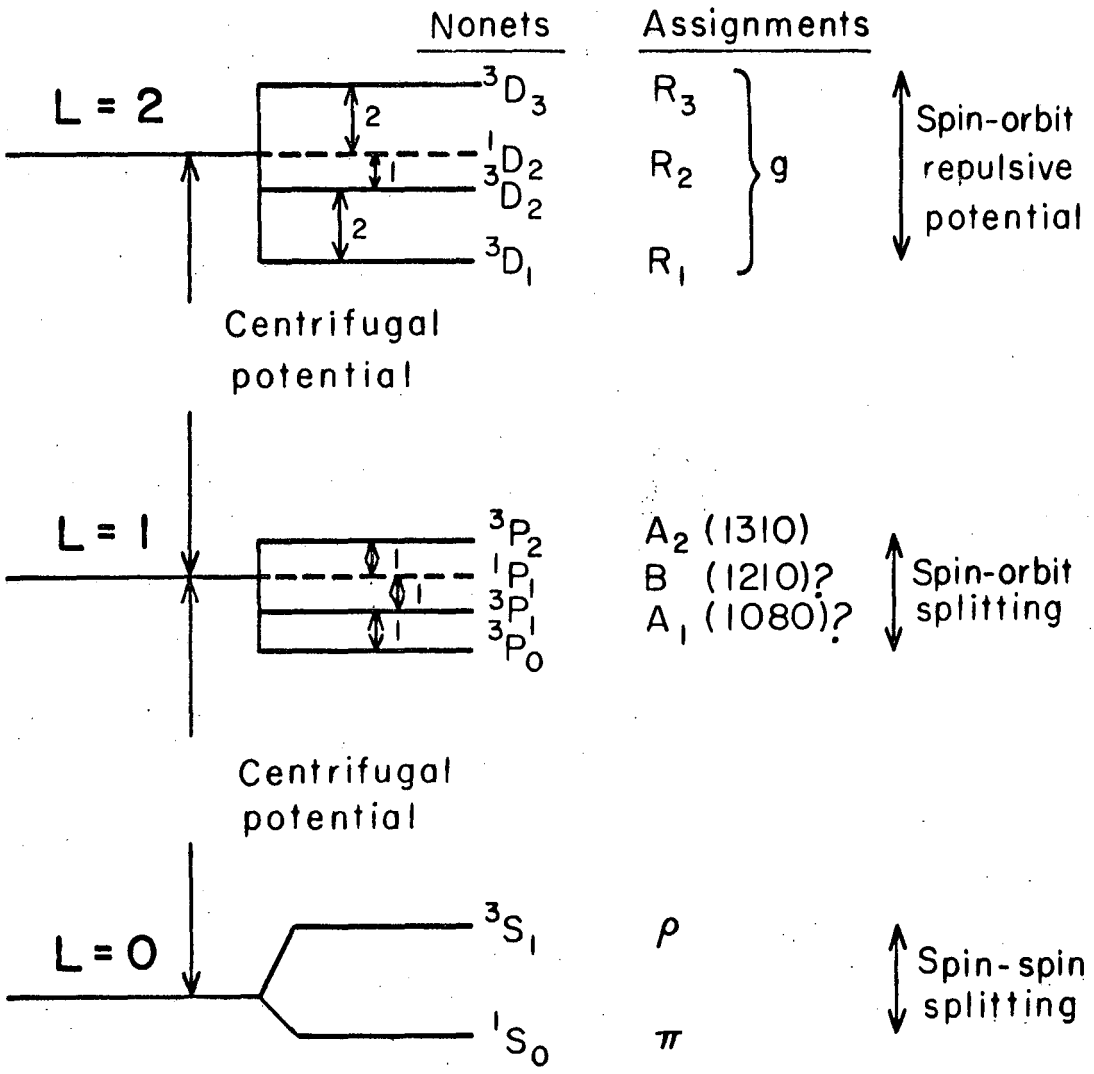

XBL677-3466

Fig. III-8

iv) Exchange degeneracy

In the Regge model for baryons one finds that a Regge trajectory contains baryons having values of J which differ by 2 units, so that $J_2 = J_1 + 2$. The separation between two such trajectories with different J values is ascribed to an exchange force. For bosons the A_2 appears to lie on the ρ trajectory, and so on through R, S, T, and U, which in the spirit of the present discussion are believed to correspond to adjacent J values ($J_2 = J_1 + 1$). Thus for bosons there appears to be an exchange degeneracy. Dalitz explains this by pointing out that the simplest object which can be exchanged between q and $\bar{q}$ must have baryon number 2/3, and thus consists of two quarks qq with mass 2Mq. The large mass of such an object would tend to suppress the exchange potential.

3. THE REGGE PLOT

To explore the model I have outlined above in further detail, we can consider the schematic Regge plot shown in Fig. III-9a. Here I have indicated schematically what the boson clusters may look like. As we do not know the spin-orbit splitting of the higher L boson clusters, I have just sketched what such clusters might be like. The indicated mass splitting should not be taken seriously, of course. Each square in Fig. III-9 represents a nonet of mesons. It must be noted that the SU(3) splitting is not shown. Presumably there can be four distinct Regge trajectories. I have indicated only the ρ trajectory. Figure III-9b shows the same plot, where now, however, L is plotted against mass squared. Here the clustering is more apparent. In a way, this represents the simplest possible situation. Should the spin-orbit splitting increase as L increases we could get bosons of different L superimposed on each other, and thus lose the cluster effect.

Other causes which can complicate or even obscure the cluster effect would be

(a) the presence of bosons belonging to higher-symmetry groups such as the $\underline{27}$ configuration, which requires the existence of states like K^+K^+, $K\pi\pi$ I = 3/2, $\pi^+\pi^+$, etc. In my estimation, there is not yet sufficient evidence to require us to invoke such configurations.

(b) boson clusters corresponding to higher radial quantum numbers n. Here we must note that, until we get a clear understanding of the $q\bar{q}$

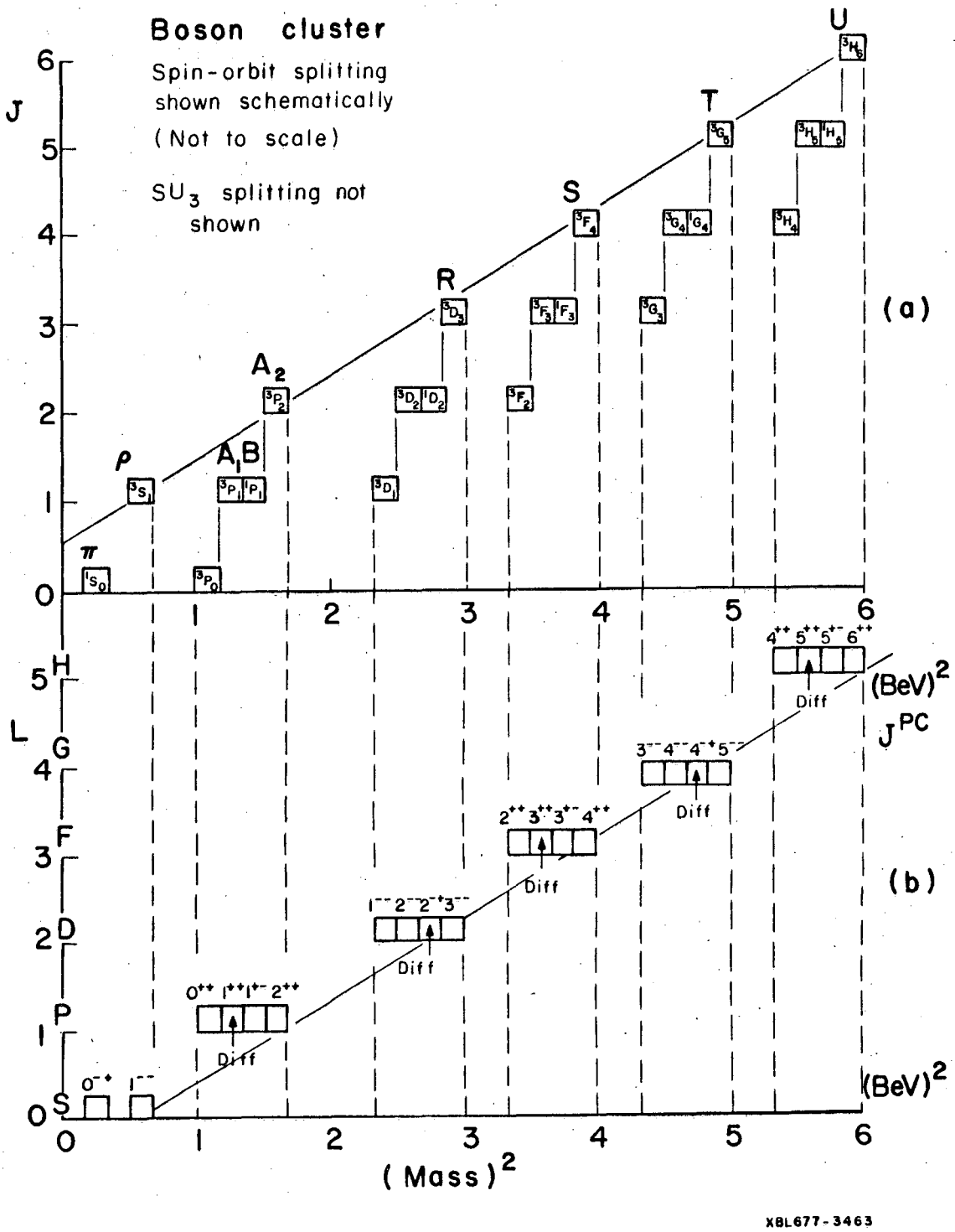
Boson cluster
Spin-orbit splitting shown schematically
(Not to scale)
SU3 splitting not shown
J
L
(a)
(b)
(BeV)2
JPC
(Mass)2
Diff
XBL677-3463

Fig. III-9

potential, it is not obvious just what n represents.

Finally, continuing in the spirit of this inquiry, we can ask what are the allowed decay modes for the members of these various nonets? Some representative decay modes are illustrated in Fig. III-10. Here again I have indicated a crude mass-squared scale. Thus, in a sense, this figure illustrates, in an approximate fashion, the mass spectrum expected for various final states. For example, the first two rows indicate the mass spectrum in the I = 1 and I = 0 $\pi\pi$ state, and so forth. A few of the presently known and identified states are marked with their names.

A comparison of these patterns with the experimental spectra is perhaps the most sensitive way in which to detect evidence for, or deviations from, the model described herein. Thus, for example, in the $\pi\rho$ or $\pi\pi\pi$ decay mode, in the region of the A meson there is only room for two distinct mesons, corresponding to the L = 1 boson cluster. If the A_1 is established as a definite meson, and if one finds any more mesons in this region, this must indicate the presence of other effects. For example, the possible existence of the $A_{1.5}$ would be such an effect; so would the A_2 if it is indeed split, as the CERN missing-mass-spectrometer work appears to indicate, and if it is shown that such a split corresponds to two distinct resonances!

In Fig. III-9 I have also indicated in each case which nonent would be produced by diffraction dissociation or pomeron exchange. That is, we could produce the corresponding isovector meson by pion bombardment or the I =1/2 meson by K bombardment. As stated in Lecture II, to be produced by diffraction dissociation the boson has to have the quantum numbers of the incident particle, i.e., 0^-, plus angular momentum ℓ. This yields $J = \ell$ and a parity of $P = (-1)^{\ell+1}$ for the resulting boson state. Bosons produced by this process are expected to have constant cross section with increasing energy. Thus for high bombarding energies these are the ones which should dominate the cluster, while the other three nonets would presumably have cross sections that go through a maximum above threshold and then die out again with increasing energy.

4. POSSIBLE DECAY SCHEMES

It is of interest to look in greater detail at how these boson resonances will decay.

Allowed strong decay modes for conjectured Boson L clusters (schematic)

(Spin-orbit splitting not to scale, SU_3 splitting not shown)

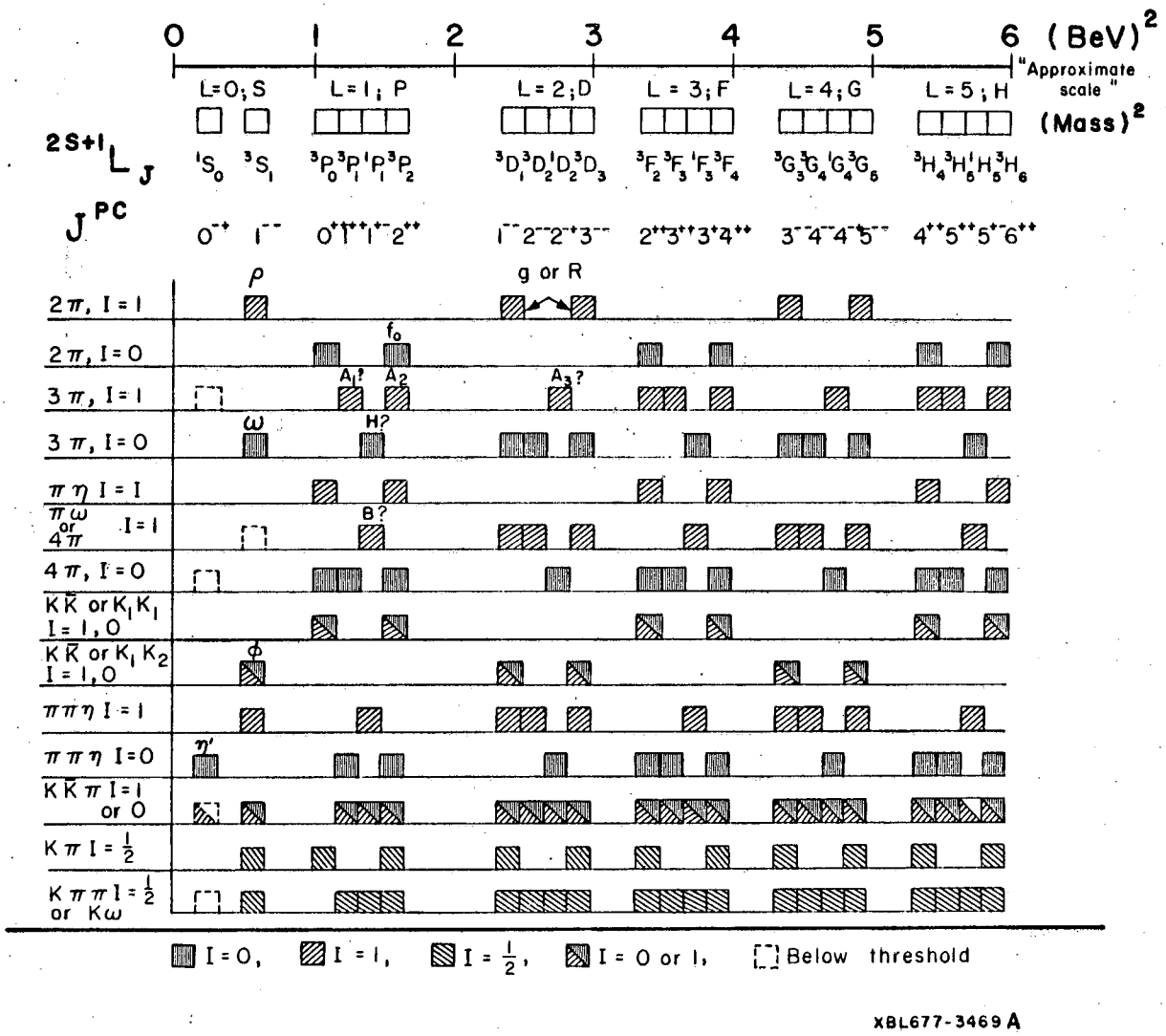

XBL677-3469 A

Fig. III-10

i) Nomenclature

To identify the various members of a boson L cluster I will use the following nomenclature: π, η, η', and K stand for the isotopic triplet, singlets, and doublet, as in Rosenfeld et al.[9] This symbol plus the quantum numbers $^{2S+1}L_J$ identify a specific $q\bar{q}$ state. For example, the A_2 is given as $\pi(^3P_2)$, the ω is given as $\eta(^3S_1)$. Furthermore I occasionally use the name of the isotriplet to refer to the entire nonet: thus A_2 nonet refers to the $^3P_2$ nonet and ρ nonet refers to the $^3S_1$ nonet.

ii) Allowed decays into well-known particles

In Tables III-2, through III-6 I have listed the allowed decays of the L = 2 to L = 5 bosons into some of the better-known particles. The entries in the tables are the angular momentum ℓ and corresponding P when the decay mode indicated is allowed via strong interactions. The threshold mass required for each given decay mode is also indicated. One very interesting feature emerges immediately from these tables: the nonet with J = L + 1 decays consistently through higher angular momentum states for the common decay modes than any of the other three nonets. Thus we might expect that the widths of the bosons in the J = L+1 nonets could be considerably narrower than the widths of the other bosons, for the same L value. I will comment on this later in connection with comparisons with experiments.

iii) The cascading to lower boson clusters

Aside from the decay into well-known mesons described in the tables above, we can also consider what transitions are allowed by pion emission from one L cluster to another. The allowed transitions with ℓ = 0 and ℓ = 1 between the two final-state particles are illustrated in Figs. III-11, III-12, and III-13. In Fig. III-14 is shown the decay from the J = L + 1 levels. As can be noted from these figures, the three nonets with J = L - 1 and J = L in the two charge conjugation states, can each decay via an ℓ = 0 transition as well as via an ℓ = 1 transition. On the other hand the nonet with J = L + 1 can only cascade down to the next lower similar nonet via an ℓ = 2 transition. The ℓ = 1 transitions within a boson cluster of given L (see Fig. III-13) are probably forbidden by energy conservation. Thus, here too, we see that the members of the J = L+1 nonets have no way of decaying with angular momentum less than 2--a feature, again, which will contribute to their particularly narrow decay widths.

Table III-2

Some possible decay schemes for L = 2 bosons; the entry refers to ℓ^P minimum for allowed decays

Decay mode	$\eta(^3D_1)$	$\eta(^3D_2)$	$\eta(^1D_2)$	$\eta(^3D_3)$	$\pi(^3D_1)$	$\pi(^3D_2)$	$\pi(^1D_2)$	$\pi(^3D_3)$	Threshold (MeV)
$J^{PC}(G)$	$1^{--}(-)$	$2^{--}(-)$	$2^{-+}(+)$	$3^{--}(-)$	$1^{--}(+)$	$2^{--}(+)$	$2^{-+}(-)$	$3^{--}(+)$	
$\pi\pi$	-	-	-	-	1^-	-	-	3^-	280
$\pi\rho$	1^-	1^-	-	3^-	-	-	1^-	-	905
$\pi\eta$	-	-	-	-	-	-	-	-	690
$\pi\omega$	-	-	-	-	1^-	1^-	-	3^-	925
$K\bar{K}$ or K_1K_2	1^-	-	-	3^-	1^-	-	-	3^-	990
πf^0	-	-	-	-	-	-	0^+	-	1390
πA_2	-	-	0^+	-	2^+	0^+	-	2^+	1450
$\rho\rho$	-	-	1^-	-	1^-	1^-	-	1^-	1530
$\rho\omega$	-	-	-	-	-	-	1^-	-	1550
ρf^0	-	-	-	-	0^+	0^+	-	0^+	2015

Table III-3

Boson nonets in L = 2 cluster

Decay mode	Mass threshold	$J_1^{P_1}, J_2^{P_2}$	$K(^3D_1)$	$K(^3D_2)$	$K(^1D_2)$	$K(^3D_3)$
			JPC=1^{--}	2^{--}	2^{-+}	3^{--}
$K\pi$	635	$0^-, 0^-$	1^-	-	-	3^-
$K^*\pi$	1030	$1^-, 0^-$	1^-	1^-	1^-	3^-
$K\rho$	1260	$0^-, 1^-$	1^-	1^-	1^-	3^-
$K^*(1400)\pi$	1540	$2^+, 0^-$	2^+	0^+	0^+	2^+
KA_2	1810	$0^-, 2^+$	2^+	0^+	0^+	2^+
Kf^0	1745	$0^-, 2^+$	2^+	0^+	0^+	2^+
$K^*\rho$	1655	$1^-, 1^-$	1^-	1^-	1^-	1^-
K^*A_2	2210	$1^-, 2^+$	0^+	0^+	0^+	0^+
K^*f^0	2140	$1^-, 2^+$	0^+	0^+	0^+	0^+

Table III-4

Some possible decay schemes for L = 3 bosons;
the entry refers to ℓ^P minimum for allowed decays

Decay mode	$\eta(^3F_2)$	$\eta(^3F_3)$	$\eta(^1F_3)$	$\eta(^3F_4$	$\pi(^3F_2)$	$\pi(^3F_3)$	$\pi(^1F_3)$	$\pi(^3F_4)$	Threshold (MeV)
J^{PC}_G	$2^{++}_{(+)}$	$3^{++}_{(+)}$	$3^{+-}_{(-)}$	$4^{++}_{(+)}$	$2^{++}_{(-)}$	$3^{++}_{(-)}$	$3^{+-}_{(+)}$	$4^{++}_{(-)}$	
$\pi\pi$	2^+	-	-	4^+	-	-	-	-	280
$\pi\rho$	-	-	2^+	-	2^+	2^+	-	4^+	905
$\pi\eta$	-	-	-	-	2^+	-	-	4^+	690
$\pi\omega$	-	-	-	-	-	-	2^+	-	925
$K\bar{K}$, K_1K_1 or K_2K_2	2^+	-	-	4^+	2^+	-	-	4^+	990
πf^0	-	-	-	-	1^-	1^-	-	3^-	1390
πA_2	1^-	1^-	-	3^-	-	-	1^-	-	1450
$\rho\rho$	0^+	2^+	-	2^+	-	-	2^+	-	1530
$\rho\omega$	-	-	-	-	0^+	2^+	-	2^+	1550
ρf^0	-	-	-	-	-	-	1^-	-	2015

Table III-5

Some possible decay schemes for L = 4 bosons;
the entry refers to ℓ^P minimum for allowed decays

Decay mode	$\eta(^3G_3)$	$\eta(^3G_4)$	$\eta(^1G_4)$	$\eta(^3G_5)$	$\pi(^3G_3)$	$\pi(^3G_4)$	$\pi(^1G_4)$	$\pi(^3G_5)$	Threshold (MeV)
$J^{PC}(G)$	$3^{--}_{(-)}$	$4^{--}_{(-)}$	$4^{-+}_{(+)}$	$5^{--}_{(-)}$	$3^{--}_{(+)}$	$4^{--}_{(+)}$	$4^{-+}_{(-)}$	$5^{--}_{(+)}$	
$\pi\pi$	-	-	-	-	3^-	-	-	5^-	280
$\pi\rho$	3^-	3^-	-	5^-	-	-	3^-	-	905
$\pi\eta$	-	-	-	-	-	-	-	-	690
$\pi\omega$	-	-	-	-	3^-	3^-	-	5^-	925
$K\bar{K}$ or K_1K_2	3^-	-	-	5^-	3^-	-	-	5^-	990
πf^0	-	-	-	-	-	-	2^+	-	1390
πA_2	-	-	2^+	-	-	-	-	-	1450
$\rho\rho$	-	-	3^-	-	1^-	3^-	-	3^-	1530
$\rho\omega$	-	-	-	-	-	-	3^-	-	1550
ρf^0	-	-	-	-	0^+	2^+	-	2^+	2015
ρA_2	0^+	2^+	-	2^+	-	-	-	-	2075

Table III-6

Some possible decay schemes for L = 5 bosons;
the entry refers to ℓ^P minimum for allowed decays

Decay mode	$\eta(^3H_4)$	$\eta(^3H_5)$	$\eta(^1H_5)$	$\eta(^3H_6)$	$\pi(^3H_4)$	$\pi(^3H_5)$	$\pi(^1H_5)$	$\pi(^3H_6)$	Threshold (MeV)
$J^{PC}(G)$	$4^{++}(+)$	$5^{++}(+)$	$5^{+-}(-)$	$6^{++}(+)$	$5^{++}(-)$	$5^{++}(-)$	$5^{+-}(+)$	$6^{++}(-)$	
$\pi\pi$	4^+	-	-	6^+	-	-	-	-	280
$\pi\rho$	-	-	4^+	-	4^+	4^+	-	6^+	905
$\pi\eta$	-	-	-	-	4^+	-	-	6^+	690
$\pi\omega$	-	-	-	-	-	-	4^+	-	925
$K\bar{K}, K_1k$ or K_2K_2	4^+	-	-	6^+	4^+	-	-	6^+	990
πf^0	-	-	-	-	3^-	3^-	-	5^-	1390
πA_2	-	-	-	-	-	-	3^-	-	1450
$\rho\rho$	2^+	4^+	-	4^+	-	-	4^+	-	1530
$\rho\omega$	-	-	-	-	2^+	4^+	-	4^+	1550
ρf^0	-	-	-	-	-	-	3^-	-	2015
ρA_2	-	-	-	-	1^-	3^-	-	3^-	2075

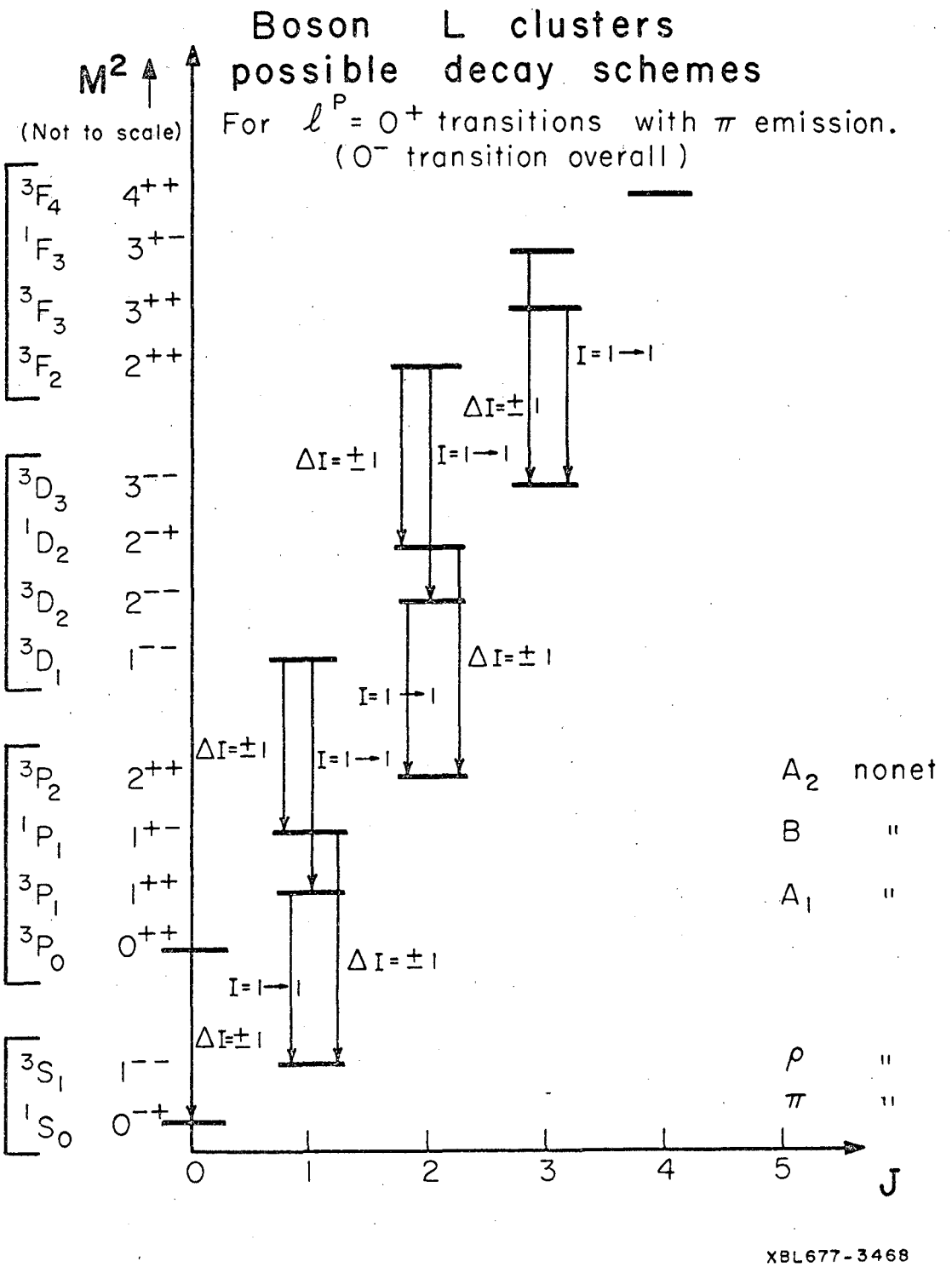
Boson L clusters
possible decay schemes
For $\ell^P = 0^+$ transitions with π emission.
(0^- transition overall)
M^2
(Not to scale)
$^3F_4$ 4^{++}
$^1F_3$ 3^{+-}
$^3F_3$ 3^{++}
$^3F_2$ 2^{++}
$^3D_3$ 3^{--}
$^1D_2$ 2^{-+}
$^3D_2$ 2^{--}
$^3D_1$ 1^{--}
$^3P_2$ 2^{++}
$^1P_1$ 1^{+-}
$^3P_1$ 1^{++}
$^3P_0$ 0^{++}
$^3S_1$ 1^{--}
$^1S_0$ 0^{-+}
$\Delta I = \pm 1$
$I = 1 \to 1$
A_2 nonet
B "
A_1 "
ρ "
π "
0 1 2 3 4 5
J
XBL677-3468

Fig. III-11

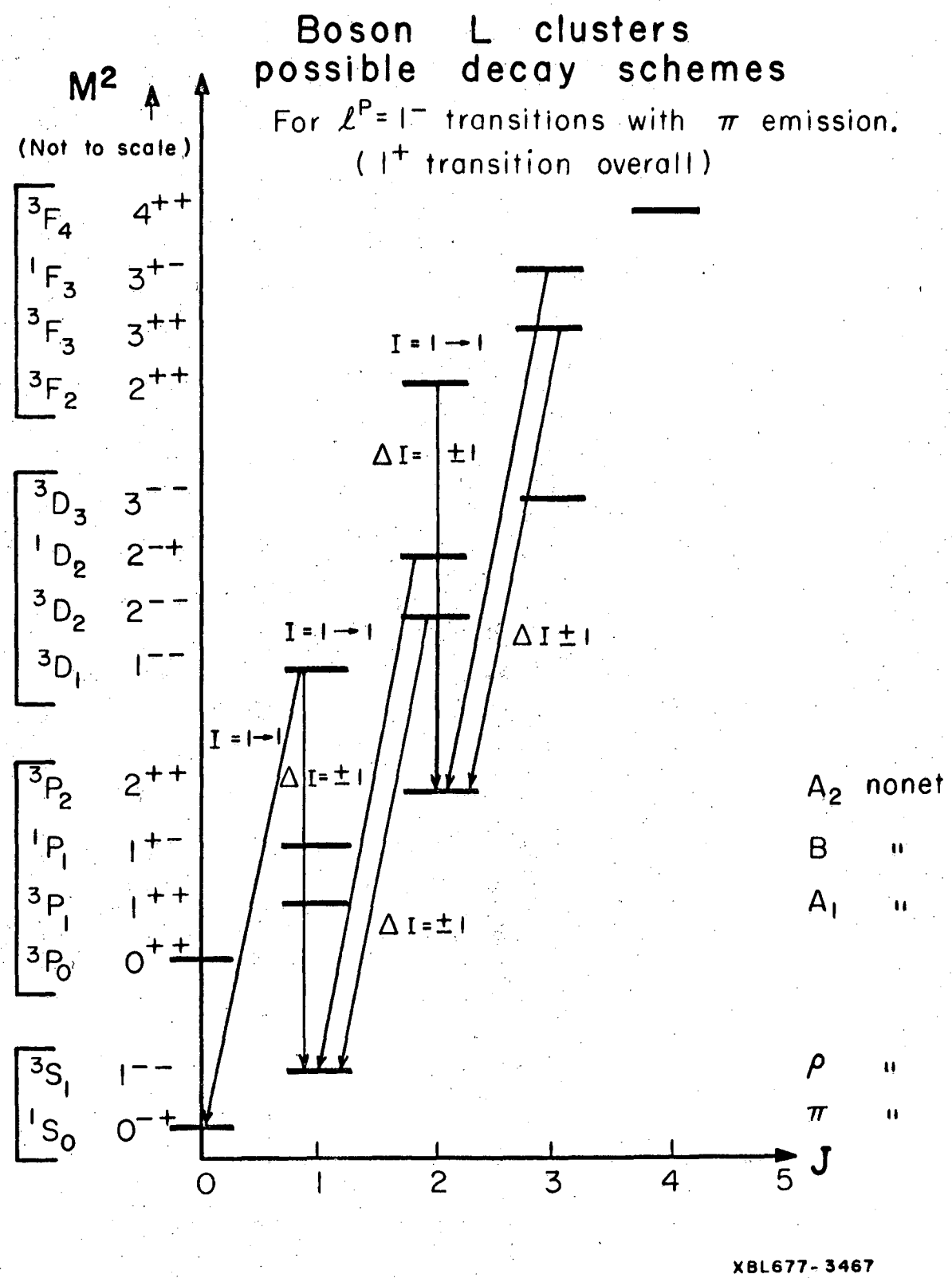
Boson L clusters
possible decay schemes
For $\ell^P = 1^-$ transitions with π emission.
(1^+ transition overall)
M^2
(Not to scale)
$^3F_4$ 4^{++}
$^1F_3$ 3^{+-}
$^3F_3$ 3^{++}
$^3F_2$ 2^{++}
$^3D_3$ 3^{--}
$^1D_2$ 2^{-+}
$^3D_2$ 2^{--}
$^3D_1$ 1^{--}
$^3P_2$ 2^{++}
$^1P_1$ 1^{+-}
$^3P_1$ 1^{++}
$^3P_0$ 0^{++}
$^3S_1$ 1^{--}
$^1S_0$ 0^{-+}
I = 1 → 1
ΔI = ±1
I = 1 → 1
ΔI ±1
I = 1 → 1
ΔI = ±1
ΔI = ±1
A_2 nonet
B "
A_1 "
ρ "
π "
0 1 2 3 4 5 J
XBL677-3467

Fig. III-12

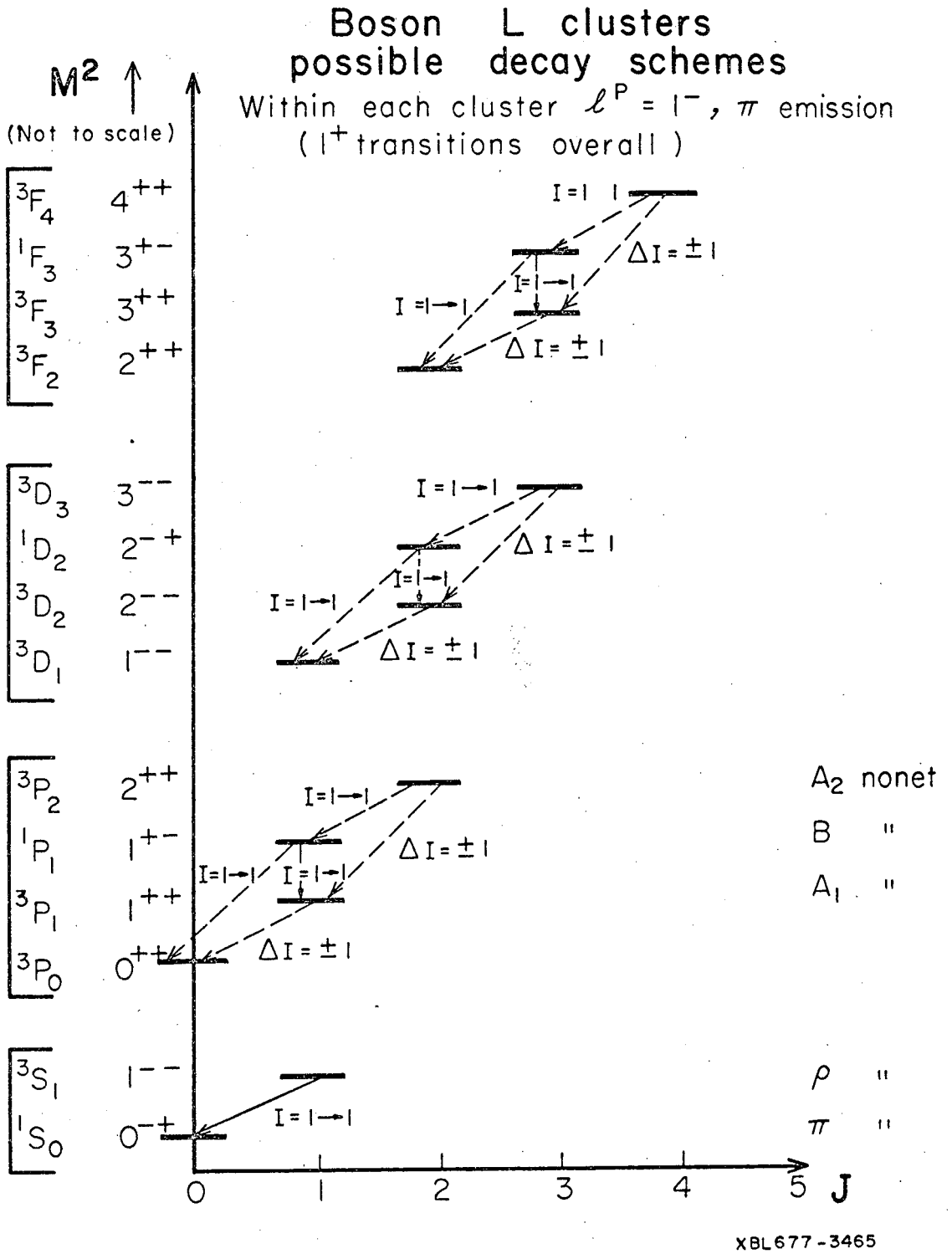

Fig. III-13

Depending on the magnitude of the spin-orbit splitting the transitions ---- are probably forbidden by energy conservation.

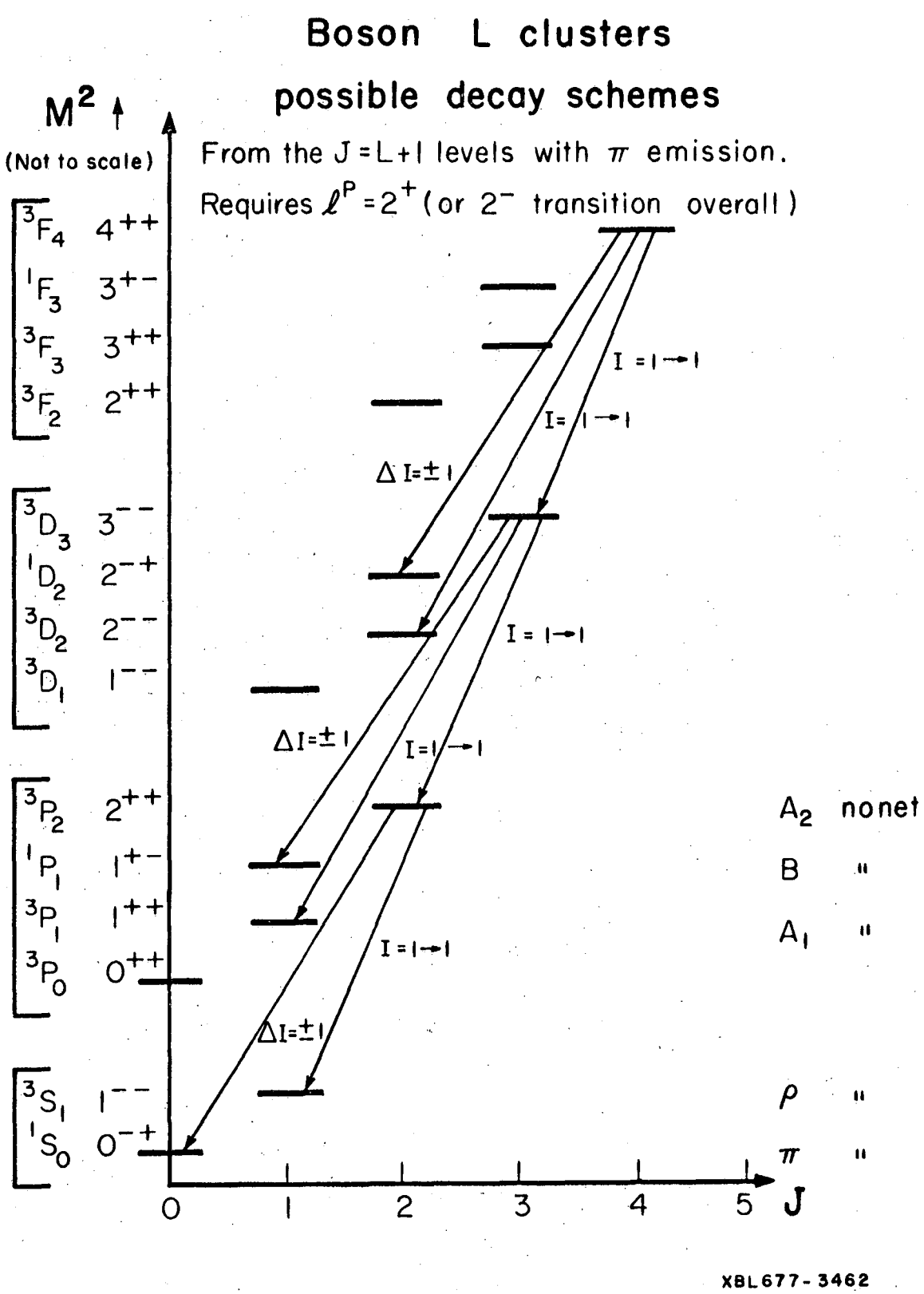

XBL677-3462

Fig. III-14

Let I_1 refer to the initial boson, and I_2 to the final boson, which is produced together with the π meson. Thus $\Delta I = 1 \to 1$ indicates that the transition has to occur between an isovector initial state and an isovector final state $+\pi$. Similarly $\Delta I = \pm 1$ refers to the change of I spin from the initial- to the final-state bosons. The selection rules for π transitions from an initial boson state $\underline{1}$ to a final boson state $\underline{2}$ $\left[I_1 (L_1)_{J_1} P_1 C_1 G_1 \to \pi + I_2 (L_2)_{J_2} P_2 C_2 G_2 \right]$ with angular momentum ℓ between $\underline{2}$ and π are:

$$G_2 = -G_1,$$
$$P_2 = P_1 (-1)^{\ell+1};$$
$$\text{for} \quad C_2 = C_1, \quad \text{then} \quad \Delta I = \pm 1;$$
$$\text{for} \quad C_2 = -C_1, \quad \text{then} \quad I_2 = I_1 = 1.$$

We can then distinguish

ℓ = even	ℓ = odd
$P_2 = -P_1$	$P_2 = P_1$
$L_2 - L_1 =$ odd	$L_2 - L_1 =$ even

This behavior is illustrated below. Thus, for example,

$$\left.\begin{array}{lll} & \pi\,(^3P_2) & \to \pi + \pi\,(^3S_1) \\ \text{ie.,} & A_2 & \to \pi + \rho \end{array}\right] \quad \Delta I = 0, \quad I_1 = I_2 = 1 \quad (\ell = 2)$$

$$\left.\begin{array}{lll} \text{or,} & \pi\,(^1P_1) & \to \pi + \eta\,(^3S_1) \\ \text{ie.,} & B & \to \pi + \omega \\ & \eta\,(^1P_1) & \to \pi + \pi\,(^3S_1) \\ \text{ie.,} & H & \to \pi + \rho \end{array}\right] \quad \Delta I = \pm 1 \quad (\ell = 0)$$

Note that the experimental identification of the B and H with given quantum numbers is still tentative.

5. MORE DETAILED COMPARISON WITH EXPERIMENTS

If we accept the experimental evidence cited above at face value we must ask: Can the narrow peaks from the CERN missing-mass spectrometer work be reconciled with the broad peaks observed in $\sigma(\bar{p}p)$? It is, of course, impossible to answer this question at present without considerably more experimental data. We need an independent

confirmation for the very narrow peaks, and we need further information on whether or not the $\bar{p}p$ data indeed correspond to bosons.

In spite of these serious problems let us explore the possibility that the two types of corresponding phenomena could belong to the same boson L clusters. To do this we will consider the following points:

i) Experimental sensitivity to different regions of t

The missing-mass spectrometer work relies on precision angle measurements on a proton in the region of the "Jacobian peak." This cuts out low-momentum-transfer data. In the region of the S(1929), T(2195), and U(2382) mesons the average momentum transfer squared value for the measurements made is $t \approx 0.3(\text{GeV})^2$. On the other hand, $\sigma(\bar{p}p)$ measurements are sensitive to all allowed values of t. The same is true for bubble chamber work, which in fact is most sensitive to the lowest allowed t values, for which the cross sections are maximal for peripheral reactions.

ii) Examples of different t distributions

If we look at the A_1 and A_2 $d\sigma/dt$ distributions vs t we note the well-known feature that the A_2 has a much broader t distribution than the A_1. This is illustrated in Fig. III-15, from the $\pi^+ p$ ABC experiment at 8 GeV/c, where the slopes for elastic scattering, A_1 production, and A_2 production are compared. The ratio of intensity at $t = 0.3$ to $t \approx 0$ is shown on the graphs. It is perhaps significant to note here that the A_2 presumably belongs to the ${}^3L_{L+1}$ nonet. Although we cannot make a rigorous argument, it is possible that differences in t distributions among the bosons in a given L cluster contribute to the difference between the phenomena discussed here.

iii) The width of higher boson resonances

As I mentioned above, the four-multiplets belonging to a given L cluster have quite different decay schemes. In particular, the nonet with the spin $J = L + 1$, i.e., ${}^3L_{L+1}$, must in nearly all cases decay via higher angular momentum states than the other three nonets. The decay width Γ for decay into two particles can be expressed as

$$\Gamma = \gamma \frac{k}{M} [(Rk)^{\ell}/\ell!!]^2,$$

when k is the c.m. momentum, ℓ the decay angular momentum, and M the mass of the boson. The coupling constant γ and characteristic

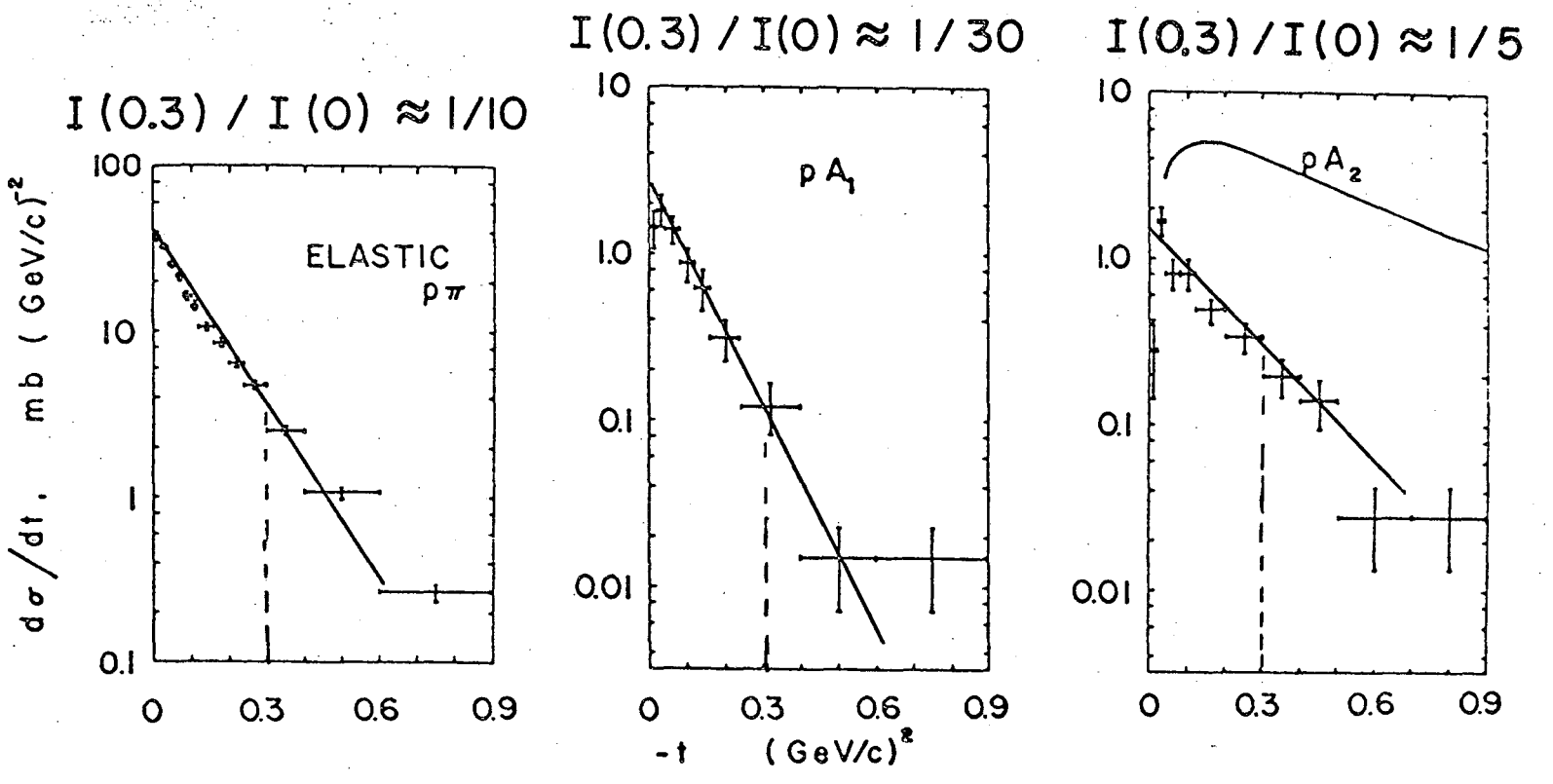
ABC Collaboration 8.0-GeV/c $\pi^+ p$
I(0.3) / I(0) ≈ 1/10
I(0.3) / I(0) ≈ 1/30
I(0.3) / I(0) ≈ 1/5
ELASTIC
$p\pi$
pA_1
pA_2
$d\sigma/dt$, mb (GeV/c)$^{-2}$
$-t$ (GeV/c)^2
100
10
1
0.1
1.0
0.01
0
0.3
0.6
0.9
XBL677-3586

Fig. III-15

radius R are, however, not known to sufficient accuracy. If we consider γ and R to be constant for a given boson L cluster, it follows that members of the $J = L + 1$ nonet have a considerably narrower decay width than members of the other three nonets. Thus, for $L = 3$ and higher we might expect one narrow nonet, while it is possible that the width of the others is comparable to the spin-orbit splitting, so that they may actually not always be fully resolved from each other.

iv) Sensitivity of the missing-mass spectrometer experiment

Next we must take into account the fact that the CERN missing-mass experiment was carried out in the region of the S, T, and U mesons in a signal-to-background ratio of $\approx 1:7$, while the magnitude of the signal in each peak consisted of ≈ 200 to 250 events. If this same number of events, constituting a signal, had been distributed over 3 or 4 times the number of bins, such a signal could not have been detected by this method. In other words, within the statistics available so far, the missing-mass measurement is most sensitive to narrow resonances.

v) Partial width for $\bar{p}p$ decay

The $\sigma(\bar{p}p)$ experiment will, of course, show up only boson resonances for which there is a finite partial width $\Gamma(\bar{p}p)$ for $\bar{p}p$ decay in a given nonet. At present it is not known to me how $\Gamma(\bar{p}p)$ depends on the quantum numbers of a particular nonet in a given L cluster.

In conclusion, then, when these various points are taken into account, it is possible that the two sets of observed phenomena correspond to the observation of different components of the same boson L clusters. Namely, it is possible that what has been observed as the S, T, and U in the CERN missing-mass-spectrometer work is the one set of very narrow bosons with $J = L + 1$. On the other hand, depending on $\Gamma(\bar{p}p)$, the $\sigma(\bar{p}p)$ experiment at Brookhaven may have observed one or more different members of the L cluster, which then can be appreciably broader. Clearly, these ideas are purely speculative at the moment, and much further experimental work is required to confirm them.

REFERENCES, SECTION III

1) M. N. Focacci, W. Kienzle, B. Levrat, B. C. Maglić, and M. Martin, Phys. Rev. Letters 17, 890 (1966).

2) R. J. Abrams, R. L. Cool, G. Giacomilli, T. F. Kycia, B. A. Leontic, K. K. Li, and D. N. Michael, Phys. Rev. Letters 18, 1209 (1967). Also T. F. Kycia, Total Cross Sections of $\bar{K}$ Mesons and Antiprotons on Nucleons up to 3.3 GeV/c, Brookhaven National Laboratory Report BNL-11372

3) Gerson Goldhaber, Rapporteur Talk, "Boson Resonances," in Proceedings of the XIIIth International Conference on High Energy Physics, Berkeley, 1966, Berkeley and Los Angeles, 1967, (University of California Press), page 103.

4) D. J. Crennell, P. V. C. Hough, George R. Kalbfleisch, K. W. Lai, J. M. Scarr, T. G. Schumann, I. O. Skillocorn, R. C. Strand, and M. S. Webster, Phys. Rev. Letters 18, 323 (1967).

5) R. L. Cool, G. Giacomelli, T. F. Kycia, B. A. Leontic, K. K. Li, A. Lundby, and J. Teiger, Phys. Rev. Letters 17, 102 (1966).

6) R. W. Bland, M. G. Bowler, J. L. Brown, G. Goldhaber, S. Goldhaber, V. H. Seeger, and G. H. Trilling, Phys. Rev. Letters 18, 1077 (1967).

7) D. V. Bugg, D. C. Salter, G. H. Stafford, R. F. George, K. F. Riley, and R. J. Tapper, Phys. Rev. 146, 980 (1966).

8) R. H. Dalitz, Rapporteur Talk, "Symmetries and the Strong Interactions," in Proceedings of the XIIIth International Conference on High Energy Physics, Berkeley, September 1966 (University of California Press, Berkeley and Los Angeles, 1967), page 215.

9) Arthur H. Rosenfeld, Angela Barbaro-Galtieri, William J. Podolsky, LeRoy R. Price, Paul Soding, Charles G. Wohl, Matts Roos, and William J. Willis, Rev. of Mod. Phys. 39, No. 1 (1967).

APPENDIX I

Three-Pion Resonances

Here we describe a new method for the utilization of the Dalitz plot designed to facilitate the search for the existence of new resonances and the determination of their quantum numbers for three-particle resonances. The method we shall describe has a counterpart in resonance formation experiments. Consider πp scattering through a direct channel resonance, $\pi p \rightarrow N^* \rightarrow \pi p$. The total cross section has very marked bumps for the low-lying resonances, but at higher masses the N^* does not always manifest itself in such an obvious way, and the methods must be refined. An example is the use of angular distributions. For a definite J^P the distribution assumes a characteristic shape at $E = M$, and varies rapidly over the range $M - \frac{\Gamma}{2} < E < M + \frac{\Gamma}{2}$. A very recent method used by the Michigan group at Argonne is the study of backward πp scattering. By the study of $\frac{d\sigma}{d\Omega}(180°)$ one obtains strong variations in this quantity as one sweeps through resonance regions. This effect is amplified, in fact, due to interference effects between the superimposing resonance amplitude and a high-energy Regge background term. This method has revealed some new resonances. The interference effects also led to a sensitive test of the assumed quantum numbers for the higher N^* resonances.

In the case of three-particles (boson), the method is to study the density distribution of events in the Dalitz plot as a function of the three-particle mass. For example, in the reaction $\pi^+ p \rightarrow \pi^+ \pi^- \pi^0 \pi^+ p$ it is possible that there is some hidden structure at the high end of the 3π mass spectrum. The method depends on the fact that the decay-matrix elements for a three-pion system follow a very characteristic symmetry pattern in the Dalitz plot for various I, J^{PG} values. A very elegant graphical representation of the density distributions for the states $I = 0$, $J^{PG} = 0^{--}$, 1^{--}, and 1^{+-}, given by Stevenson et al.[1] based on the "simplest" matrix element first suggested by Gell-Mann,[2] is in Fig. A-1. A thorough discussion of this problem has recently been carried out by Zemach[3] (see Fig. A-2). In this note we wish to discuss a method by which one can carry out a pattern search as a function of the three-pion mass. Let us consider the state $I = 0$ and $J^{PG} = 0^{--}$, 1^{--}, 1^{+-}, 2^{--}, and 2^{+-}.

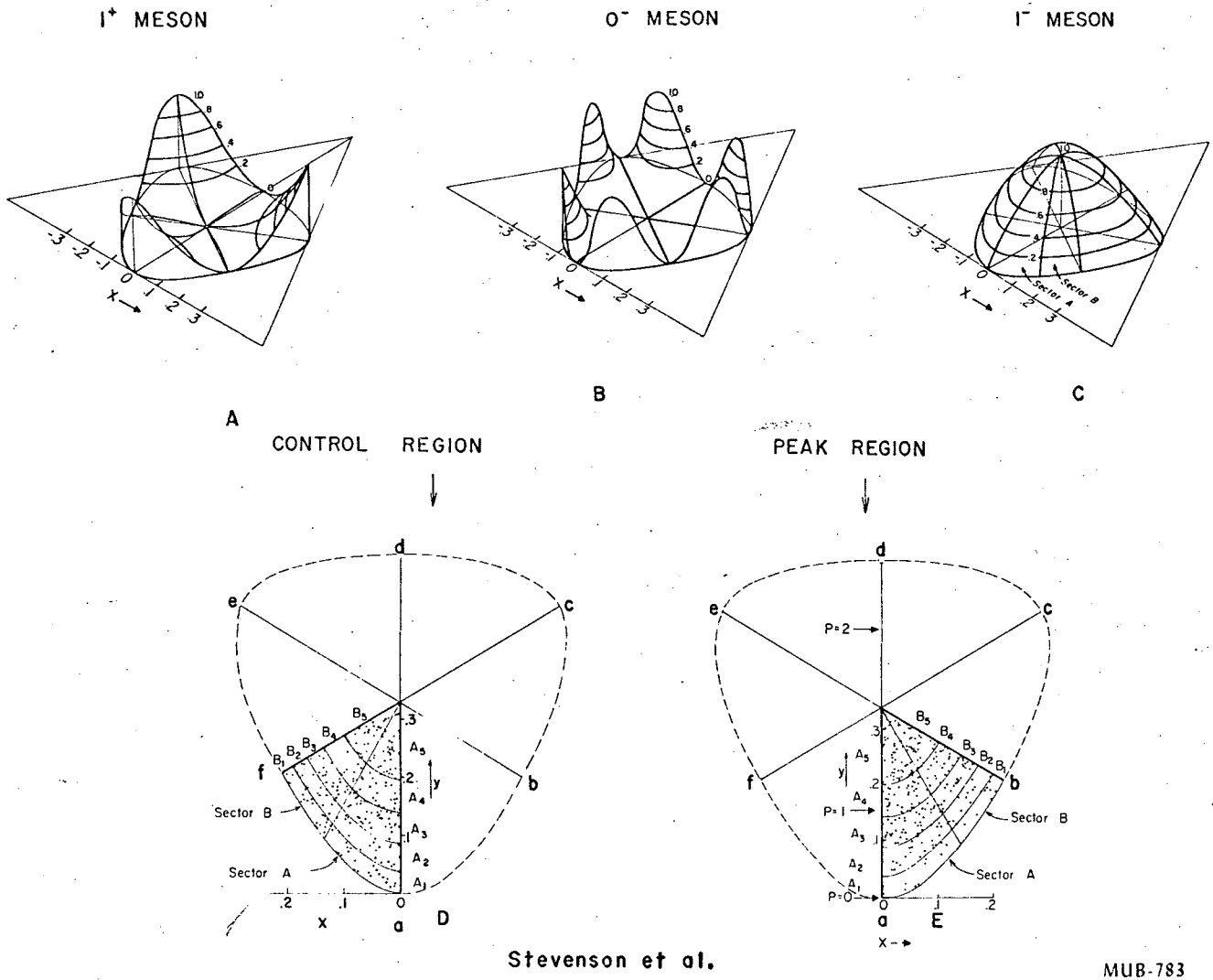
1+ MESON
0- MESON
1- MESON
A
B
C
CONTROL REGION
PEAK REGION
Sector A
Sector B
Stevenson et al.
MUB-783

Fig. A-1

Zemach

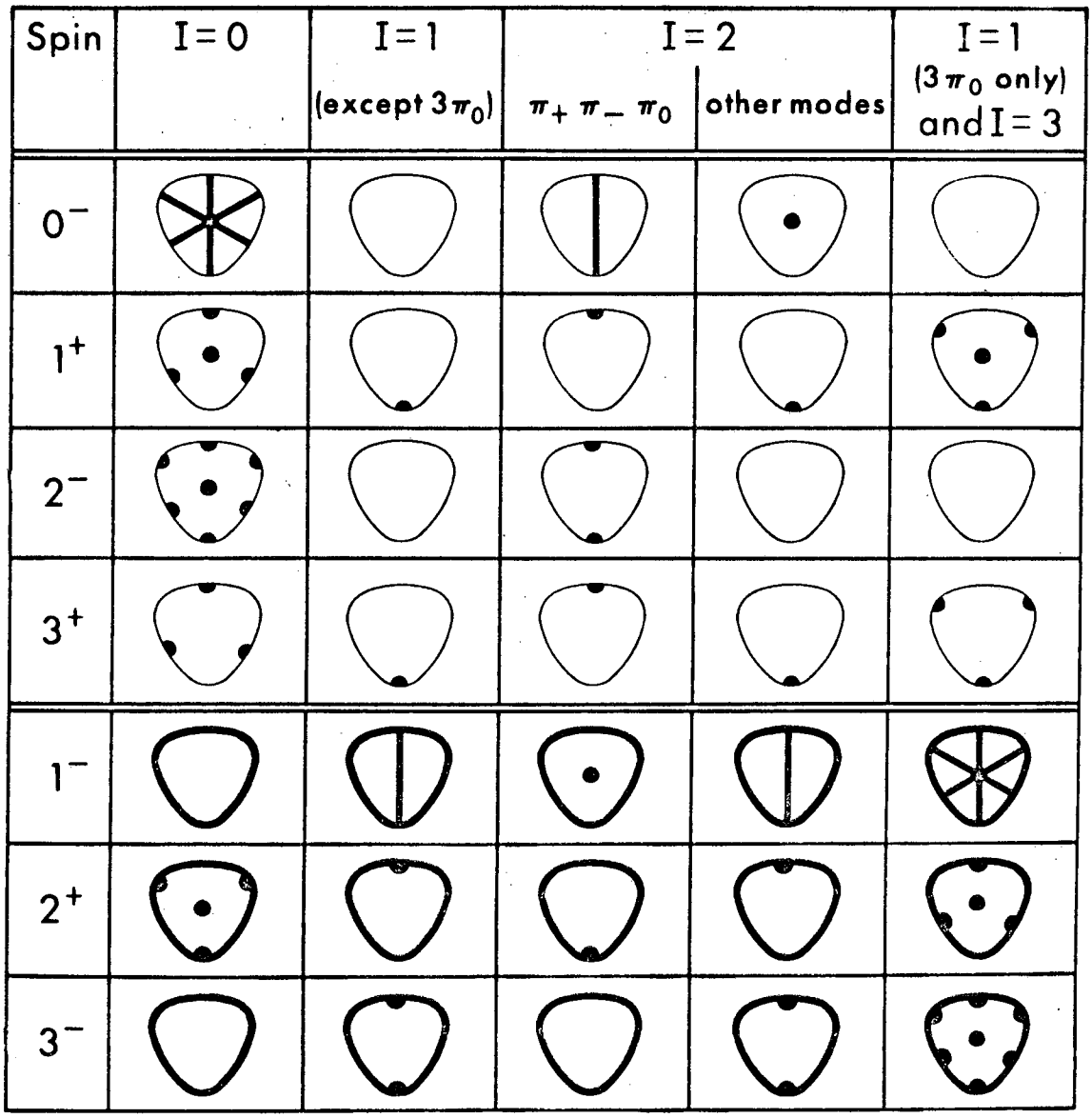

XBL678-3614

Fig. A-2

The corresponding "simplest" matrix elements are given in Table A-1. The Dalitz contour maps for the corresponding density distributions are given in Figs. A-3 through A-7. These were calculated for a mass of the three-pion system of M = 782 MeV. The contour maps are computed in 5% steps labeled by the 20 letters A to T. Alternate letters are left blank for clarity.

Table A-1

The square of the matrix elements for the angular momentum-parity states I = 0, $J^P = 0^-, 1^-, 1^+, 2^-, 2^+$

$$\lambda(0^-) = [(E_2 - E_3)(E_3 - E_1)(E_1 - E_2)]^2$$

$$\lambda(1^-) = (\vec{P}_1 \times \vec{P}_2 + \vec{P}_2 \times \vec{P}_3 + \vec{P}_3 \times \vec{P}_1)^2 = q^2$$

$$\lambda(1^+) = [\vec{P}_1(E_2 - E_3) + \vec{P}_2(E_3 - E_1) + \vec{P}_3(E_1 - E_2)]^2$$

$$\lambda(2^-) = \sum_{(ijk)} \left[\frac{2}{3}(E_j - E_k)^2 P_i^4 + 2(E_j - E_k)(E_k - E_i)\left((\vec{P}_i \cdot \vec{P}_j)^2 - \frac{1}{3} P_i^2 P_j^2\right)\right]$$

$$\lambda(2^+) = q^2 (E_1 \vec{P}_1 + E_2 \vec{P}_2 + E_3 \vec{P}_3)^2$$

We can plot the three-pion mass distribution for $\lambda(J^P)$ less than and greater than $\lambda_M(J^P)$ where $\lambda_M(J^P)$ is a suitable median value of $\lambda(J^P)$ such that about 1/2 the events with quantum numbers J^P have a $\lambda(J^P)$ greater than $\lambda_M(J^P)$. By limiting $\lambda(J^P)$ to certain values--e.g., $0.7 \leq \lambda(1^-) \leq 1.0$ for the ω meson[4]--we are considering definite regions in the Dalitz plot at which $\lambda(J^P)$ is near its maximum value. These regions correspond to small fractions of the area and thus phase-space effects become considerably reduced relative to a given matrix element.

The values chosen for $\lambda_M(J^P)$ together with the corresponding percentage of events and percentage of area (i.e., phase space) are given in Table A-2. The regions occupied in the Dalitz plot for the various matrix elements with $\lambda(J^P) \geq \lambda_M(J^P)$ are shown in Fig. A-8. Notice that these maxima lie in practically disjoint regions, so that each region corresponds to a certain J^P value which can be studied separately.

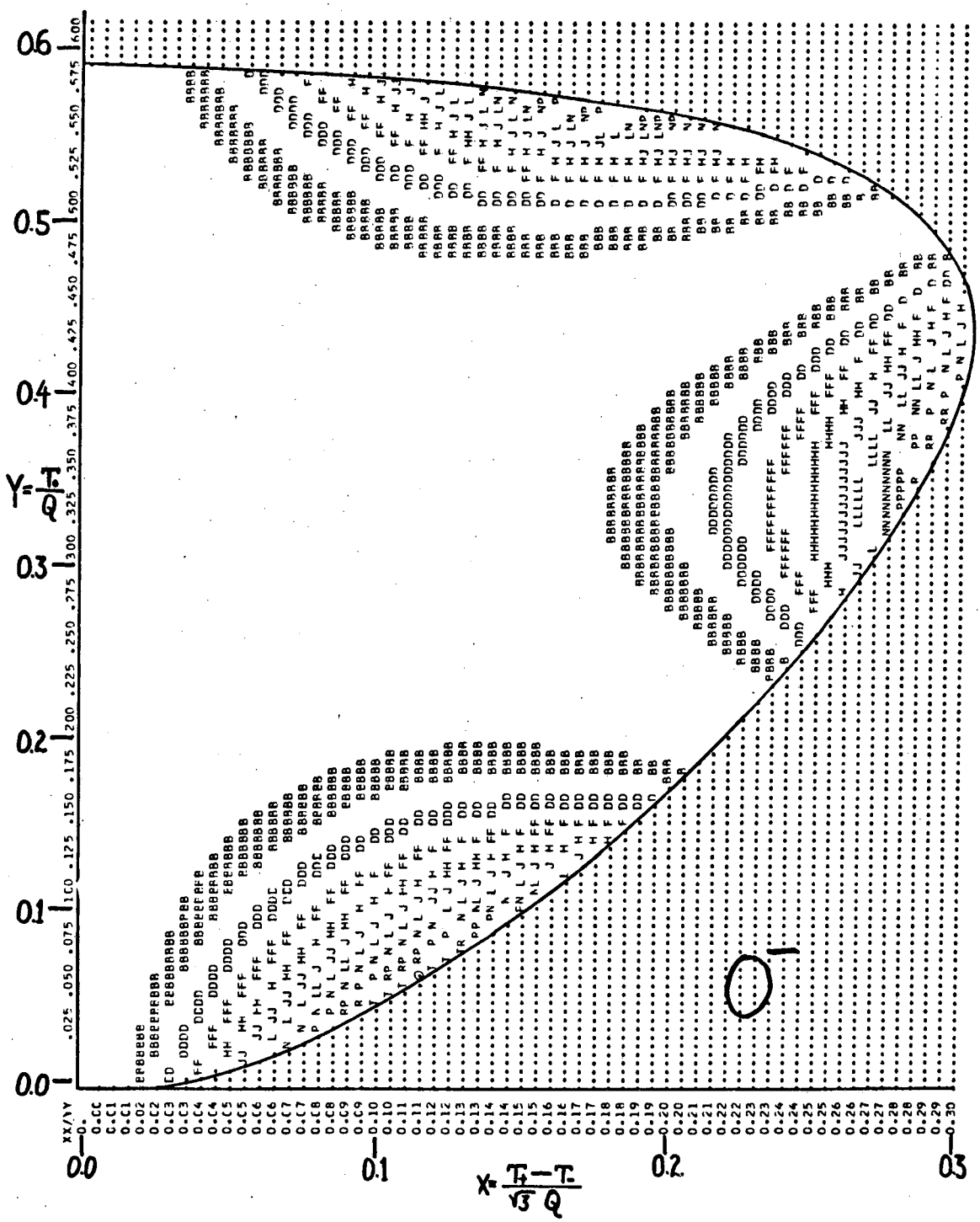

Fig. A-3

MUB-6764

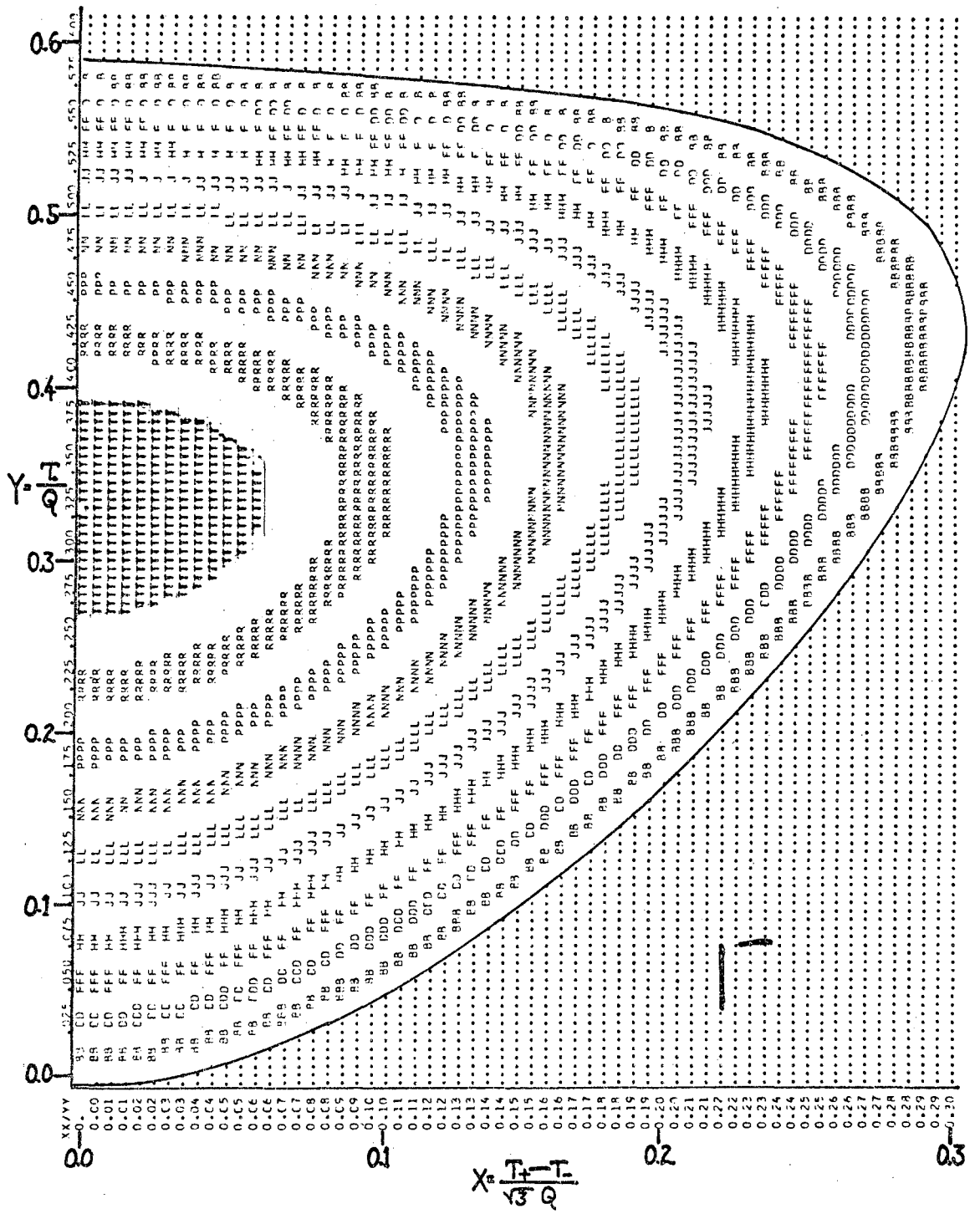

Fig. A-4

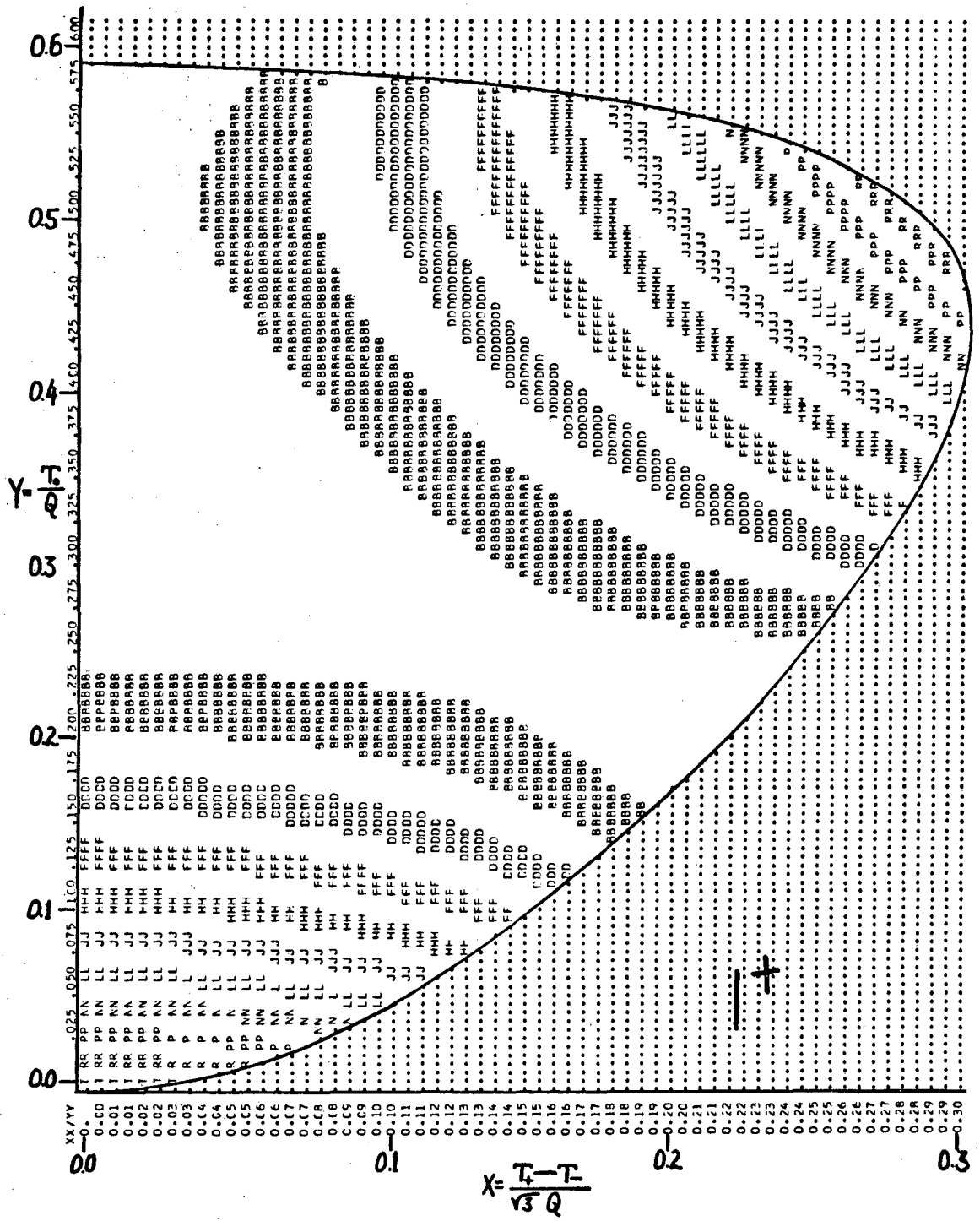

Fig. A-5

MUB-6765

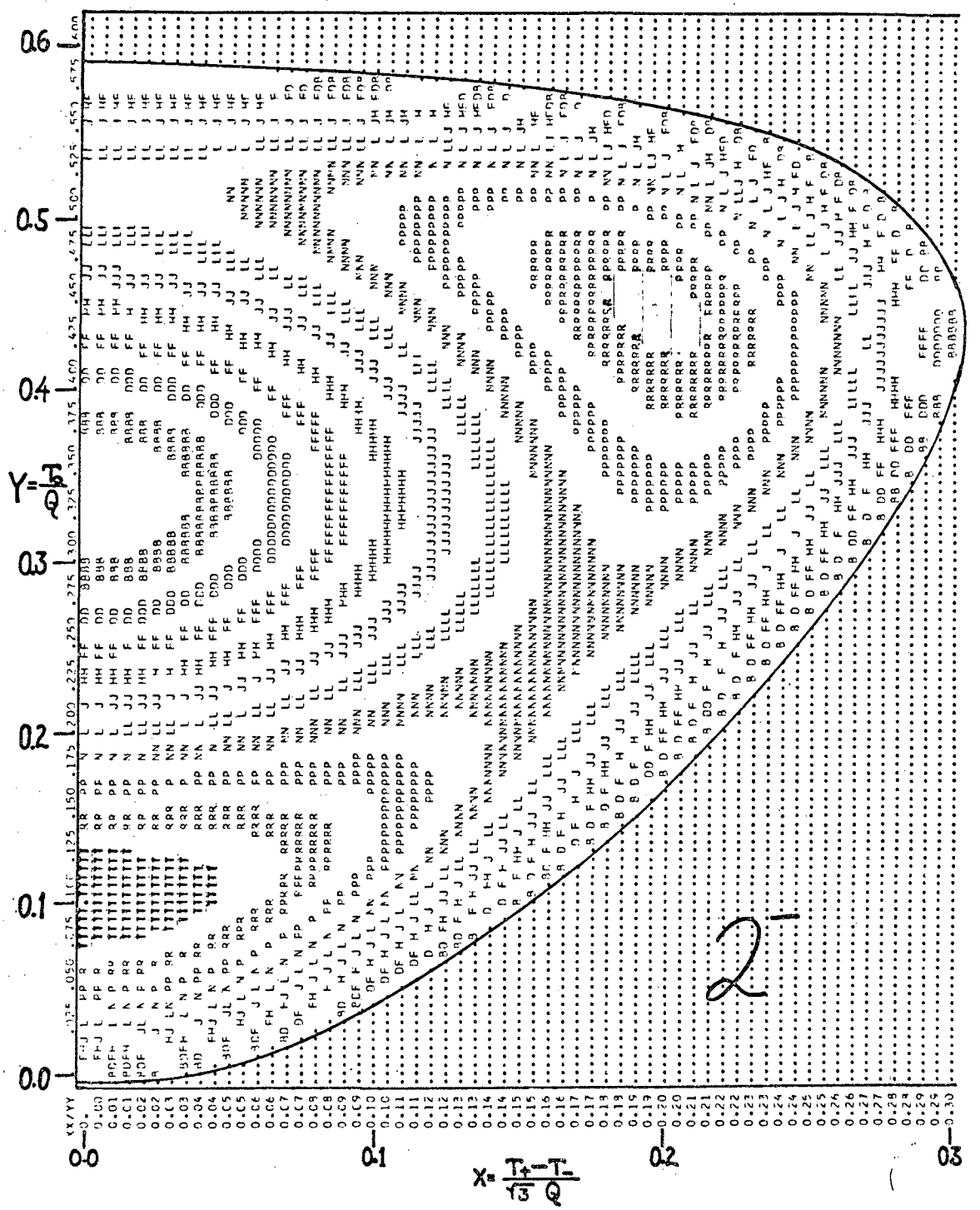

Fig. A-6

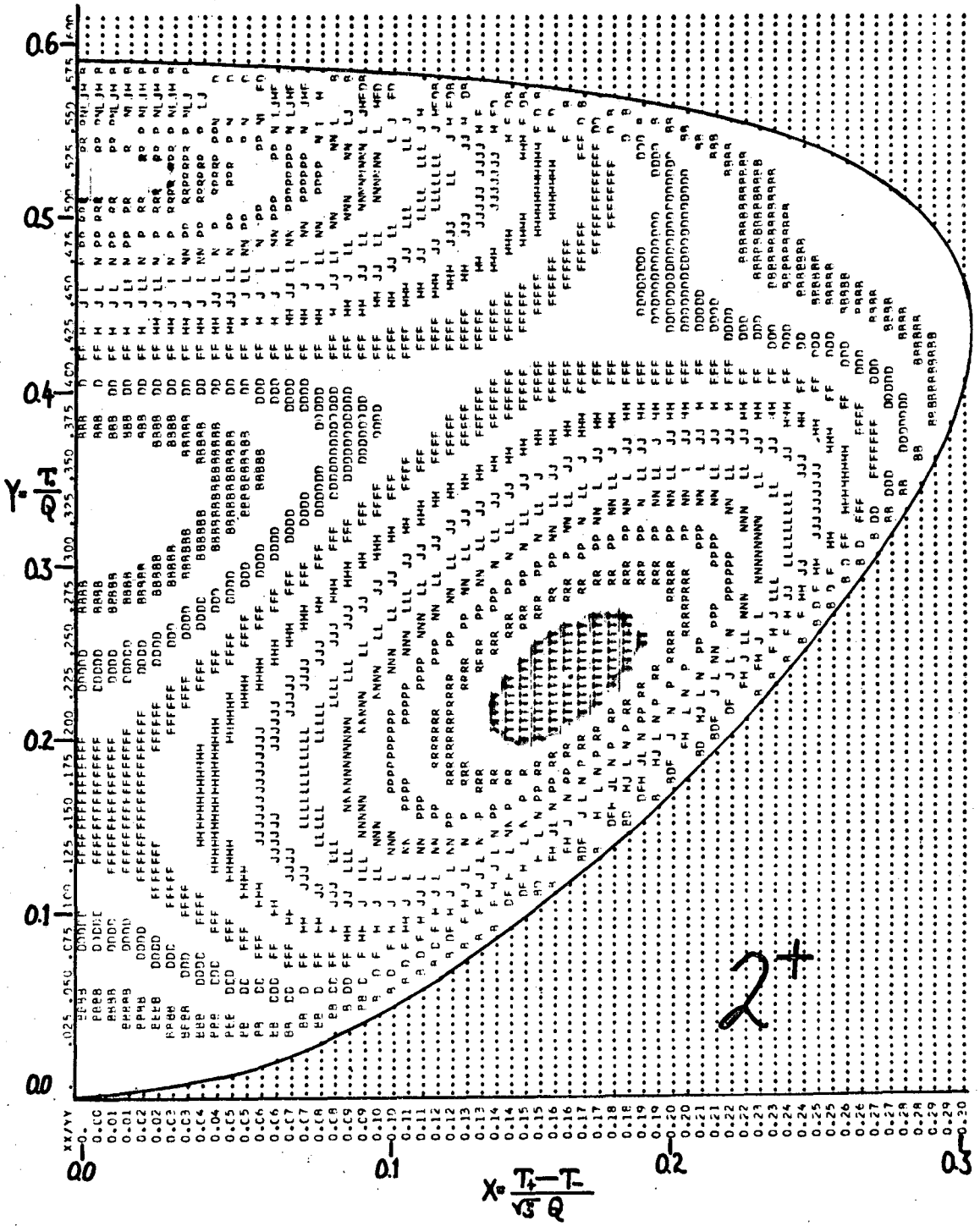

Fig. A-7

MUB-6766

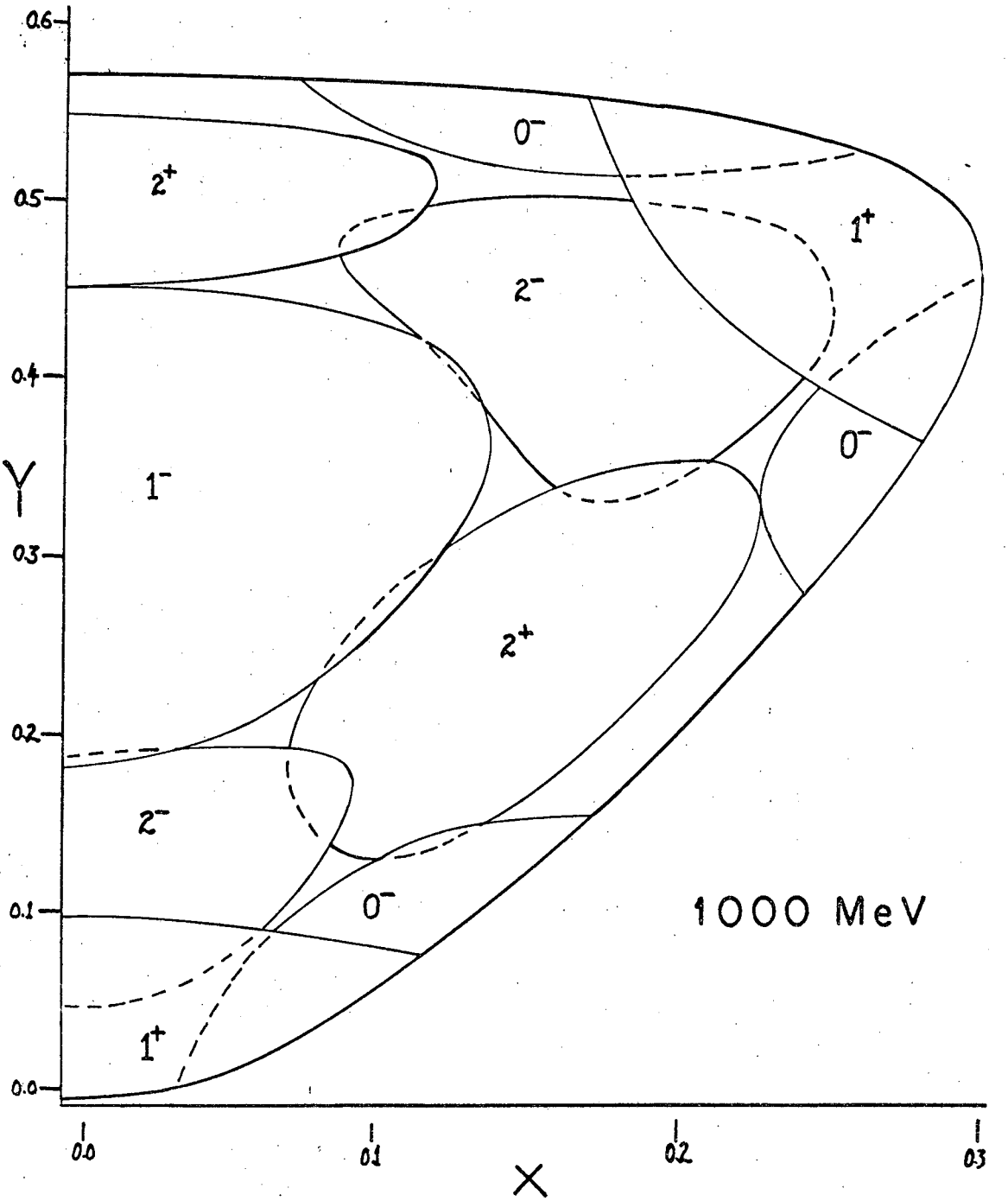

Fig. A-8

Table A-2

Percentage of area and percentage of integral over the matrix element above the value $\lambda_M(J^P)$

Three-pion mass

		500 MeV		1000 MeV		1500 MeV		2000 MeV	
J^P	$\lambda_M(J^P)$	Area (%)	Integral (%)	Area (%)	Integral (%)	Area (%)	Integral (%)	Area (%)	Integral (%)
0^-	0.3	8.4	48.5	14.1	61.5	14.9	63.2	14.9	63.3
1^-	0.7	30.0	51.2	28.4	49.7	27.4	48.8	26.9	48.6
1^+	0.4	15.8	45.4	17.8	52.3	16.8	52.1	16.1	51.5
2^-	0.7	21.7	35.9	28.1	43.4	27.4	43.3	27.0	43.0
2^+	0.6	18.7	41.4	24.2	48.3	24.4	48.7	24.3	48.7

Notice also that as the ℓ values are summed, the maxima almost cover the plot, so that the expected uniform population of the plot for phase space is being explicitly shown.

The shape and area of the normalized Dalitz plot change considerably with total energy of the three-pion system (i.e., from a near circle in the nonrelativistic case to a triangle in the highly relativistic regions). For example, from M = 500 MeV to M = 2000 MeV, A(500)/A(2000) = 1.62, where A corresponds to the normalized area.

The comparison of the corresponding Dalitz plots at 500 MeV and 2000 MeV for the $J^P = 1^-$ and 1^+ matrix element is shown in Fig. A-9. We note that although the area and shape are changing, the percentage of events with $\lambda(J^P) \geq \lambda_M(J^P)$ varies only slowly with M.

Figure A-10 shows this technique applied to the ω meson, a 1^- resonance. The matrix element peaks in the center; the central curve encloses 50% of the events but only 30% of the area. Figure 10 shows the radial density distribution (background accounts for the events where the ω density should be zero).

Figure A-11 shows the projection onto the $\pi^+\pi^-\pi^0$ axis of the central and outer regions. Notice that the background is considerably reduced in the central region plot. Also notice that the η shows up only in

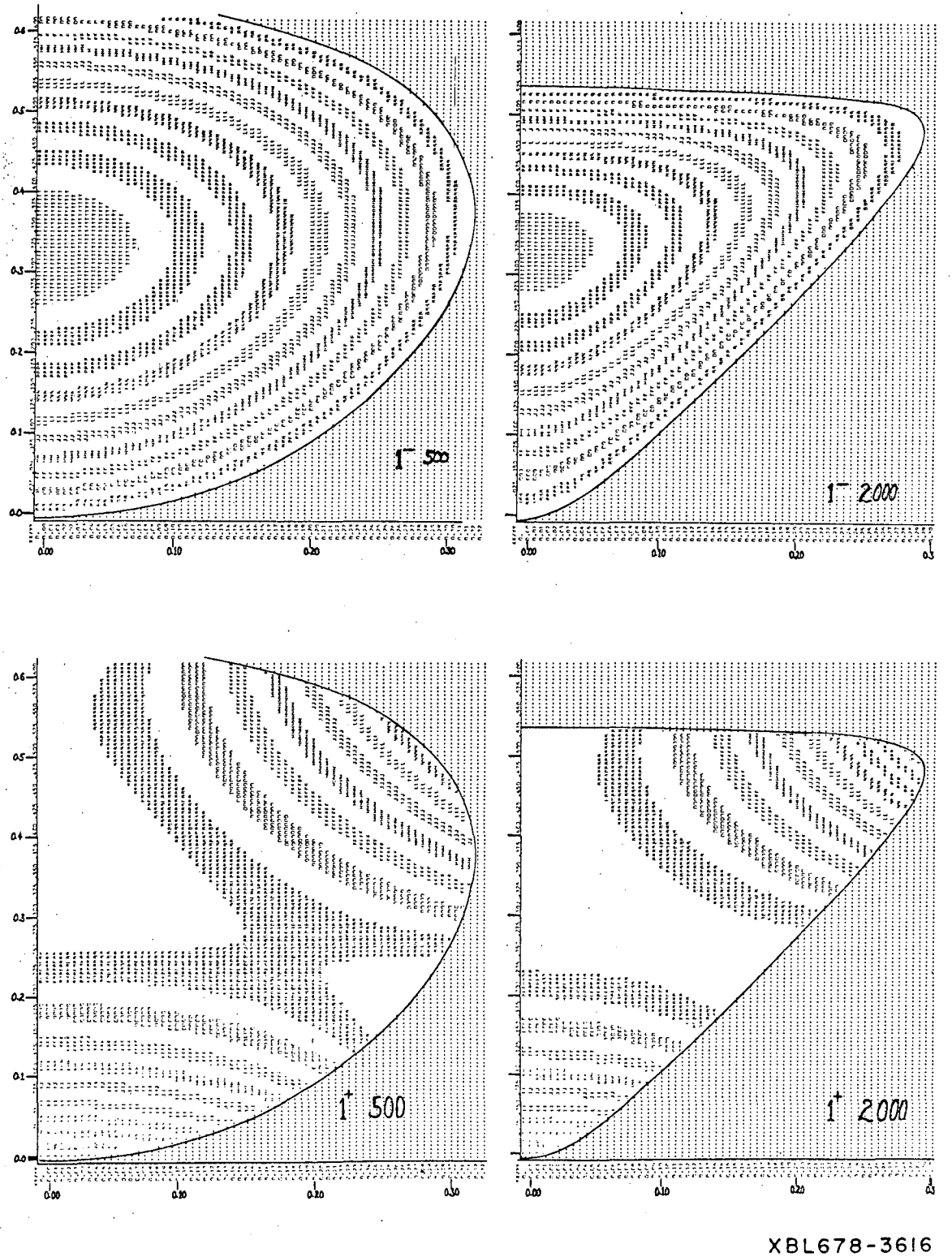

XBL678-3616

Fig. A-9

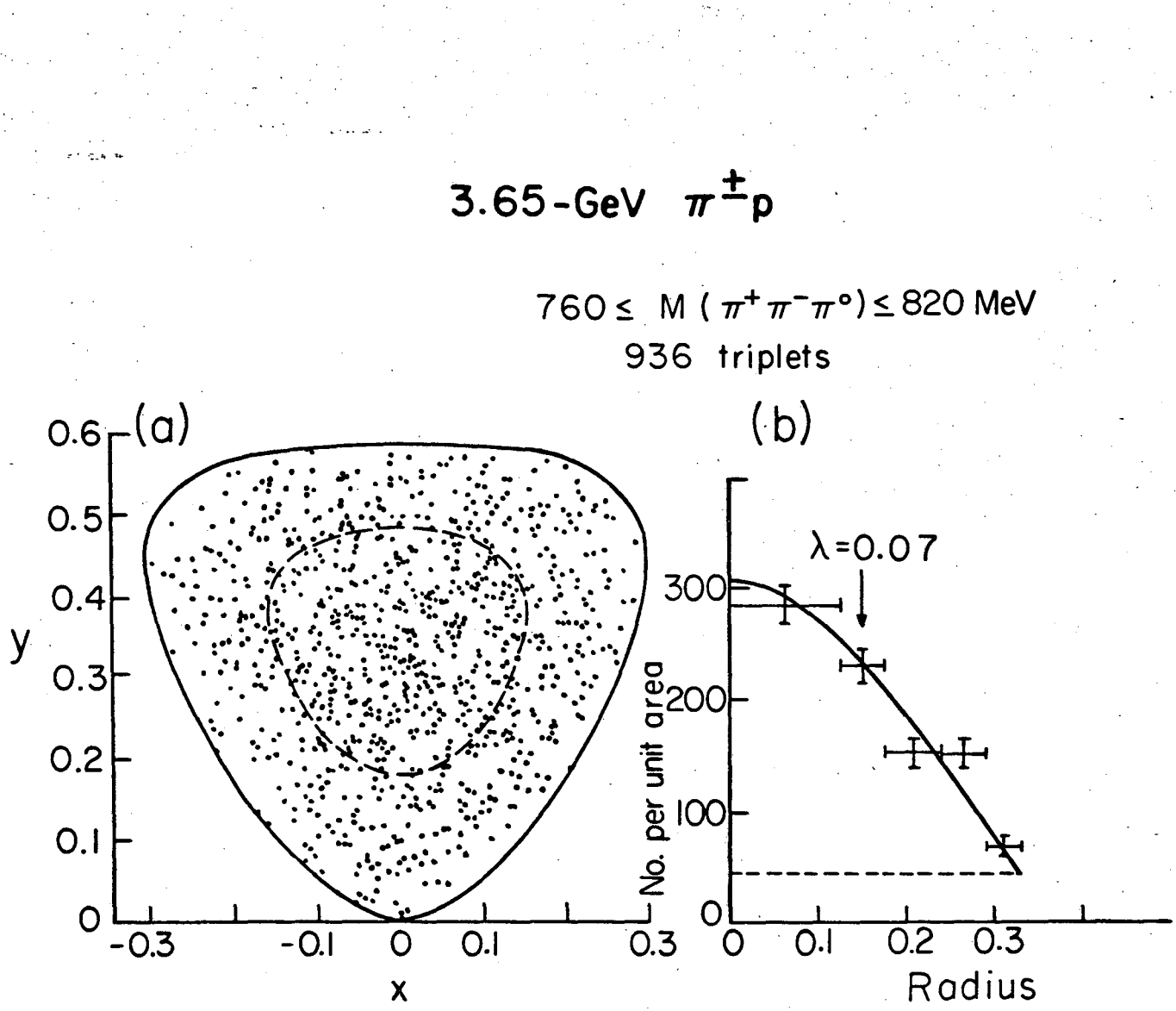
3.65-GeV $\pi^{\pm}p$
760 ≤ M ($\pi^+\pi^-\pi^0$) ≤ 820 MeV
936 triplets
(a)
(b)
y
x
0.6
0.5
0.4
0.3
0.2
0.1
0
-0.3
-0.1
0
0.1
0.3
λ=0.07
No. per unit area
300
200
100
0
0.1
0.2
0.3
Radius
XBL678-3617

Fig. A-10

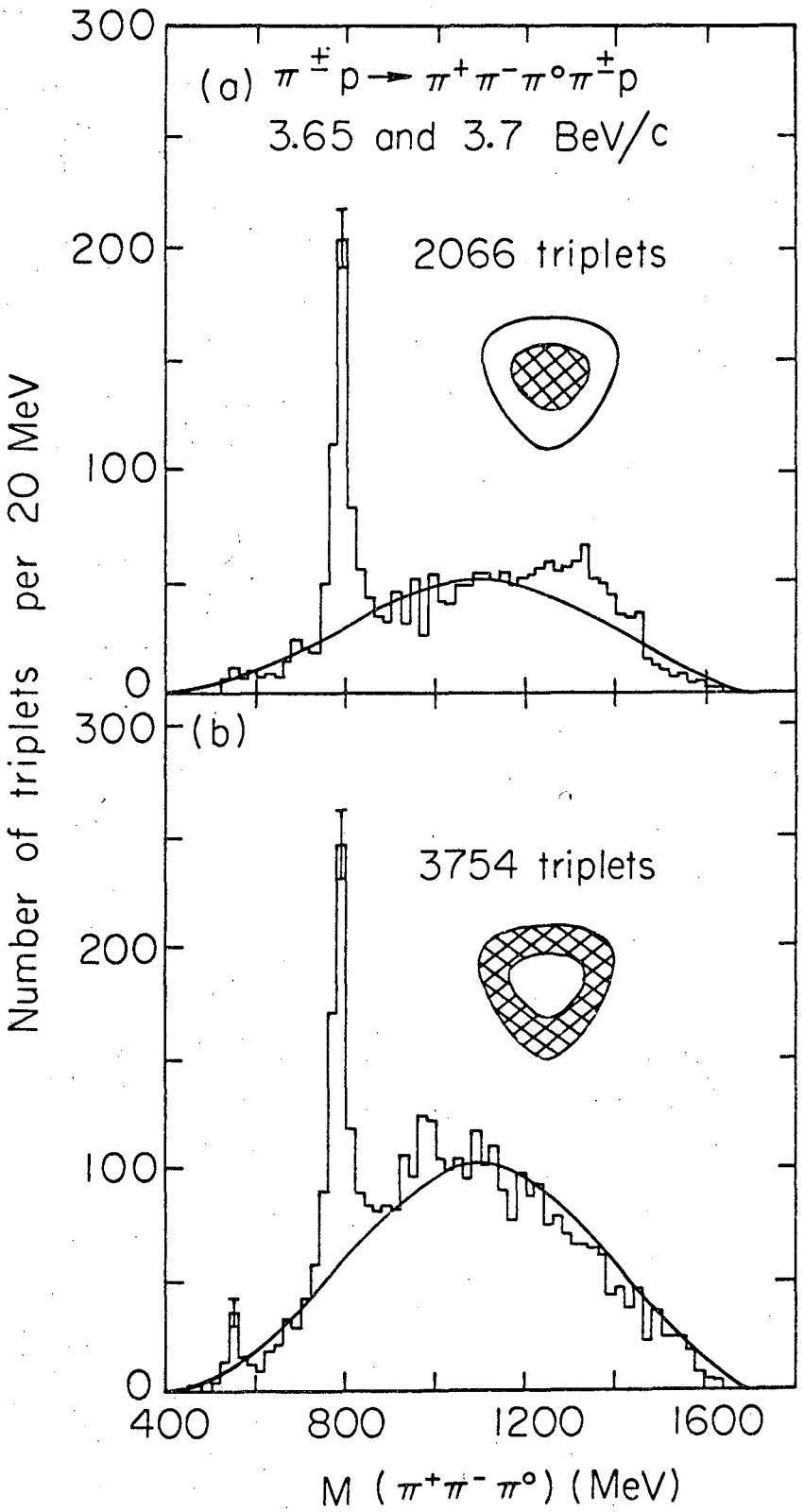

Fig. A-11

MUB-6020

the outer region; if we had not known about the η we could have found it this way.

Figure A-12 shows the same data in a different form. The y axis is the $\lambda(1^-)$ matrix element; we see that the mass sweep shows the resonance best where its matrix element is largest, as expected. The figure corresponds to choosing concentric regions in the Dalitz plot.

Figure A-13 shows the same data plotted vs the 2^+ matrix element. The statistics are limited (3000 events are shwon and probably we would need 10 000 to 20 000 events to detect a real effect over the fluctuations). The A_2 meson (a 2^+ meson) should show up in this plot. Figure A-14 shows the same data plotted against the 2^- matrix element.

One further difficulty in the application of this method should be mentioned. In analysis of a resonance with a two-step decay, such as the A_1 or A_2, there will be ρ bands across the Dalitz plot corresponding to $A_2 \to \rho^{\pm}\pi^{\mp}$ (notice $A_2 \not\to \rho^0\pi^0$). Hence the recognition of the appropriate pattern for the A_2 meson is altered by these bands. Similar calculations taking these effects into account will be needed.[5]

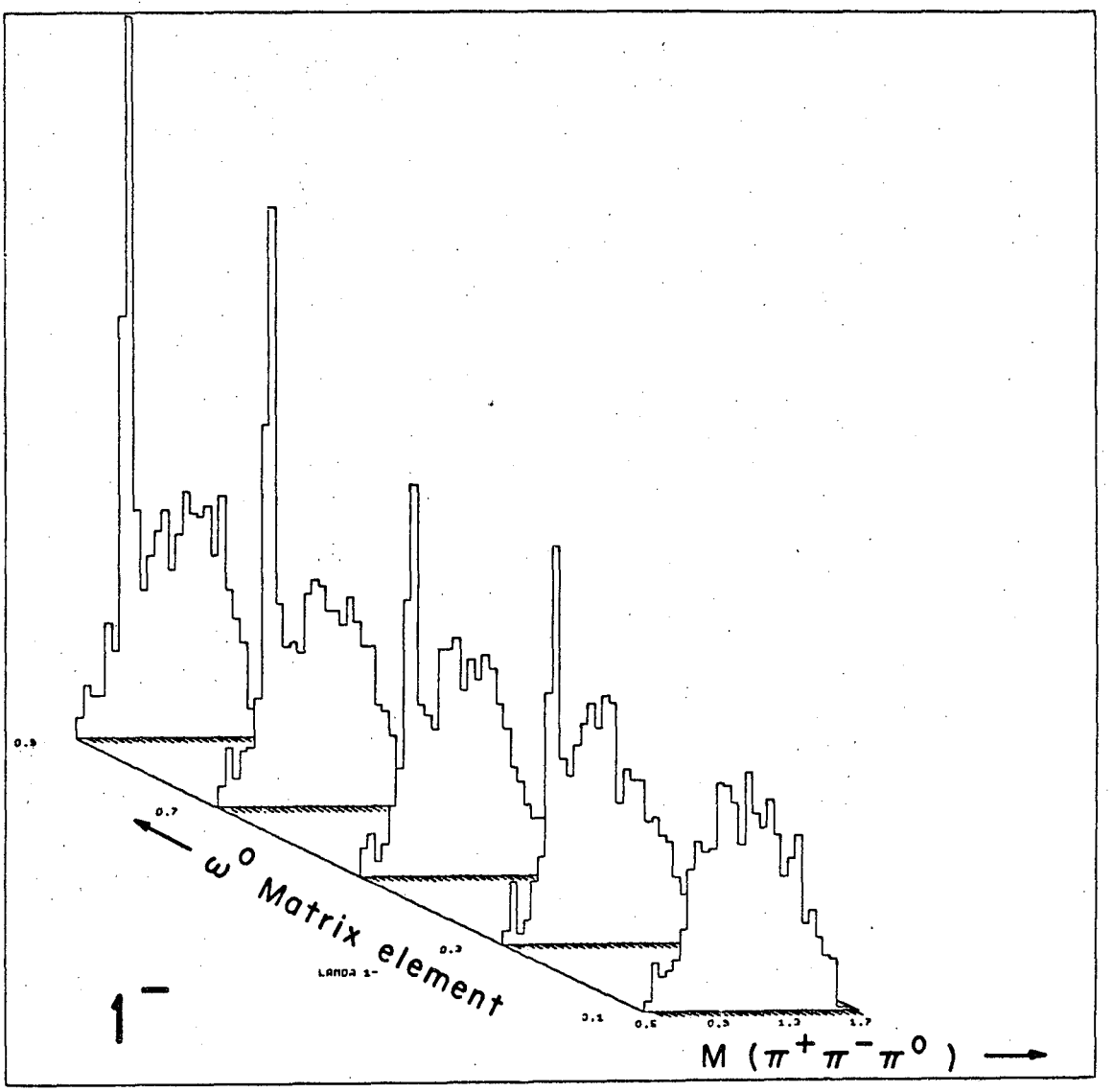

XBL678-3613

Fig. A-12

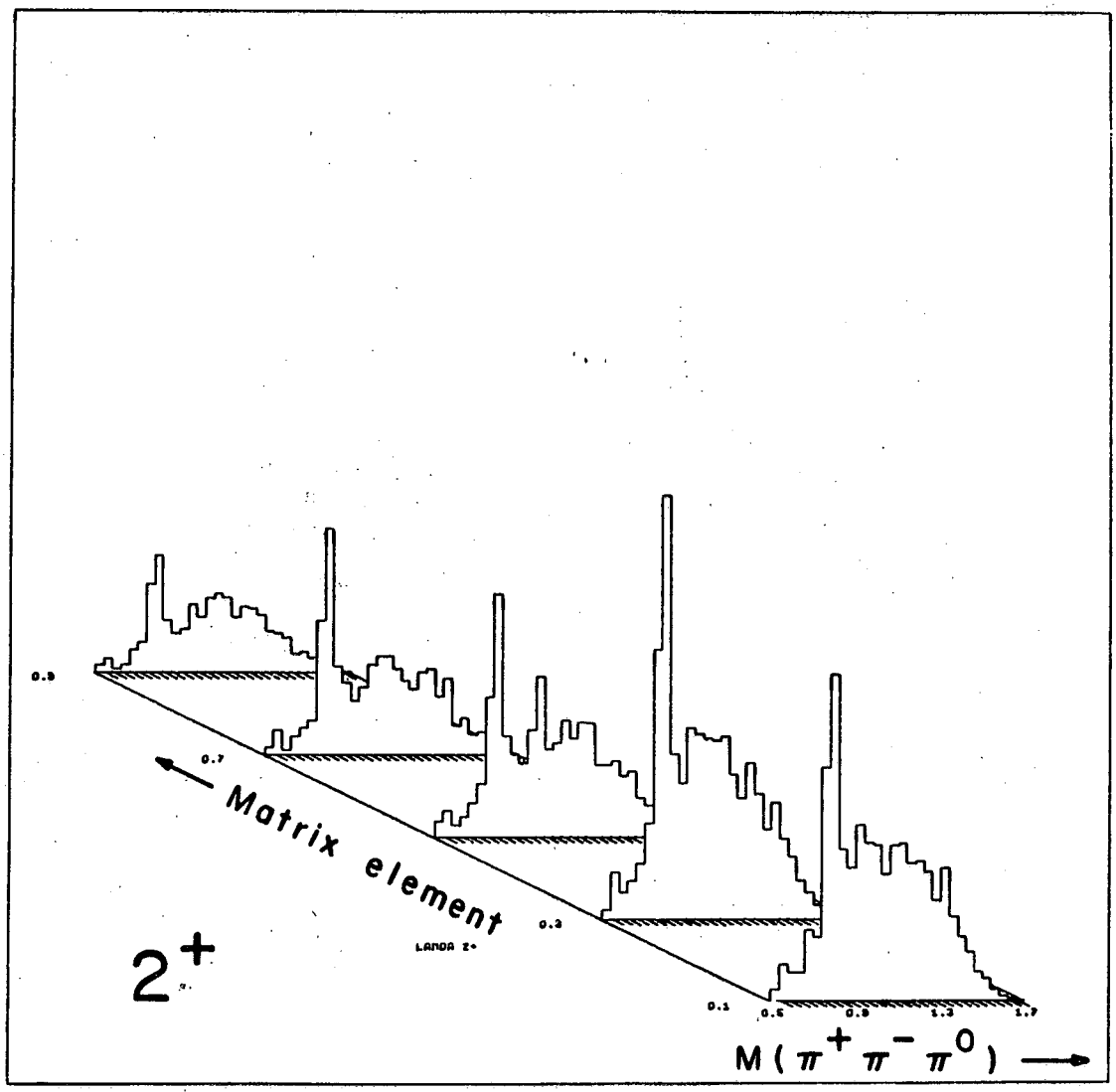

XBL678-3612

Fig. A-13

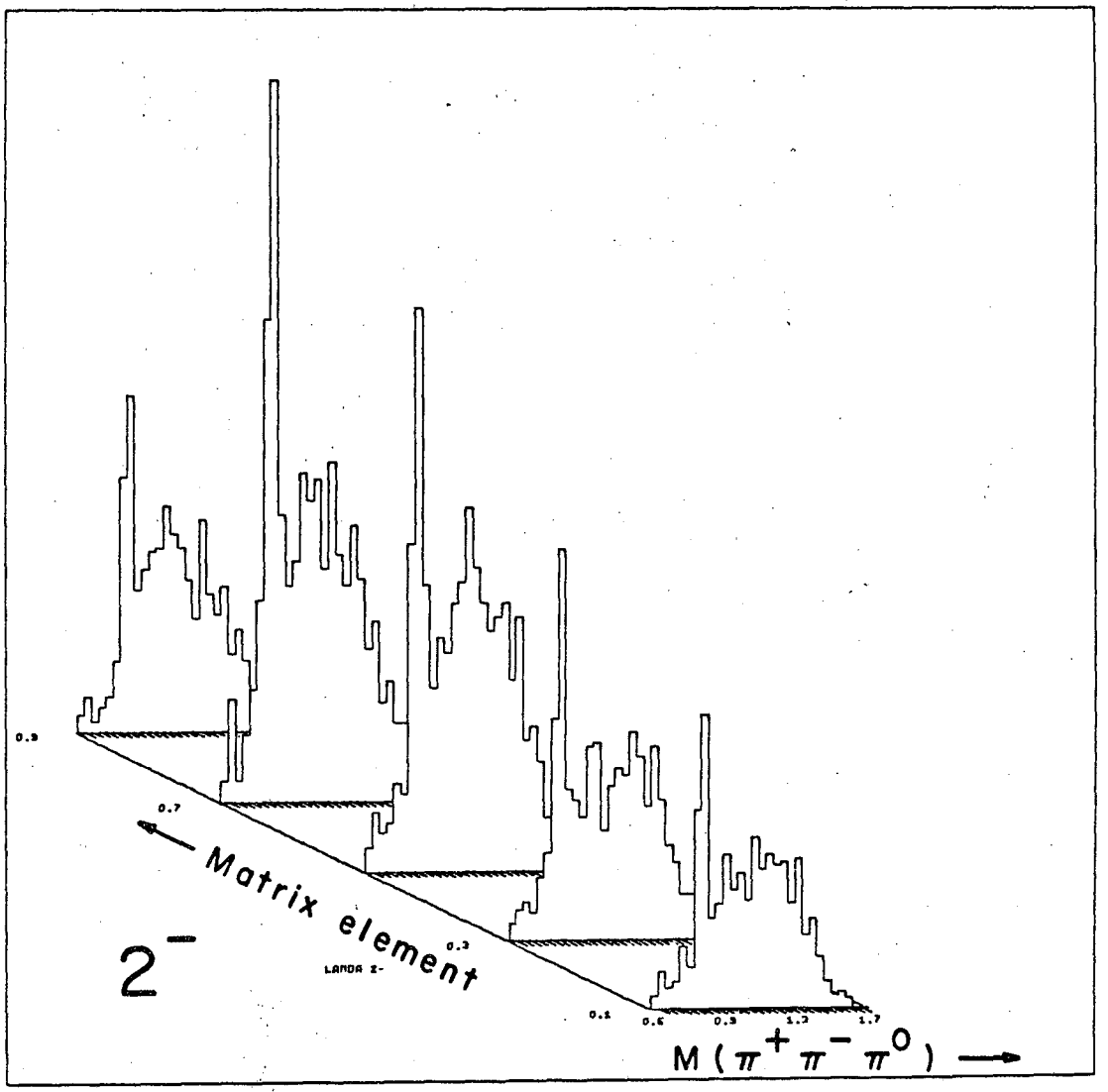

XBL678-3611

Fig. A-14

REFERENCES

1) M. L. Stevenson, L. W. Alvarez, B. C. Maglić, and A. H. Rosenfeld, Phys. Rev. 125, 687 (1962).

2) M. Gell-Mann, as quoted by B. C. Maglić, L. W. Alvarez, A. H. Rosenfeld, and M. L. Stevenson, Phys. Rev. Letters 7, 178 (1961).

3) C. Zemach, Phys. Rev. 133 B, 1201 (1964).

4) G. Goldhaber, S. Goldhaber, J. Kadyk, and B. Shen, Phys. Rev. Letters 15, 118 (1965).

5) G. Goldhaber, Spin Analysis for the I = 0 Three-Pion System, Lawrence Radiation Laboratory Report UCID-2608, 1965.

APPENDIX II

Tables of allowed and forbidden two-body decay modes

Table I: B = Y = 0 Nonstrange mesons

From Alvarez Memo No. 474 by
R. Huff and J. Kirz Revised May 29, 1967

In the following tables we give various allowed and forbidden two-body decay modes for various initial states, as well as the selection rules which are operative for the forbidden decays. The selection rules are applied in the following order:

1. J Angular momentum conservation. This entry for the single-photon refers to the familiar selection rule forbidding $0 \to 0$ radiative transitions.
2. S Symmetry, i.e., Bose-Einstein or Fermi-Dirac statistics. For the two-photon states, (S) refers to the $J=1$ states, but not to the higher odd angular momentum states, these latter being forbidden only for odd parity (C. N. Yang, Phys. Rev. 77:242).
3. P Parity conservation.
4. C Charge conjugation invariance.
5. I,G I-spin conservation and G-conjugation invariance, which are really equivalent when charge conjugation invariance holds, although we list both in the tables for pedigogical reasons. We use IG and I* to stand for the entries "I and G" and "I or G", respectively.

The appearance of one of these symbols in the tables means that the state in question is forbidden by the corresponding selection rule, but is allowed by all selection rules earlier in the above list. We have enclosed C in parenthesis in the tables to indicate that C applies to the neutral state of a multiplet, but not to the charged states of the same multiplet. Thus, for the multiplet X with quantum numbers $(J^P I^G = 0^+ 1^+)$, C forbids $X^0 \to \pi^+\pi^-$, but does not forbid $X^+ \to \pi^+\pi^0$ (although the latter is forbidden by I). However, for non-photon decays, if C completely forbids the decay of the neutral member of a multiplet X into a given pair of multiplets, then the decay of the charged members of X into the same pair of multiplets is forbidden by I or G, so we list this along with (C). This means a stronger selection rule for the neutral decay than for the charged, since C is valid for both strong and electromagnetic interactions, but I and G need only be valid for strong interactions.

Tables of allowed and forbidden two-body decay modes

Table I: B = Y = 0 Nonstrange mesons

We have listed the quantum numbers of the initial state in the form $J^{P(C)}{}_I{}^G$, but it should be kept in mind that the C eigenvalues refer only to the neutral member of a multiplet. This notation is more symmetric than $I(J^{PG})$ because J and P are the spin and parity in co-ordinate space, while I and G are the spin and parity in isotopic spin space, at least for the non-strange mesons. The final states are listed in order of increasing masses, and the sum of masses of the two particles are given in Mev. We do not mean to imply, however, that the decay probabilities of the various allowed modes for a given initial state will decrease in the same order. After all, matrix elements also have something to do with the rates, and not all matrix elements are equal.

We have made the tentative assignments $f(1250) = 2^{++}0^{+}$ and $\varphi(1020) = 1^{--}0^{-}$. Also the $\mathcal{K}(725)$ has $I = \frac{1}{2}$, with $J^P = \text{even}^+$ or odd^-, but the symbols enclosed in square brackets apply to the special case $J^P = 0^+$.

Note that all decays that are I- and/or G-forbidden can only occur by virtual emission and reabsorption of a photon, which means that these decay rates are down by a factor of at least α^2 relative to modes which are allowed by I and G. Decays involving one or two real photons are also down by α or α^2, respectively, and we have indicated these factors in the tables by @ or @@, respectively. Thus blanks in the tables indicate strong decays fully allowed by all five selection rules.

The $\Delta I=0$ or ± 1 selection rule for electromagnetic interactions impedes the decay of I=2 mesons into I=0 mesons and a gamma ray. The need for the emission and absorption of an additional photon in this case is denoted by @I,

Tables of allowed and forbidden two-body decay modes

Table I; B = Y = 0 Nonstrange mesons

$J^{P(C)}$	I^G	$\gamma\gamma$	$\gamma\pi$	$\pi^0\pi^0$	$\pi\pi$	$\gamma\eta$	$\pi\eta$	$\gamma\rho$	$\gamma\omega$	$\pi^0\rho^0$
		0	140	270	280	550	690	750	780	885
$0^{+(+)}$	0^+	@@	J			J	IG	@	@	P
	1^-	@@	J	IG	IG	J		@	@	P
	2^+	@@	J			J	IG	@	@ I	P
$0^{+(-)}$	0^-	C	J	C	C	J	C	C	C	P
	1^+	C	J	C	(C)I	J	(C)G	(C)@	C	P
	2^-	C	J	C	(C)G	J	(C)I	(C)@	C	P
$0^{-(+)}$	0^+	@@	J	P	P	J	P	@	@	C
	1^-	@@	J	P	P	J	P	@	@	C
	2^+	@@	J	P	P	J	P	@	@I	C
$0^{-(-)}$	0^-	C	J	P	P	J	P	C	C	
	1^+	C	J	P	P	J	P	(C)@	C	IG
	2^-	C	J	P	P	J	P	(C)@	C	
$ven^{+(+)}$	0^+	@@	C			C	IG	@	@	C
	1^-	@@	(C)@	IG	IG	C		@	@	C
	2^+	@@	(C)@			C	IG	@	@I	C
$ven^{+(-)}$	0^-	C	@	C	C	@	C	C	C	
	1^+	C	@	C	(C)I	@	(C)G	(C)@	C	IG
	2^-	C	@	C	(C)G	@I	(C)I	(C)@	C	
$ven^{-(+)}$	0^+	@@	C	P	P	C	P	@	@	C
	1^-	@@	(C)@	P	P	C	P	@	@	C
	2^+	@@	(C)@	P	P	C	P	@	@I	C
$ven^{-(-)}$	0^-	C	@	P	P	@	P	C	C	
	1^+	C	@	P	P	@	P	(C)@	C	IG
	2^-	C	@	P	P	@I	P	(C)@	C	
$odd^{+(+)}$	0^+	(S)	C	S	P	C	P	@	@	C
	1^-	(S)	(C)@	S	P	C	P	@	@	C
	2^+	(S)	(C)@	S	P	C	P	@	@I	C
$odd^{+(-)}$	0^-	(S)	@	S	P	@	P	C	C	
	1^+	(S)	@	S	P	@	P	(C)@	C	IG
	2^-	(S)	@	S	P	@I	P	(C)@	C	
$odd^{-(+)}$	0^+	(S)P	C	S	C	C	IG	@	@	C
	1^-	(S)P	(C)@	S	(C)G	C		@	@	C
	2^+	(S)P	(C)@	S	(C)I	C	IG	@	@I	C
$odd^{-(-)}$	0^-	(S)P	@	S	IG	@	C	C	C	
	1^+	(S)P	@	S		@	(C)G	(C)@	C	IG
	2^-	(S)P	@	S	IG	@I	(C)I	(C)@	C	

Tables of allowed and forbidden two-body decay modes

Table I: B = Y = 0 Nonstrange mesons

$J^{P(C)}$	I^G	$\pi\rho$ 890	$\pi\omega$ 920	$K\bar{K}$ 990	K_1K_1[a] K_2K_2 995	K_1K_2[a] 995	$\gamma\varphi$ 1020	$\eta\eta$ 1100	$\pi\varphi$ 1160	$\frac{K\bar{K}}{K\bar{K}}$ 1220	
$0^{+(+)}$	0^+	P	P			C	@		P	P	
	1^-	P	P			C	@	IG	P	P	
	2^+	P	P	I	I	C	@I	I	P	P	
$0^{+(-)}$	0^-	P	P	C	C		C	C	P	P	
	1^+	P	P	(C)I*	C		C	C	P	P	
	2^-	P	P	(C)I	C	I	C	C	P	P	
$0^{-(+)}$	0^+	G	C	P	P	P	@	P	C		
	1^-		(C)G	P	P	P	@	P	(C)G		
	2^+	G	(C)I	P	P	P	@I	P	(C)I	I	
$0^{-(-)}$	0^-		IG	P	P	P	C	P	IG		
	1^+	G		P	P	P	C	P			
	2^-		IG	P	P	P	C	P	IG	I	
$\text{even}^{+(+)}$	0^+	G	C			C	@		C	[P	
	1^-		(C)G			C	@	IG	(C)G	P	
	2^+	G	(C)I	I	I	C	@I	I	(C)I	P	I
$\text{even}^{+(-)}$	0^-		IG	C	C		C	C	IG	P	
	1^+	G		(C)I*	C		C	C		P	
	2^-		IG	(C)I	C	I	C	C	IG	P]	I
$\text{even}^{-(+)}$	0^+	G	C	P	P	P	@	P	C		
	1^-		(C)G	P	P	P	@	P	(C)G		
	2^+	G	(C)I	P	P	P	@I	P	(C)I	I	
$\text{even}^{-(-)}$	0^-		IG	P	P	P	C	P	IG		
	1^+	G		P	P	P	C	P			
	2^-		IG	P	P	P	C	P	IG	I	
$\text{odd}^{+(+)}$	0^+	G	C	P	S	P	@	S	C		
	1^-		(C)G	P	S	P	@	S	(C)G		
	2^+	G	(C)I	P	S	P	@I	S	(C)I	I	
$\text{odd}^{+(-)}$	0^-		IG	P	S	P	C	S	IG		
	1^+	G		P	S	P	C	S			
	2^-		IG	P	S	P	C	S	IG	I	
$\text{odd}^{-(+)}$	0^+	G	C	C	S	C	@	S	C	[P	
	1^-		(C)G	(C)I*	S	C	@	S	(C)G	P	
	2^+	G	(C)I	(C)I	S	C	@I	S	(C)I	P	I
$\text{odd}^{-(-)}$	0^-		IG		S		C	S	IG	P	
	1^+	G			S		C	S		P	
	2^-		IG	I	S	I	C	S	IG	P]	I

[a] It is not assumed that K_1K_1, K_2K_2, or K_1K_2 are produced as $K\bar{K}$. They may have S=0 or ± 2

Tables of allowed and forbidden two-body decay modes

Table I: B = Y = 0 Nonstrange mesons

$J^{P(C)}$	I^G	γf	$\eta\rho$	$\eta\omega$	$\begin{matrix}K\bar{K}^* \\ \bar{K}K^*\end{matrix}$	πf	$K\bar{K}$	$\rho^0\rho^0$	$\rho\rho$	$\rho\omega$
		1250	1300	1330	1380	1390	1450	1500	1500	1530
$0^{+(+)}$	0^+	C	P	P	P	P				IG
	1^-	C	P	P	P	P		IG	IG	
	2^+	C	P	P	P	P	I			IG
$0^{+(-)}$	0^-	@	P	P	P	P	C	C	C	C
	1^+	@	P	P	P	P	(C)I*	C	(C)I	(C)G
	2^-	@I	P	P	P	P	(C)I	C	(C)G	(C)I
$0^{-(+)}$	0^+	C	C	C		IG	[P			IG
	1^-	C	(C)G	C			P	IG	IG	
	2^+	C	(C)I	C	I	IG	P I			IG
$0^{-(-)}$	0^-	@	IG			C	P C	C	C	C
	1^+	@		IG		(C)G	P (C)I*	C	(C)I	(C)G
	2^-	@I	IG	I	I	(C)I	P (C)I	C	(C)G	(C)I
$\text{even}^{+(+)}$	0^+	C	C	C		IG				IG
	1^-	C	(C)G	C				IG	G	
	2^+	C	(C)I	C	I	IG	I			IG
$\text{even}^{+(-)}$	0^-	@	IG			C	[C	C	G	C
	1^+	@		IG		(C)G	(C)I*	C		(C)G
	2^-	@I	IG	I	I	(C)I	(C)I] I	C	G	(C)I
$\text{even}^{-(+)}$	0^+	C	C	C		IG	[P			IG
	1^-	C	(C)G	C			P	IG	G	
	2^+	C	(C)I	C	I	IG	P I			IG
$\text{even}^{-(-)}$	0^-	@	IG			C	P	C	G	C
	1^+	@		IG		(C)G	P	C		(C)G
	2^-	@I	IG	I	I	(C)I	P I	C	G	(C)I
$\text{odd}^{+(+)}$	0^+	C	C	C		IG	P			IG
	1^-	C	(C)G	C			P	IG	G	
	2^+	C	(C)I	C	I	IG	P I			IG
$\text{odd}^{+(-)}$	0^-	@	IG			C	P	C	G	C
	1^+	@		IG		(C)G	P	C		(C)G
	2^-	@I	IG	I	I	(C)I	P] I	C	G	(C)I
$\text{odd}^{-(+)}$	0^+	C	C	C		IG	[C			IG
	1^-	C	(C)G	C			(C)I*	IG	G	
	2^+	C	(C)I	C	I	IG	(C)I] I			IG
$\text{odd}^{-(-)}$	0^-	@	IG			C		C	G	C
	1^+	@		IG		(C)G		C		(C)G
	2^-	@I	IG	I	I	(C)I	I	C	G	(C)I

Tables of allowed and forbidden two-body decay modes

Table I: B = Y = 0 Nonstrange mesons

$J^{P(C)}$	I^G	$\omega\omega$	$\eta\varphi$	$\frac{K^*\bar{K}}{K^*K}$	$\rho\varphi$	$K^*\bar{K}^*$	ηf	$\omega\varphi$	$N\bar{N}$	ρf
		1560	1570	1610	1770	1775	1800	1800	1880	2000
$0^{+(+)}$	0^+		P		IG		P			C
	1^-	IG	P				P	IG		(C)G
	2^+	I	P	I	IG	I	P	I	I	(C)I
$0^{+(-)}$	0^-	C	P		C	C	P	C	C	IG
	1^+	C	P		(C)G	(C)I*	P	C	(C)I*	
	2^-	C	P	I	(C)I	(C)I	P	C	(C)I	IG
$0^{-(+)}$	0^+		C	[P	IG					C
	1^-	IG	C	P			IG	IG		(C)G
	2^+	I	C	P I	IG	I	I	I	I	(C)I
$0^{-(-)}$	0^-	C		P	C	C	C	C	C	IG
	1^+	C	IG	P	(C)G	(C)I*	C	C	(C)I*	
	2^-	C	I	P] I	(C)I	(C)I	C	C	(C)I	IG
$\text{even}^{+(+)}$	0^+		C		IG					C
	1^-	IG	C				IG	IG		(C)G
	2^+	I	C	I	IG	I	I	I	I	(C)I
$\text{even}^{+(-)}$	0^-	C			C		C	C	C	IG
	1^+	C	IG		(C)G		C	C	(C)I*	
	2^-	C	I	I	(C)I	I	C	C	(C)I	IG
$\text{even}^{-(+)}$	0^+		C		IG					C
	1^-	IG	C				IG	IG		(C)G
	2^+	I	C	I	IG	I	I	I	I	(C)I
$\text{even}^{-(-)}$	0^-	C			C		C	C		IG
	1^+	C	IG		(C)G		C	C		
	2^-	C	I	I	(C)I	I	C	C	I	IG
$\text{odd}^{+(+)}$	0^+		C		IG					C
	1^-	IG	C				IG	IG		(C)G
	2^+	I	C	I	IG	I	I	I	I	(C)I
$\text{odd}^{+(-)}$	0^-	C			C		C	C		IG
	1^+	C	IG		(C)G		C	C		
	2^-	C	I	I	(C)I	I	C	C	I	IG
$\text{odd}^{-(+)}$	0^+		C		IG				C	C
	1^-	IG	C				IG	IG	(C)I*	(C)G
	2^+	I	C	I	IG	I	I	I	(C)I	(C)I
$\text{odd}^{-(-)}$	0^-	C			C		C	C		IG
	1^+	C	IG		(C)G		C	C		
	2^-	C	I	I	(C)I	I	C	C	I	IG

Tables of allowed and forbidden two-body decay modes

Table I: B = Y = 0 Nonstrange mesons

$J^{P(C)}$	I^G	ωf	$\varphi\varphi$	$\Lambda\bar{\Lambda}$	φf	$\Lambda\bar{\Sigma}$ / $\bar{\Lambda}\Sigma$	$\Sigma\bar{\Sigma}$	ff
		2030	2040	2230	2270	2310	2390	2500
$0^{+(+)}$	0^+	C			C	I		
	1^-	C	IG	IG	C			IG
	2^+	C	I	I	C	I		I
$0^{+(-)}$	0^-		C	C		I	C	C
	1^+	IG	C	C	IG		(C)I*	C
	2^-	I	C	C	I	I	(C)I*	C
$0^{-(+)}$	0^+	C			C	I		
	1^-	C	IG	IG	C			IG
	2^+	C	I	I	C	I		I
$0^{-(-)}$	0^-		C	C		I	C	C
	1^+	IG	C	C	IG		(C)I*	C
	2^-	I	C	C	I	I	(C)I*	C
$\text{even}^{+(+)}$	0^+	C			C	I		
	1^-	C	IG	IG	C			IG
	2^+	C	I	I	C	I		I
$\text{even}^{+(-)}$	0^-		C	C		I	C	C
	1^+	IG	C	C	IG		(C)I*	C
	2^-	I	C	C	I	I	(C)I*	C
$\text{even}^{-(+)}$	0^+	C			C	I		
	1^-	C	IG	I	C			IG
	2^+	C	I	I	C	I		I
$\text{even}^{-(-)}$	0^-		C			I		C
	1^+	IG	C	I	IG			C
	2^-	I	C	I	I	I		C
$\text{odd}^{+(+)}$	0^+	C			C	I		
	1^-	C	IG	I	C			IG
	2^+	C	I	I	C	I		I
$\text{odd}^{+(-)}$	0^-		C			I		C
	1^+	IG	C	I	IG			C
	2^-	I	C	I	I	I		C
$\text{odd}^{-(+)}$	0^+	C		C	C	I	C	
	1^-	C	IG	C	C		(C)I*	IG
	2^+	C	I	C	C	I	(C)I*	I
$\text{odd}^{-(-)}$	0^-		C			I		C
	1^+	IG	C	IG	IG			C
	2^-	I	C	I	I	I		C